Experimental Investigation and Performance Evaluation of Natural Draft Double-Pot Biomass Cookstove Using New *Aircrete* Insulation

BY:

WAGANESH ADMASE WAGAYE

A Thesis Submitted to the Department of Thermal and Aerospace Engineering
School of Mechanical, Chemical, and Material Engineering

Presented in Partial Fulfillment of the Requirement for the Degree of Master of science in Thermal Engineering

Office of Graduate Studies

Adama Science and Technology University

August 2021

Adama, Ethiopia

Experimental Investigation and Performance Evaluation of Natural Draft Double-Pot Biomass Cookstove Using New *Aircrete* Insulation

BY

Waganesh Admase Wagaye

Advisor Dr. Dawit Gudeta

A Thesis Submitted to the Department of Thermal and Aerospace Engineering
School of Mechanical, Chemical, and Material Engineering

Presented in Partial Fulfillment of the Requirement for the Degree of Master of science in Thermal Engineering

Office of Graduate Studies

Adama Science and Technology University

August 2021

Adama, Ethiopia

DECLARATION

First, I hereby declare that this M.Sc. thesis entitled "**Experimental Investigation and Performance Evaluation of Natural Draft Double-Pot Biomass Cookstove Using New *Aircrete* Insulation**" is my original work and that all sources and materials used for this thesis have been duly acknowledged. This thesis has been submitted in partial fulfillment of the requirements for MSc. degree in Thermal Engineering at Adama Science and Technology University, School of Mechanical, Chemical, and Material Engineering. I solemnly declare that this thesis is not submitted to any other institution anywhere for the award of any academic degree, diploma, or certificate. Quotation from this thesis is allowable without special permission if an accurate acknowledgment of the source is made.

Waganesh Admase	____________________	__________________
Candidate	Signature	Date

This is to certify that the above statement made by the candidate is correct to the best of my knowledge and belief. This has been submitted for examination with my approval.

Dr. Dawit Gudeta	____________________	__________________
Advisor	Signature	Date

Approval Page

We, the undersigned members of the Board of Examiners of the final open defense by **Waganesh Admase** have read and evaluated her thesis entitled "**Experimental Investigation and Performance Evaluation of Natural Draft Double-Pot Biomass Cookstove Using New *Aircrete* Insulation**" and examined the candidate. Therefore, this is to certify that the thesis has been accepted in partial fulfillment of the requirement of the Degree of Master of science in Thermal Engineering.

Name	Signature	Date
Waganesh Admase	____________________	________________
Name of the Student		
____________________	____________________	________________
Advisor		
____________________	____________________	________________
External Examiner		
____________________	____________________	________________
Internal Examiner		
____________________	____________________	________________
Chair Person		
____________________	____________________	________________
Head of Department		
____________________	____________________	________________
School Dean		
____________________	____________________	________________
Post Graduate Dean		

ACKNOWLEDGMENT

First, I would like to thank almighty God for his grace in the completion of this work. I would also like to express my gratitude to my advisor Dr. Dawit Gudeta for his valuable guidance, encouragement, and constructive comments from the beginning until the completion of this thesis. I would then like to thank Dr. Addisu Bekele for sharing his academic experience, knowledge, and guidance during my Master's study and Dr. Gezahegn Habtamu for his valuable advice and constructive comments for the completion of this thesis.

I express my sincere thanks to the mechanical, chemical, and material science engineering departments and lab assistants for their contribution from the start to the completion of the prototype. My heartfelt and deepest gratitude goes to all of my family who was always on my side persistently throughout my entire academic life. I never forget to thank all of my academic friends for their encouragement and support all along.

ABSTRACT

Biomass has been and still now is one of the most abundant renewable energy resources for cooking and heating applications in both household and industrial levels. However, ineffective and improper use of biomass fuels for cooking results in socio-economic and environmental problems. Those problems can be reduced by properly designing efficient and improved biomass cookstoves with enhanced performance. Thus, the major objective of this thesis is to design and experimentally investigate the performance of a locally constructed double-pot improved biomass cookstove using an Aircrete wall as new insulating material. Numerical simulation using ANSYS Fluent was carried out to compare the performance of cookstove models with different geometrical parameters. An experimental investigation is done to study the performance of the selected model with better performance and good agreement is obtained between the numerical and experimental results. For thermal conductivity test of insulating material, four samples of Aircrete walls with different ratio of, water, cement, foam, and light weight gravel was prepared. The test result showed that a sample with a ratio of 2.272% water, 58.25% cement, 17.54% foam, and 21.93% light weight gravel has a lower thermal conductivity of 0.1839 W/m.K and porosity 37.03% were selected as an insulating material for the development of the cookstove. Water boiling tests were conducted using 2.5kg of water and using eucalyptus wood log of moisture content of 10.03% as a feedstock. The result showed that for an average fire power input of 6.686 kW the overall efficiency, boiling time, and average specific fuel consumption were found to be 35.8 %, 15.166 min, and 140 g/l. The average deviation in the numerically predicted and experimental values of zonal temperature is 2.446 %. The result of exhaust gases emission showed that the average amount of CO and CO_2 *emission from the stove was found to 0.21% and 6.448 % volume, respectively. The use of Aircrete insulation results in a relative reduction of heat loss through the combustion chamber wall which is only found as 3% of total loss.*

Keywords: Improved Biomass Cookstove (IBC), *Aircrete* insulation, Foam, *Infralyt* smart gas analyzer

Table of Contents

List of Figures

List of Tables

List of Abbreviations and Acronyms

μ	Dynamic viscosity of flue gas (kg/m s)	ϵ_{fl}	The emissivity of flue gas
k	Thermal conductivity (W/m K)	α_{fl}	Absorptivity of flue gas
g	Gravity (m/s^2)	L_b	Characteristic length
ρ_g	The density of flue gas (kg/m3)	h_{ci}	Convective heat transfer coefficient for the inner wall of the stove
v	Kinematic viscosity of air/flue gas (m^2/s)	h_{co}	Convective heat transfer coefficient for the outer wall of the stove
h_s	Enthalpy of superheated steam at atmospheric pressure (kJ/kg of steam)	h_{ri}	Radiative heat transfer coefficient for the outer wall
C_p	Specific heat of air/flue gas (kJ/kg K)	h_{rof}	Radiative heat transfer coefficient of flame for inner wall
R_e	Reynolds no for combustion zone	h_{roc}	Radiative heat transfer coefficient of char from the outer side
k	Thermal conductivity of air/flue gas (W/m K)	h_{chr}	Char radiative temperature
L	length (mm)	h_{ro}	Radiative heat transfer of outer surface
Q_{fl}	Heat gain by a flue in zone 1	h_{rfl}	Radiative heat transfer coefficient of flue gas
Q_{ac}	Supplied heat by the fuel combustion	TSF	Three stone fire

Q_{fr}	Heat transfer by radiation from a flame to pot	G_r	Gras hoff's
Q_{loss}	loss through combustion wall	T_f	Film temperature (K)
$Q_{moisture\ loss}$	moisture loss	CFD	Computational fluid dynamics
Q_d	loss through the door opening in the feeding zone	IAR	Inlet area ratio
$Q_{H_2 loss}$	heat loss due to hydrogen in the fuel	ICS	Improved biomass cookstoves
Q_{cr}	Radiation from char to pot	GHS	Greenhouse gases
P_r	Prandtl number	kW	Kilowatt
m_{act}	Actual mass flow rate	PM	Particulate matter
$C_{p,fl}$	Flue gas heat capacity (kJ/kg K)	WHO	World Health Organization
C_d	Coefficient of discharge	℃	Degree Celsius
A	Cross-sectional area	T_{ch}	Char temperatures
T_a	Ambient temperature	T_{p1}	Pot 1 surface temperature
T_{fl}	Flue gas or flame temperature	ϵ_{ch}	Emissivity of char
M	The moisture content of the fuel on a weight basis (%)	F_{c-p}	View factor between char bed and pot bottom
P	The firepower of the stove (kW)	F_{c-w}	view or configuration factor between char bed and inner wall
v_{th}	Theoretical velocity ($\frac{\mathrm{m}}{s^2}$)	F_{c-d}	configuration factor fuel feeding door
NCV	The net calorific value of fuel (kJ/kg of dry fuel)	HTE	Heat transfer efficiency

σ	Stephen Boltzmann constant (W/m^2K^4)	Q_{pot1}	Heat transfer to the pot 1
EDM	Eddy dissipation model	Q_{pot2}	Heat transfer to pot 2
EDC	Eddy dissipation concept	m	Moisture content
Δt_c	Boiling time	T_{wi1}	Inner wall temperature of zone 1
T_{fla}	Flame temperature	T_{wo1}	Outer wall temperature of zone 1
T_{flu1}	The temperature of flue gas 1	T_{flu2}	The temperature of flue gas 2
T_{zon2}	The temperature at zone 2	T_{wo2}	Outer wall temperature of zone 3
$Tz_{one\ 3}$	The temperature at zone 3	T_{zone4}	The temperature of gas at zone 4
T_{wi2}	Inner wall temperature of zone 2	T_e	Exit temperature
T_{zone5}	The temperature of gas ate zone 5	T_{wo3}	Outer wall temperature in zone 3
t	Time	BCS	Biomass cookstoves
WBT	Water boiling test	η_{th}	Thermal efficiency
CO	Carbon monoxide	CO_2	Carbon dioxide
M	Saturated mass	D	Dry mass
S	A mass suspended in water	P	Porosity
GIT	Grid independence test	T_{p1}	The temperature of pot 1
Tp_2	The temperature of pot 2	H	Height of pot

CHAPTER ONE

1. INTRODUCTION

1.1 Background of the Study

Biomass is one of the most abundant renewable energy resources for cooking and heating application at both the household and industrial levels. Biomass stove is one of the primitive devices that used for the conversion of biomass fuels to thermal energy forms and presently around 38% of the world's population are relays on using biomass cookstoves. To satisfy this cooking application (Mapelli *et al*., 2013). In most developing countries, more than 50% of the population depends on the traditional use of biomass for cooking which results from the need for improvement of biomass utilization (Njiru *et al.,* 2018; Sime *et al.,* 2020; Tucho, 2020). Millions of people mainly in low- and middle-income countries are still relying on solid fuels (wood, animal dung, charcoal, crop wastes, and coal) which are burnt in an inefficient and highly polluting stove for cooking and heating application (Scharler *et al.,* 2020). Furthermore, in Sub-Saharan Africa, around 753 million people (i.e. 80% of the population) use biomass as an energy source (Adem and Ambie, 2017).

In Ethiopia, approximately 70-80% of the primary energy share is taken from biomass (Bantelay D., 2014). The unstable economy and poverty of the country might not change the use of wood as a feedstock and this challenges mostly the low-income population. For this reason, several governmental and nongovernmental organizations such as GIZ, SNV, and the Ethiopian ministry of energy are being worked on the development of different types of biomasses cookstoves by improving the performance and some researchers are also worked on the improvement of the existing cookstoves in the country. Cooking stoves such as; Metal stoves, *Tikikil,* and *lackech,* and *Injera* baking stoves like; *Gonze* and *Mirt* cookstoves are the most commonly used by the end-users and abundantly available in the local market.

Many problems are associated with the ineffective use of biomass fuel for cooking. Globally, around 4 million premature deaths mainly women and children are from respiratory health problems (such as bronchitis and pneumonia) associated with incomplete combustion that is the primary cause of indoor air pollution (Ali and Wei, 2017; Beyene *et al*., 2018; WHO, 2018). Pollutant emissions emitted into homes reduce the indoor air quality, causing several diseases associated with the inhalation of smoke from solid fuels, such as higher blood pressure, acute respiratory infections, cataracts, blindness, adverse effects on pregnancy, low birth weight, infant mortality, and, especially, chronic obstructive pulmonary diseases (Chica and Pérez, 2019). In addition, due to wastage use and scarcity of biomass fuels, people in rural areas are forced to travel long distances from their homes to fetch wood which is mainly carried out almost entirely by women and children. Figure 1.1 shows traditional, unhealthy, polluting, and inefficient ways of open fire burning of wood-based biomass fuels for cooking. In order to eliminate those problems associated with improper use of biomass as a feedstock for cooking, double-pot improved biomass cookstove using new *Aircrete* insulation material is a very interesting option to save energy from cooking stoves and to reduce the side effects that come with the inefficient way of burning of biomass fuel.

Figure 1.1 Inefficient way of burning biomass fuel (Balmes, 2019)

However, the design modification on the cookstoves was attempted based on an experimentally trial and error approach. Accordingly, as a country Ethiopia, the available cookstoves are not do not come up with the best fit that modern engineering can offer. recently, a handful of literates have been done numerical modeling of the heat transfer analysis in the biomass cooking stoves at a global level with a better understanding of cookstove guideline principles (Sedighi and Salarian, 2017).

Double-pot improved biomass cookstove is a device that is used to convert chemical energy from solid biomass fuel to thermal energy or heat by using a combustion principle. The system contains five basic heat flow regions. The combustion of fuel takes place on the combustion chamber section only and then the other section extracts the extra heat from the first section which is the combustion zone. Previously the two-pot biomass cookstoves have been done by some scholars i.e. *(*Chica and Pérez, 2019; and Pande *et al*., 2019) using a ceramic blanket as an insulating material and the thermal efficiency reported as 20.9% and 32.23± 2.36 respectively. The conducted researches showed that metals have high thermal conductivity, for that reason, utilizing the heat from the stove that is wasted through the wall of the stove needs more investigation in the improvement of cookstoves performance. As a result, the aim of the present study is to design and experimentally investigate the performance of double-pot biomass cookstoves by using a new *Aircrete* insulation material.

1.2 Biomass Cookstoves

The use of fire for cooking dates back to 100,000 years ago, and cooking was presumably done over an open fire (mainly for cooking/roasting meat) with the fuel arranged in a pyramid shape. Biomass cookstoves are devices that help to convert the chemical form of the fuel to thermal or heat energy and directs the heat from the combustion towards a cooking pot. Those cookstoves are used to burn wood, charcoal, animal dung, or crop residue as fuel for cooking and heating food in developing countries. Besides, they are used at both the domestic and institutional levels.

1.3 Classification of Biomass Cookstoves

Biomass cookstoves can be classified in several ways as new cookers designed with new improvements are continuously proposed, which requires a continuous update of those cookstove classifications. According to Kshirsagar and Kalamkar, (2014), the classification of biomass cookstoves is based on different criteria. Figure 1.2 shows a diagrammatic representation of a classification of different biomass cookstoves.

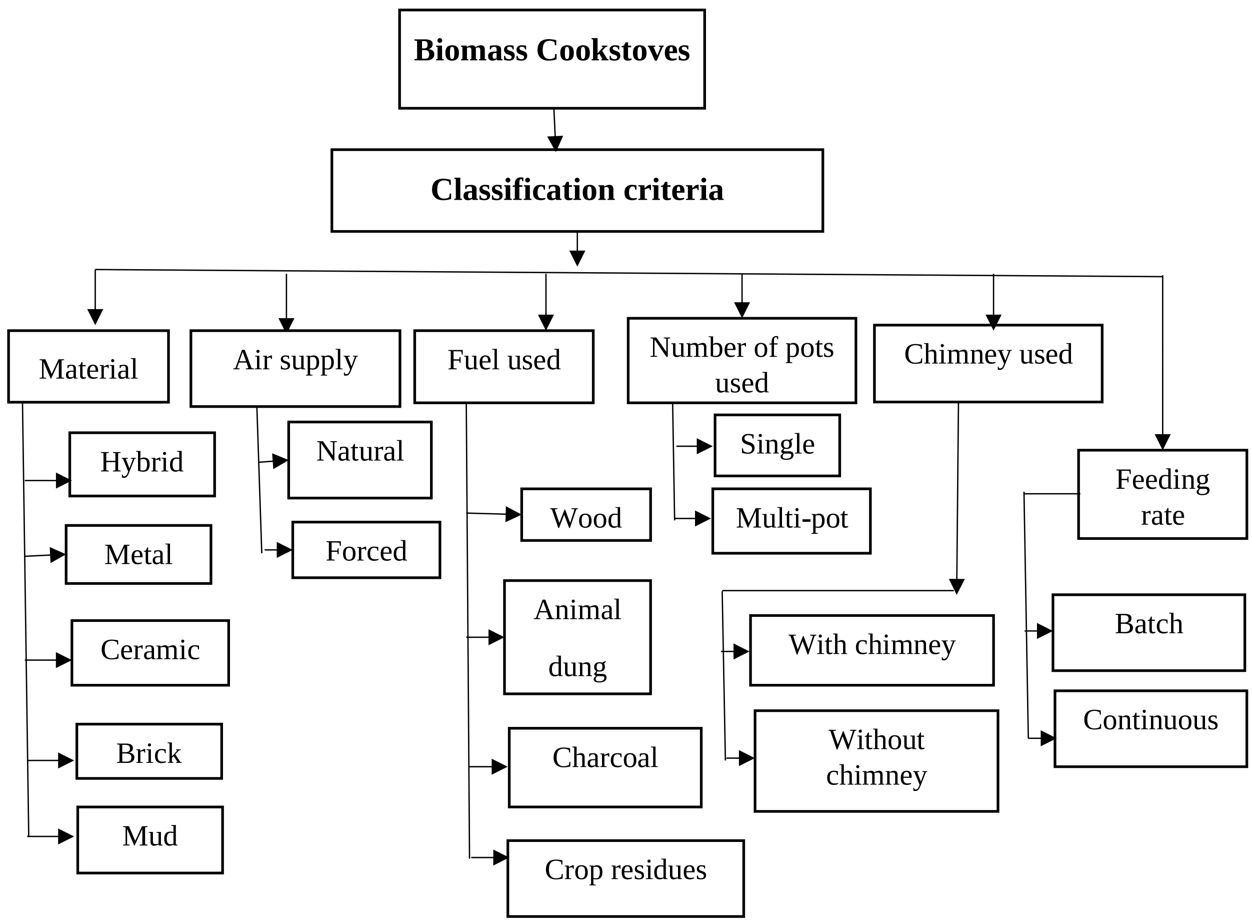

Figure 1.2 Biomass cookstove classification

1.4 Improvement of Biomass Cookstoves

Cookstoves are designed to get better cooking efficiency and release fewer pollutants. The improved cookstoves (ICS) must meet the cooking energy demands of people living in the rural area of developing countries. It is the improved use of biomass in households which, leads to reduced fuel consumption (Schirnding, 2001). On the other hand, the use of improved cookstove reduces the fuel collection burden placed on women and children and also saves time. Women in their free time can engage in other income-generating activities and children may spare more time to get an education, especially girl-child. Improved cookstoves should be designed in such ways that are acceptable to the users. The improvement in the design of the stove must be (Ram *et al.*, 1984);

- Inexpensive as compared to use open fires.

- Durable to withstand heavy use without cracking for at least a year and preferably longer.
- Able to be constructed with locally available resources and tools.

1.5 Statement of the Problem

The cookstove's design modifications were primarily based on a trial-and-error technique. As a result, locally accessible stoves fall short of modern engineering's optimum design. With a better knowledge of guiding principles, researchers have recently applied numerical modeling and computational fluid dynamics (CFD) technologies for cookstove design. Only a few researchers throughout the world have utilized the numerical modeling technique for heat transfer and combustion in solid-fuel cooking stoves. For cooking, the majority of people in underdeveloped countries rely on firewood. Given the country's unstable economy and poverty, the situation is unlikely to alter soon. from the existing literature, cooking stove modeling has not yet progressed to the point where it can be utilized as a tool for stove design.

Inefficient burning of these biomass fuels affects the end-users by exposing them to death,(i.e. each year, close to 4 million people die from inhaling smoke while cooking using polluting stoves paired with solid fuels and kerosene (World Health Organization (WHO, 2018)). In addition to this, the improper gathering of biomass fuels damages the local environment, collecting and buying of biomass fuels reduces the productivity and development of the community, and burning of biomass fuels increases greenhouse gases (GHG) by releasing contaminating gases. Since the use of biomass as fuel will continue, improving the way of using it is the only solution to improve the lifestyle of end-users by upgrading the performance of the stove and minimizing the emission, health problems, indoor air pollution, and death. Besides, there is a wide range of problems that comes from the world’s population. Therefore, in the present work effort has been made to upgrade the performance of the two-pot biomass cookstove by improving the construction material and minimizing the heat loss through the body of the stove. According to the most recent pieces of literature, biomass cooking stoves were produced utilizing clay soil and concrete walls as insulating materials. therefore, more research is needed to develop insulation materials for biomass cookstove production. For this reason, there is a need for research towards the design and development of improved biomass cook stoves with better efficiency, less heat loss, less fuel consumption, and less emissions, and the stated problems can be minimized by implementing the newly designed cooking system.

1.6 Objective of the Study

The general and the specific objectives of the research are followed below.

1.6.1 General Objective

The general objective of this research is to design, construct and evaluate the performance of natural draft double-pot biomass cook stove using *Aircrete* insulated wall by using CFD and experimental techniques.

1.6.2 Specific Objectives

The specific objectives are:

- Designing a double-pot biomass cookstove with a modified geometry.
- Evaluating the effect of height of the combustion chamber on the performance of a double-pot biomass stove using computational fluid dynamics simulation.
- Develop the prototype of the natural draft double-pot cookstove from locally available materials and conduct an experimental test.
- Validate the numerical results with experimental results.

1.6.3 Significance Of the Study

This work is basically significant for people who live in rural areas that use traditional solid biomass cookstoves. The benefit of implementing and distributing the stove can be categorized into two. The first one is internal importunacy for the users and the other one is external benefits. The internal benefit for a household is in terms of minimizing the production of gases that are hazardous to the lives of women and children, reduced fuel consumption, and cooking time. The external benefit includes less pressure on forest and energy resources and reducing greenhouse gases. Where wood is being harvested faster than it is being grown, the use of more efficient stoves can reduce demand for wood to sustainable levels. Generally, the present stove is expected to improve the lifestyle of the end-users by improving the performance of the stove. Implementing the newly introduced stove can reduce the health problems of women and children caused by indoor air pollution.

1.7 Scope and Limitation

The scope of this research is to design, analyze, and validate numerical versus experimental results of double-pot biomass cookstoves. The prototype of the model of the present stove was developed.

Material selection of stove components is undertaken. The thermal efficiency, specific fuel consumption, and emissions of the stove during the experiment were measured and recorded in order to compare and develop confidence about the developed model. Using pure insulation is the limitation of the work because there is no completely insulated material for this purpose and materials with low thermal conductivities are very expensive and are not easily available. In addition to that, making the stove a multi-branch at once did not investigate.

1.8 Organization of the Study

This thesis is composed of 7-chapters. After the first chapter introduces about the background of the study, biomass cookstove, and its classification, a literature review was presented in chapter two with its summary and gap. The third chapter presents the material and methodology section of the work followed by chapter four which presents the theoretical formulation and analysis with numerical simulation of the cooking system. The fifth chapter describes the conceptual design working principle, construction process, and the experimental setup of the cookstove prototype, Chapter six presents the major finding and results of a numerical and experimental analysis with their implication. The last chapter includes the conclusion of the whole work and recommendations for further study.

CHAPTER TWO

2. LITERATURE REVIEW

2.1 Introduction

Many studies and researches have been done on biomass cookstoves to improve the efficiency and performance of such stoves. One of the innovative ideas in the design of biomass cookstoves is achieved by introducing improved biomass cookstoves (ICS) which empowered the lives of end-users for the last thirty and more years. The design modification is intended to make those cookstoves as efficient as possible by optimizing the geometry and minimizing the heat loss during the combustion process. The complex geometry and characteristics of the combustion process in biomass cookstoves are the major challenge in studying and predicting the performance of those systems (Husain *et al*., 2019).

In this section, previous works associated with the development of biomass cookstoves, different types of biomass cookstoves such as traditional, improved, and advanced biomass cookstoves were presented. Different factors which affect the performance of cookstoves and different types of solid fuels were presented in detail. Stove designing principle and stove construction material and utilization of biomass energy and environmental effect were also discussed. Finally, CFD-based studies on improved biomass cookstoves are presented and the chapter is closed with a respective summary and literature gap.

2.2 Development of Biomass Cookstoves

Based on their state of art biomass cookstoves can be broadly categorized as, traditional (open fire), improved, and advanced type.

2.2.1 Traditional (Open Fire) Biomass Cookstoves

Based on the performance of cookstoves the most inefficient (three stone) cookstoves are categorized under traditional type and the emissions and energy lost in those types of cookstoves are quite high which is due to unshielded fire way of burning of fuel wood as shown in Figure 2.1. The thermal efficiency of traditional biomass cookstoves is very low. The converting capacity of chemical energy in the fuel into the necessary heat for cooking or heating is inefficient (Foley and Moss, 1983; Memon *et al.,* 2020). Moreover, such traditional stoves result from deaths to human beings due to harmful emissions and it contributes to global warming to the environment.

Figure 2.1 Traditional (open fire) biomass cookstoves (Fekadu *et al*., 2019)

2.2.2 Improved Biomass Cookstoves

Improved biomass cookstoves (ICS) are the modified version of traditional biomass cookstoves that are designed to run on the same fuel such that animal dung, wood, and crop wastes with better efficiency and cleaner operation (Garcia, 2010). The objective of ICS is to get better cooking efficiency, less emission (producing cleaner gas), and less cooking time than is feasible with traditional cookstoves. Figure 2-2 shows the diagram of simple ICS.

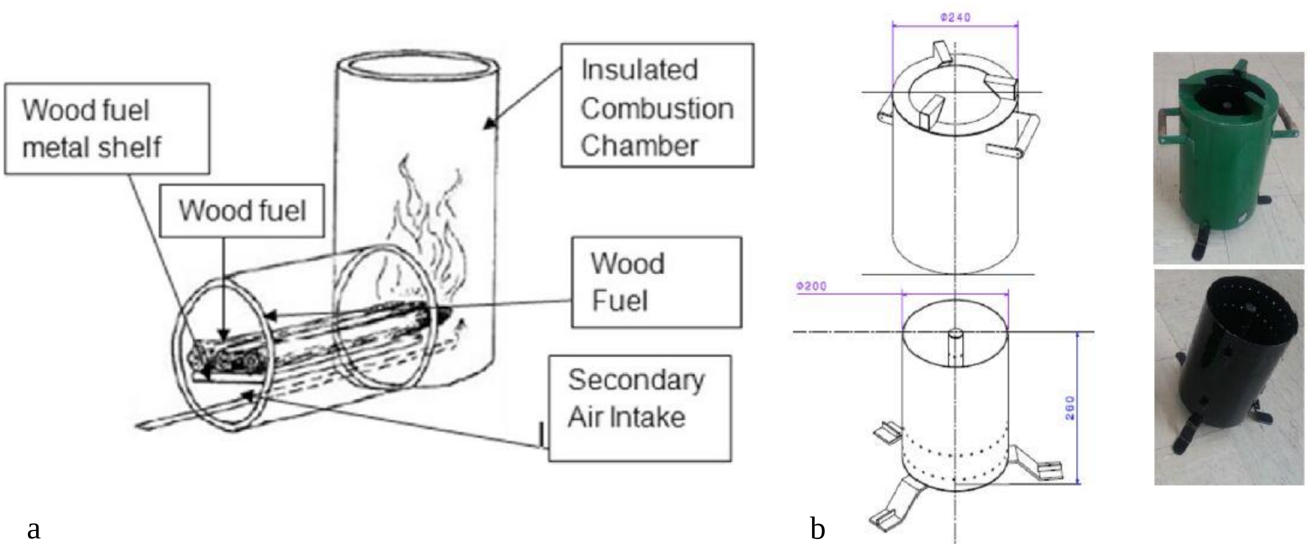

Figure 2.2 Schematic diagram of simple ICS (a) (Agenbroad *et al*., 2011) (b) (Adem and Ambie, 2017)

In addition to that ICS are led to reducing consumption of feedstock's (Kumar *et al.*, 2013; Mehetre *et al.*, 2017; Urmee and Gyamfi, 2014). The aim of increasing thermal efficiency is achieved by shielding the fire to restrict the flow of fire on different and unwanted surfaces. Figure 2.3 indicates the actual improved biomass cooking utilities for household-level cooking.

Figure 2.3 Improved biomass cookstove (Amare *et al*., 2015)

Mamuye *et al*. (2018) work on a comparison of emissions and fuel use performance of two stoves. The main objectives of this study were assessing the emissions of CO, $CO_{2,}$ and fine particulate matter ($PM_{2.5}$) of improved *Merchaye* and *Lakech* charcoal stoves in comparison with traditional metal stoves, specific fuel consumption (SFC) of the two ICS; and the factors that affect cookstove adoption. The results showed that the *Merchaye* stove reduced emission of CO, $CO_{2,}$ and $PM_{2.5}$ by 28, 22, and 27 % respectively in comparison to a traditional charcoal stove. Whereas, the *Lakech* stove reduced emission of CO, $CO_{2,}$ and $PM_{2.5}$ by 15, 8, and 13 %, respectively.

Okafor and Unachukwu (2012) investigated experimentally the thermal efficiency, cooking time, and fuel consumption of nozzle type improved wood cook stove fabricated with mild steel sheet thickness of 2 mm and made of double walls separated by 20 mm thickness glass wool insulator and measure the evaluations by using water boiling test by performance measuring method with 5 kg of fuelwood were used to boil 2.5 L of water in the two 28 cm diameter pots. Six pieces of fuelwood of about 20mm diameter were added to the developed combustion chamber. tests showed with 0.30kg of fuel wood to boil 2.5 litter water 29 min, with 0.28 kg of fuel wood burning rate 0.40, specific fuel consumption 0.85 and 34 % of thermal efficiency. From the result, it was obtained that the possibility of maximizing thermal efficiency of biomass gasifier stove can be achieved by differing the shape.

i. Natural Draft Versus Forced Draft Cookstoves

Previously, both traditional and improved household cookstoves were designed and developed free convection-driven called 'natural draft'. Because of its low cost and ease of manufacturing, the most recent improved cookstoves are also natural drafts. However, most future promising improved cookstoves are forced to draft or uses a fan to increase the combustion efficiency by creating high-velocity air jets that mix the fuel and air. Cookstoves with fans not only reduce emissions through improved combustion but also improve heat transfer to the cooking vessel. Figure 2.4 indicates natural and forced types of cookstoves respectively from left to right.

Figure 2.4 Natural and forced draft improved biomass cookstoves (Kar *et al*., 2012)

ii. Chimney Stoves Versus Stoves Without Chimney

The chimney is a tube that is able to release emissions and smoke from the cookstove away from the users. Some of the improved biomass cookstoves are developed with smoke-released chimneys. Attaching chimneys to biomass cookstoves ensures the entire stove has a rapid air movement through the chamber, leading to better combustion and less indoor air pollution. However, cookstoves with chimneys are more expensive due to the presence of the chimneys. Almost all traditional cookstoves have been built without a chimney, this makes them comparatively inefficient.

2.3 Factors Affecting the Performance of Biomass Cookstove

It is important to determine the effect of various operating and geometric parameters on the performance of the cookstove.

2.3.1 Insulation

Different kinds of literatures showed that insulation has a significant effect on the thermal efficiency of improved biomass cookstoves. Insulation of the cookstove is very important to increase the performance, as it reduces heat loss through the heated walls (Shebaz *et al*., 2020). With proper insulation of the cookstove, efficiency was found to be increased by 8% and consumption of fuel was found to be reduced by almost 5% (Sedighi and Salarian, 2017). Nevertheless, the thickness of the insulation also affects the efficiency of the stove. If the thickness of the insulation is out of range based on considerations, it may reduce the thermal efficiency (performance) of the stove (Memon *et al.*, 2020). The conductivity of material highly influences the selection of insulating material (Njoku *et al*., 2019). Glass wool, ceramic wool, fire brick, etc. are widely used as cookstoves' insulation. With the increase in the thickness of insulating material, efficiency increases since it reduces heat losses. But after a certain thickness of insulation, the decrease in the heat loss reduces and makes it economically non-beneficial to add more insulation thickness. The optimum thickness of insulation should be selected by the parametric study of the cookstove under consideration.

2.3.2 Chimney Height

An increase in chimney height enhances the combustion efficiency due to the higher draft (Ayub, 2018). The decrease in chimney height means the decrease in cookstove height, which is good from the economics point of view. Faisal *et al.* (2018) studied the effect of chimney high to get optimal chimneys height of double pots biomass stove. Optimal chimneys height needs to provide the best performance of the stove. An experimental study was done by varied the chimney heights. Water boiling test as the standard method was used to obtained stove performance for each chimney height variation. The results showed that the best performance stove was the one with a 1.65 cm chimney height.

Setiawan *et al.* (2018) present the results of numerical modeling of temperature distribution and flow pattern in a biomass cooking stove using CFD simulation. The biomass stove has been designed to suit the household cooking process. A chimney installed at the end of the stove releases the exhaust gas into the ambient air. During the tests, the height of the chimney was varied to find the highest temperatures at both pots. Results showed that the height of the chimney at the highest temperatures of the pots is 1.65 cm. This chimney height was validated by developing a model for computational fluid dynamics. Both experimental and simulations results show a good agreement and help in tune-fining the design of biomass cooking stove.

2.3.3 Excess Air Ratio

It is a parameter, which controls the availability of oxygen in the cookstove for the combustion process and temperature of flame (Pal *et al.,* 2016). Excess air ratio is defined in terms of the percentage of oxygen in the flue gases. With an increase in excess air ratio, the flame temperature decreases. It was found in the work that the maximum fuel burning rate but at those harmful gases will be quite high and efficiency will be low. The value of excess air ratio can be found for the optimum value of combustion efficiency (Jain and Sheth, 2019).

2.3.4 Inlet Area Ratio

Inlet area ratio is one of the parameters which affect the performance of cookstoves. As the air comes into the stove combustion chamber through the vents, it needs to be evacuated as well. This is done from the top of the stove beside the container (Kshirsagar and Kalamkar, 2016). For an efficient combustion process to happen, the value of the inlet area ratio is found to be more than 0.7.

2.3.5 Pot Gap Width

Optimizing the gap width of the pot is compulsory to improve the boiling effect and performance of a cookstove. The efficiency of biomass cookstoves increases with a decrease in pot gap width, (Obi *et al*., 2016). A very small pot gap width is not desirable, because it leads to blockage with soot deposition, which will decrease its efficiency (Kshirsagar and Kalamkar, 2016). The pot gap depends on the rate of fuel combustion. The minimum gap required for a burning rate greater than 2 kg h^{-1} is 15 mm (Obi *et al.,* 2016). If the pot gap is too large, flue gas will not make complete contact with the pot surface, and if it is too small, then the air supply becomes limited.

2.3.6 Turbulent Flow Creation

Swirling (formation of turbulent flow) air flow conditions can be created in a cookstove to increase combustion efficiency and gives a stable flame (Shebaz *et al*., 2020). Deng *et al*. (2015) suggested a gasifier stove with central holes for gasification gas and channels around them for swirling airflow. With this design, the thermal efficiency of the stove was observed to be increased by 10% and gasification efficiency by 2%.

2.3.7 Proper Grate

One of the performance factors in the design of cookstoves is the improved design of the grate. Implementation of a Proper grate can increase efficiency and reduces the number of pollutants (Shebaz *et al*., 2020). It was found that the mean efficiency of a traditional cookstove can be increased by 7% when it is equipped with a grate (Jawurek *et al.,* 1996).

2.3.8 Proper Use of Skirt

It is a metallic part that is placed circumferentially around the pot. It is used to guide the flame on the pot increasing heat transfer, decreasing fuel combustion, and hence efficiency (Shebaz *et al*., 2020). 25–30% improvement in fuel consumption and CO emission are observed when pot with skirts was used.

2.3.9 Material for Cookstove

The material used for manufacturing has a role to play in deciding the efficiency of the cookstove. The heat loss through the wall of the stove is influenced by the conductivity of the barrel material (Shebaz *et al*., 2020). In the same way, the heat absorbed and retained by the material is a type of loss of heat as well. These phenomena are heavily influenced by the selection of the material of the cookstove. The selection of material has an impact on the cost of the cookstove (Shebaz *et al*., 2020), which needs to be kept in mind while designing the cookstove.

Boafo *et al*. (2020) designed, developed, and tested three improved biomass cookstoves with different combustion chamber materials (aluminum, ceramic clay, and mild steel) under the Water Boiling Test (WBT) protocol. The stove's design specifications were carefully altered to prevent significant variations in performance. The result of energy efficiency, specific fuel consumption, and emission performance parameters of the three stoves indicated that the ceramic clay combustion chamber was able to achieve the set target of the work.

2.3.10 Advanced Biomass Stoves

Advanced biomass stoves (ABS) are recently developed, factory-manufactured cookstoves based on modern technology and product development research. The standards include higher efficiency, lower emissions, better safety, and enhanced durability (Juriso J., 2018). These next-generation cookstoves commonly have advanced features such as induced or forced airflow for cleaner burning. ABS enable factory-based production, undergoes thorough quality testing, and hence increases the possibility of accurate reproduction of the design in all the stoves. Although the current ABS show significant emissions reductions over traditional stoves, liquefied petroleum gas-like emission levels are still there. To increase the combustion and heat transfer efficiencies of cookstoves through different mechanisms, few components need to be modified. (Kshirsagar and Kalamkar, 2014). Different literates have studied advanced cookstoves to improve these performances of such stoves.

Panwar and Rathore (2008**)** have addressed the design and performance evaluation of a 5-kW producer gas stove. it works in natural draft mode. Babul wood (*Prosopis juliflora*) was selected as feedstock for testing of wood gas stoves. The fire hole of the stove was filled with dried fuel wood to within 5 cm of the top. the amount of CO_2 and CO emission inside the kitchen has been reduced, which was measured at a distance of 1 m from wood gas stoves with the help of gas analyzers. It was found in the range of 18–2 and 1–3 ppm, respectively. The outside temperature of the stove during testing was recorded as 105.1 degree Celsius., As result showed the thermal efficiency of the stove was recorded at about 26.5%.

Chica and Perez (2019) have developed a model of solid biomass gasifier stove and development and performance evaluation of an improved biomass cookstove for isolated communities from developing countries. The objectives of the work were the elimination of smoke and harmful emissions from the indoor air (kitchen), versatility that allows cooking several meals at once, thermal efficiency target of 20%, safe external wall temperatures, and simple, fast and safe biomass ignition. Energy characterization was conducted by means of the Water Boiling Test (WBT) and can be fed with different types of biomasses. Thermal efficiency, specific fuel consumption, specific energy consumption, and time to boil were calculated and evaluated by the WBT and found to be 20.91 %, 115.86 g/L, 2061.55 kJ/L, 31.6 min, respectively.

2.4 Biomass Fuels

Fuel choice is strongly influenced by the accessibility, affordability, and convenience of the fuel, as well as dependent on the economic and technical options of a household and the respective social and cultural determination.

2.4.1 Solid Biomass

Solid biomass is a combustible renewable organic energy resource that comes from plants or their derivatives and animal manure (McKendry, 2002). The most leading world energy resource especially for heating and cooking applications contributed from wood biomass fuel (Jana & Bhattacharya, 2017; Sinha *et al*., 1994).

Table 1 Comparison of different biomass fuels (Shebaz *et al*.,2020)

Fuel	**PM (g Kg^{-1})**	**CV (MJ Kg^{-1})**	***η* %**
Crop strew	5.6	16	16
Fire wood log	1.8	18	18
Wood branches	2.6	17	14
Anthracite chunk	1.1	21	14
Bituminous chunk	12	28	14
Anthracite briquette	0.59	21	32
Bituminous briquette	71	28	32
Crop strew pellet	2.1	14	37
Wood pellet	0.85	16	29
Natural gas	0.16	51	57
LPG	0.27	49	44

Jasper *et al*. (2021) assessed the performance of a cooking stove improved with sawdust as an insulation material. An insulated fire stove prototype of 26 cm saucepan diameter was designed, constructed, and cast with sawdust and clay as the first layer and sawdust alone as the second layer. The developed stove was tested using a water boiling test to establish its operating performance. The thermal efficiency of the stove was assessed using indigenous wood fuels used in rural Uganda (*Senna spectabilis*, *Pinus caribaea*, and *Eucalyptus grandis*). Computational fluid dynamics was used to simulate the temperature and velocity fields within the combustion chamber and for generating temperature contours of the stove. Obtained results indicated that *S. spectabilis* had the highest thermal efficiency of 35.5 ± 2.5%, followed by *E. grandis* (25.7 ± 1.7%) and lastly *P. caribaea* (19.0 ± 1.2%) in the cold start phase when compared with traditional stoves.

Kausley *et al*. (2010) was presents a detailed theoretical study of solid fuel combustion in a domestic stove and the different steady-state as well as unsteady state combustion models have been formulated, which include the description of all the chemical and physical processes taking place during the solid fuel combustion inside the stove. The result showed that the steady-state models involve the calculation of effective maximum flame temperature, suction of combustion air created by hot flue gases inside the stove, and the propagation of ignition front inside the stove. The model shows good agreement with the experimental results.

2.4.2 Sources and Potentials of Solid Biomass Feedstocks

Carbon content organic fuels that are found in plants and animals can be a raw material for a biomass cookstove. The feedstocks for biomass cookstoves from different sources are shown in Figure 2.5. The most widely used and freely collected solid biomass fuel especially in rural areas is wood (Jana and Bhattacharya, 2017).

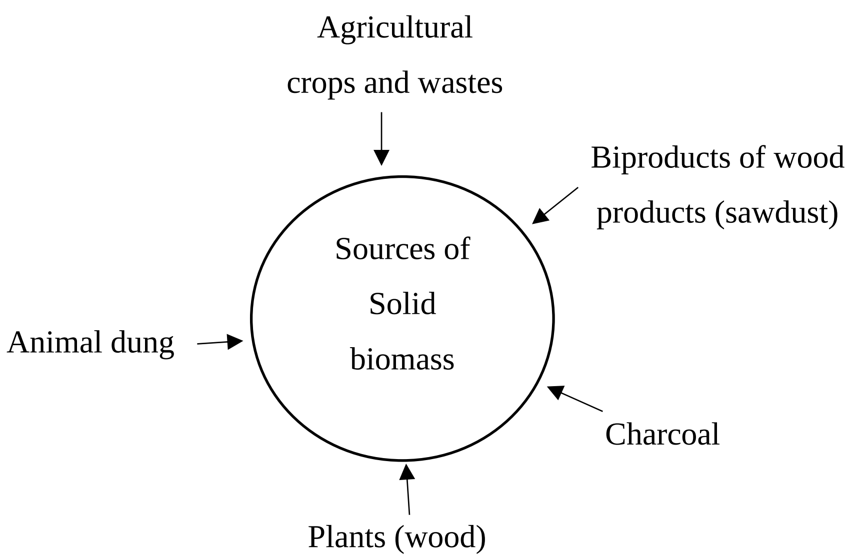

Figure 2.5 Biomass energy sources (Jana and Bhattacharya, 2017)

Wood fuel is the principal source of household energy in developing countries. In regions where wood fuel is scarce, crop residue and animal dung are important sources of cooking and heating applications (Jetter *et al.,* 2012).

2.5 Biomass cookstoves in Ethiopia

Ethiopia is a country that primary energy supply is highly dependent on solid biomass fuels and around 92 % of the population relies on biomass cookstoves. However, the adoption and the implementation of improved cookstoves are quite slow (Manaye *et al*.,2020).

2.6 Stove Construction Materials

Cookstoves can be prepared from various construction materials. Some of the stove manufacturing input materials are mud, clay, concrete, sheet metal, and the other modern stoves are built from hybrid materials.

- ✓ Mud stoves are stoves constructed from a material such as clay, sand, straw, grass, sawdust, or dung. Typically, the mixture consists of soil/clay and organic binding material, with dung for extra adhesion. Mud stoves are the cheapest type of stoves comparatively.
- ✓ Metallic stoves are stoves constructed from steel, sheet metal, or heavy metals like cast iron.
- ✓ Cement stoves are mainly ICS models constructed of cement. The “Mirt” stove, made from cement and pumice in Ethiopia since the early 1990s, has reported a life span of eight years with a fuel efficiency of up to 40% over the TSF (Beyene *et al.*, 2013).
- ✓ Hybrid stoves are modern prefabricated stoves that use more than one type of material like mud, cement, metals, or ceramics. Almost all modern charcoal stoves are the hybrid type where the combustion chamber is made of ceramic material and the outer body is metallic.

2.7 Cookstove Design Principles

Bryden *et al*. (2005) studied a proper design principle for constructing biomass cookstoves. Improved biomass cookstoves must take into consideration the geometrical design of the stove, proper material selection, energy used for specific preparation of food, and the safety of end-users. The latest ICS has to undertake the exhaust emissions form that must be undertaken so that the indoor air pollution possibly maintain and the life of the user won’t be at risk (Thompson *et al*., 2011). Sufficient air circulation needs for efficient combustion and the amount of heat produced from the desired fuel can be strong enough to burn the fuel. Improving the geometry of the stove can able to maintain the heat transferred to the pot. For this reason, the heat that reaches the pot must be under consideration during the design of ICS (Bantu *et al*., 2018).

2.8 Utilization of Biomass Energy and Environmental Impact

Most households in developing countries heavily depend on solid biomass fuel (tree) for this reason degradation of forests becomes exacerbate (Wassie and Adaramola, 2021; LaFave *et al*. 2021). Indoor air pollution from inefficient burning of biomass exposed around 4 million global deaths annually and contributes a countable saddle on climatic change (Downward *et al*., 2018).

Half of the populations of developing countries are relying on the burning of biomass efficiently and this brought indoor and environmental air pollution (Adem and Ambie, 2017).

2.9 CFD Based Studies on Biomass Cookstoves

Computational fluid dynamics (CFD) has become a powerful tool for pure and applied research applications, and it focuses on the investigations of systems involving fluid flow, heat and mass transfer, combustion, and other associated phenomena such as the study of chemical reactions through simulations. It can provide a more detailed analysis in less time and at a lower cost than a physical model alone but experimental validation of the CFD model is required (Pande *et al.*, 2019). Even though more than five hundred researches have been done on biomass cookstoves for the last thirty years, studies on numerical simulation modeling of them are fewer than thirty (MacCarty and Bryden, 2015),

Núñez *et al.* (2020) studied the CFD analysis of heat transfer, fluid flow, and gas-phase chemical reaction of natural-draft *plancha*-type biomass cookstoves under steady-state conditions. For CFD implementation, section no-slip condition was taken in all solid surfaces of the stove, the inlet gas was air at ambient temperature, the inlet gauge pressure was taken as equal to local ambient static pressure and convective heat transfer coefficient on the external part of the cookstove was taken as constant with a value of 5 W/m^2K. Finally, the thermal efficiency of the stove was found at 6.53% at 5 kW of firepower.

Parajuli *et al.* (2019) developed a model combining transient heat transfer, combustion chemistry, and fluid flow that can predict the performance parameters (i.e., efficiencies, excess air ratio, boiling time, etc.) of double-pot enclosed mud cookstoves. The study was conducted by dividing the stove into three parts such that zones 1, 2, and 3 which were for pot 1, pot 2, and the chimney, respectively. Conduction, convection, and radiation heat transfer were presented and from the results, the overall efficiency of the stove for input firepower of 5.1 kW was 17.1%, excess air ratio was 1.97, time to boil was 43 minutes while the temperature of the outer wall after 1 hour was 49°C.

Pande *et al.* (2019) worked on mathematical and experimental approaches for an elbow-type natural type biomass cookstove to study the effect of inlet air area and for the establishment of higher cookstove performance. The developed model for the analysis has been taken the assumption that the gap between pot 1 and pot 2 is negligible. The stove was developed by using ceramic wool as insulation material to reduce the heat escaping to the environment and tasted experimentally using Baboo wood as a fuel. The computational result from the assumption of steady-state operation condition, constant inlet area ratio, and two-dimensional analysis is 2.202 kW firepower, thermal efficiency from experimenting and modeling of the stove was and 35.197 % (with an error of 7.09 %) while the combustion efficiency was 98.39 % and 98.05 %, respectively with 0.35 % of error.

Kshirsagar and Kalamkar (2015) investigated a new operational parameter called “inlet area ratio” and its influence on direct combustion of rocket cookstove performance with shielded combustion and unshielded pot. The heat reaching to the bottom of the pot was calculated by neglecting heat loss and the convective heat transfer inside of the stove was also calculated by taking the flow in laminar flow. The model results showed that the higher combustion efficiency is attempted at the inlet area is between 0.9 to 0.7. The model predicted values for the given input data, in the range of 20.2 to 28.7%, which was within the plausible range of thermal efficiency for a natural draft, insulated; rocket-type biomass cookstoves with unshielded pot and 3.69 kW firepower has only 92.8% combustion efficiency.

Ali and Wei (2017) studied combustion and heat transfer analysis of biomass cookstoves using ANSYS Fluent Simulation to reduce indoor air pollution. The model has been designed to improve the combustion efficiency of the stove and reduce indoor air pollution. The developed stove was a modified one-pot L-shaped rocket type shielded with a 3 mm cast-iron plate. The results showed that the cooking time and fuel cost were reduced by 50% and hazardous emissions by 80%. Generally, the CFD analysis results suggested that the improved cookstove resulted in improved combustion and heat transfer. Finally, the authors concluded that the reduction in the size of the combustion chamber and introducing a secondary air in the combustion process of the cookstove was able to improve the heat transfer rate of the cookstove and reduce the emissions from the stove.

Ayantu (2016) has been done on the optimization of the design of *tikikil* stove and carried out an experimental evaluation of *tikikil* stove and the modified design model of *tikikil* stove which use a CFD study aid to predict the better design model depends on the performance of each stove model. In comparison to the CFD design stove, the CFD design stove performed with 50% more efficient than *Ugastove* which accounted for 31.1% efficiency.

Pande *et al.* (2019) worked on the mathematical model and experimental test of two-pot biomass cookstoves. The study overcame the difficulty of developing and designing two-pot biomass cookstoves mathematically to predict and evaluate the thermal performance of the stove using heat and mass transfer equations. The model presented the heat interaction between the body of the stove and the pots, different zonal combustion temperatures, thermal efficiency, and excess air ratio. In experimental testing, the mass of fuel required to boil water in pot 1 and the time is taken were taken while the metallic cast-iron stove was insulated with ceramic wool. From three sets of experiments, the average values showed that for firepower 2.72 kW, 35.77% thermal efficiency, 28.33 minutes to boil, and 9.93 g/MJ/d carbon monoxide emission were recorded.

Tabet (2016) has been studied the prediction of indoor air pollutants from downdraft single pot biomass cookstoves using experimental and CFD analysis. From the experimental result found at a minimum average concentration of oxygen, the concentration of CO leads high with the value between 1680 and 10240 mg/Nm3; during this time the dry flue gases were 4 and 10% vol. The result from the computational analysis also showed the CO emissions caused by the region where lacks oxygen at low temperatures.

Pande *et al.* (2019) presented the effect of variation inlet area ratio on the performance of multi-pot natural type draft biomass cookstoves. Data for boundary conditions were taken from the experiment. Insulating the external part of the stove with ceramic wool to reduce the heat loss, the experimental test was conducted. The Fluent software comprises the effect of combustion through a non-premixed combustion model. The results showed that the value of IAR was inversely proportional to the feeding rate. The analyzed CFD results indicated that the value of the IAR was 0.7 which is the same for any natural draft solid biomass cookstove.

Sagouong and Tchuen (2018) performed an approach to mathematical modeling of traditional stoves that are commonly used in rural areas. Heat transfer governing equations were considered and used for evaluating the nodal temperature and its effects. The authors concluded that amongst their studied stoves, the best heating device was that with an inverted and truncated cone and was the best for cooking since it reduced fuel consumption and therefore has a positive impact on deforestation.

Husain *et al.* (2019) carried out design modification of improved biomass one-pot cookstove to obtain uniform air-fuel distribution. In the experimental model, the transport of volatiles and air into the zone of the reaction of the developed biomass cook stove governed the turbulent convective mode of heat transfer. To attempt the mathematical model of the introduced model based on operation less than 2 m/s air inlet velocity i.e. equivalent to a speed of 4000 rpm. K (turbulent kinetic energy of the flow) and ε (turbulent energy dissipation rate) (k-ε) turbulence model used to determine the length. From CFD simulation results using an optimized IAR, the maximum temperature achieved was 1073 to 2073 K inside the cookstove. It was concluded that linear dependency of firepower and temperature is on air to fuel ratio and air velocity. The maximum output power and temperature values were obtained when the grate of the stove was placed at a height of 25 mm.

Pundle *et al.* (2019) presented a two-dimensional axisymmetric steady-state CFD model of a biomass burning natural draft rocket cookstove. The study solved the Reynolds-averaged conservation of mass, momentum, energy, and species transport. The inlet flow rates were chosen with a burn rate of 2.5 kW. At the outlet of the pot skirt, the boundary conditions were specified as atmospheric pressure. The water Boiling Testing (WBT) method and Douglas fir wood with 9.2% moisture content were used during the experiment. It was reported that entrainment of secondary air increases the turbulent mixing when used in conjunction with a central baffle but reduces the thermal efficiency of the stove by increasing the heat loss through the wall.

2.10 Literature Summary and Gap

In the literature review, the development trends of biomass cookstove starting from traditional to improved one and then advanced type of biomass cookstoves have been reviewed. Most of the kinds of literature associated with a traditional type of biomass cookstoves revealed that those types of cookstoves are inefficient, polluting, and unhealthy whereas the improved biomass cookstoves have better cooking efficiency, cleaner operation, and less cooking time. Advanced biomass cookstoves are recently developed, factory-manufactured cookstoves based on modern technology and product development research. Their standards include higher efficiency, lower emissions, better safety, and enhanced durability.

The study of different factors affecting the performance of biomass cookstoves also indicates that improving the insulation of cookstoves has a greater role in the improvement of overall efficiency and reduction in fuel consumption of cookstoves. Literature also showed that optimization of geometrical parameters affects the effective use of heat from the combustion chamber. In addition, most of the researches indicate that increasing the thermal efficiency, decreasing fuel consumption, reducing the time of cooking, decreasing the toxic gases that are emitted during using the cookstove are the main targeted objectives. One of the causes for the lower efficiency of cookstoves is caused by the inefficient use of heat from the combustion chamber due to the heat loss around the cookstoves.

In literature, efforts have been made to improve the performance of biomass cookstoves using different improvement means but little effort has been reported on improving the insulation material and finding new insulation material of cookstoves for reduced heat loss and thus, better efficiency. Even though cookstove developments are highly dependent on the geometry of the combustion chamber, predicting and analyzing a different model of cookstoves with different geometry to increase the thermal efficiency of double-pot cookstoves using ANSYS Fluent have not been investigated comprehensively and exhaustively by previous studies. Thus, upgrading the combustion efficiency by using new and better insulating material and improving the overall thermal efficiency of double-pot cookstoves by designing different models with different geometry using ANSYS Fluent software to select a better one is the main aim of the current study.

CHAPTER THREE

3. RESEARCH METHODOLOGY

3.1 Introduction

Under this section, the methodology and techniques to achieve the objectives of the study are presented in detail. Research design techniques, different data sources and collection methods, necessary materials, instruments that are used to collect data as well as data analysis method as an input for the design of double-pot wood biomass cooking stove are presented.

3.2 Data Sources and Collection Method

Both the primary and secondary data collection methods were used as input for the whole research.

i. **The primary data** such as ambient temperature, different zonal temperatures, the initial and final temperature of the boiling water, as well as water moisture contents and mass of the wood fuel were obtained by direct measurement.

ii. **Secondary data** are obtained from different sources on the internet such as books, documents from websites, works of literature local and international journal articles, and data from a deep literature review.

3.3 Methodology

This study uses theoretical approaches, numerical simulation, and experimental tests as the main methodology. Basically, the present study is investigated by studying the effect of insulations and varying the geometrical parameters of the combustion chamber in a cook-stove on the performance of biomass cook-stove. The theoretical approaches have been attempted using governing equations such as continuity, energy, and momentum equations to predict the performance of the stove whereas the numerical analysis of this study has been done using ANSYS fluent simulation. In the end, the numerical results are validated with the experimental and the latest previous works.

Both numerical and experimental approaches were used to study the performance of the present cookstove. The ANSYS fluent software is chosen for the geometrical and numerical analysis of this work. The reason to use such a computational model is to predict and analyze the actual cookstove which will save time and money for doing repeated experiments. Also, it helps to obtain the performance parameters in the combustion analysis of a cookstove. Conservation of mass, conservation of energy, conservation of momentum, and specious transport equation were utilized as basic equations in fluent to solve the flow variables of the combustion process in a cookstove.

3.4 Water boiling test

Water boiling test is one of the standard technical protocols for the determination of the performance of cooking stoves by measuring the output parameters at three different phases i.e., cold start phase at (high firepower), hot start phase at high firepower and simmer phase at low firepower (Quist *et al*., 2020; Tadesse *et al*, 2020). The reason for selecting this testing method is due to its simplicity, relatively short time of test, and approximately the same testing procedure as the actual cooking process. The evaluation of the performance of the cookstove was established from three sets of water boiling tests and each test has three different phases which are called, cold stare, hot start, and simmering phase. The first two phases are the cooking period and the last one is the low power phase which is keeping the temperature of the content of the pot for 45 minutes.

Set 1: cold start (High power); The test starts with the stove at room temperature and a pre-weighed bundle of wood being used to boil a specified amount of water in a standard pot.

Set 2: hot start (High power); To execute the second step of the test, the cooking water is replaced with a fresh pot of cold water. As a result, water is now boiled on a hot stove to determine the differences in performance between the hot and cold stages of the stove.

Set 3: simmering (Low power); A specific amount of water is boiled, and then the water is simmered for a specific amount of time at just below the boiling point, using a pre-weighed bundle of wood (45 minutes). Only the performance of the principal pot on a multi-pot stove will be evaluated during water simmering.

Temperatures of the water, the weight of fuel, and water were recorded for each of the three sets of the experiment. The thermal efficiency, firepower, mass flow rate, cooking time, specific fuel consumption, and exhaust emissions are all investigated based on the experimental data. The boiling point of water for Adama city at an altitude (elevation) of 1648 m was 94.506℃ during the assessment of thermal efficiency.

$$T_b = \left(100 - \frac{h}{300}\right) ℃ \tag{1}$$

where T_b is the local boiling point of water to account for the variations as a result of elevation.

3.5 Measuring Devices

During the experimental test, some laboratory equipment was used for measuring application. To calculate the thermal efficiency of the developed stove, some measurements have been taken using different lab equipment before, during, and after the experimental test. An *infralyt* smart gas analyzer was used for measuring O_2, CO, and CO_2, K-type thermocouple thermometer with a digital temperature indicator ranges from 0℃ – 1300℃, was used to measure the temperatures of ambient, surface and water sample, flame, and wall of the stove. Additionally, electronic balance with five-gram precision and 64 kg capacity were used to measure the weights for the experimental test. The accessories that are used during the water boiling test are:

- ✓ Stop watch
- ✓ Thermocouples
- ✓ Tap measure
- ✓ *Infralyt* smart gas analyzer
- ✓ Digital thermometer
- ✓ Weight balance

3.6 General Work Flow of the Research

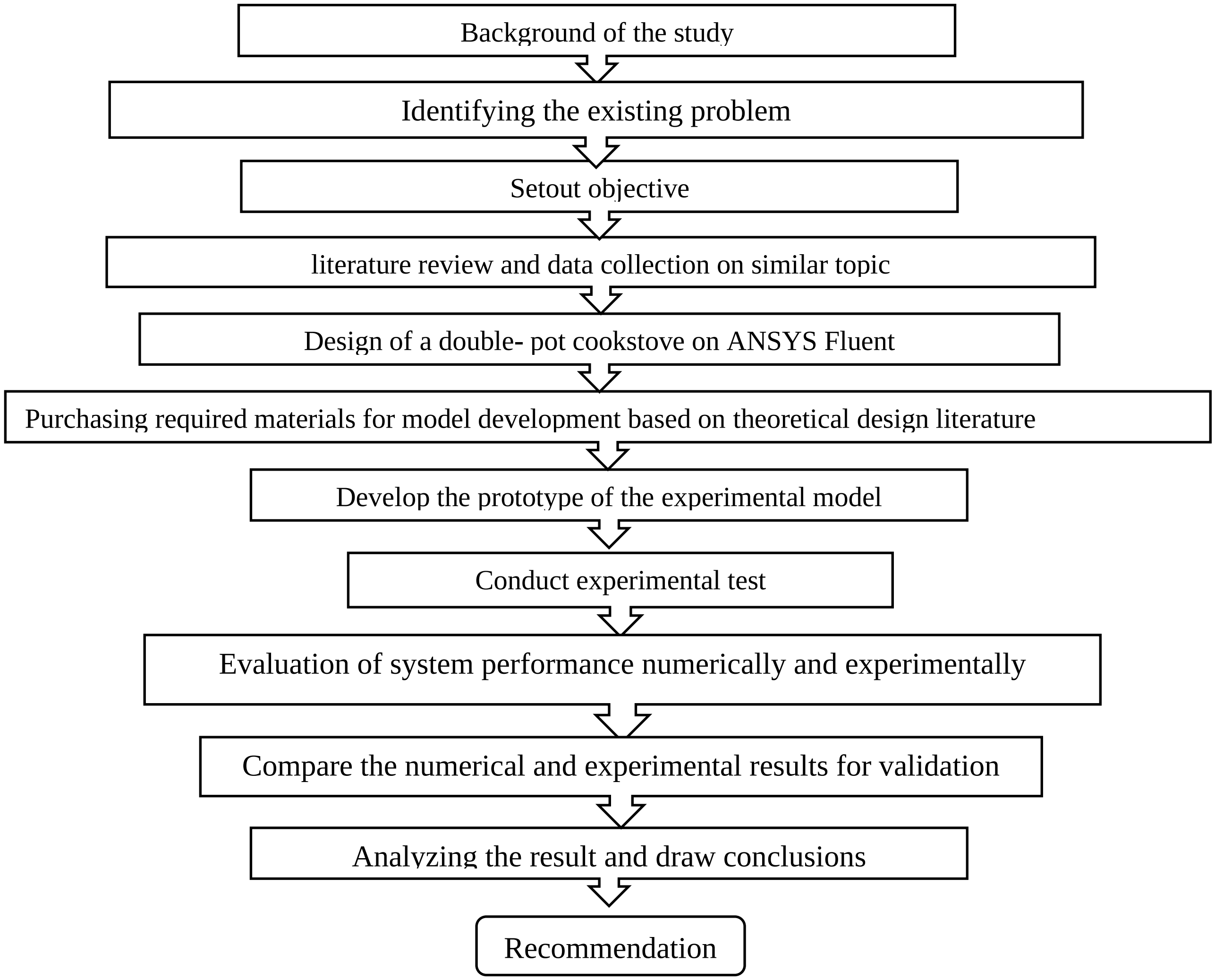

Figure 3.1 The general work flow of the research

CHAPTER FOUR

4. THEORETICAL AND NUMERICAL ANALYSIS OF DOUBLE-POT BIOMASS COOKSTOVE

4.1 Introduction

In this chapter, the thermal analysis, proximate analysis of the fuel, CFD analysis of the double-pot biomass cookstove, and performance parameters of the stove are presented in detail. The energy transfer in the body of the stove is driven by temperature differences between the body of the stove. Different zonal heat transfers and energy losses have been examined by the three modes of heat transfer equations. In general, this section will discuss the heat and energy transfer in the stove and the heat losses due to conduction, convection, and radiation that exist in a medium.

4.2 Model description

Figure 4.1 shows the schematic diagram of the present cooking stove used for the mathematical heat transfer model including five different zones. The first zone is called zone 1 (combustion chamber zone) which the combustion process is takes place. the next region is termed zone 2 which flue gas passes to come in contact with the pot 2 segment (zone 3). The energy transferred to the secondary pot section cooks the food in pot 2 and moved on to the last section (5) which is the chimney section passing through section 4 and lastly the emissions with released with low temperatures through the chimney. The reason to choose this kind of geometry is to utilize the energy lost from the combustion zone. In addition, the feeding zone on the combustion chamber is on the side of the stove that is for the safety of the end-users since most of the time the user cooks from the front side of the stove. The combustion zone plays an important role in the combustion process. So that, the grate is added as a bed of the fuel feed zone which can allow enough air to the combustion chamber. In general, the geometry of the present stove is not that complex; in such a manner that can be manufactured by any handicraft man.

4.3 Heat Transfer Analysis of Double-Pot Biomass Cookstove

Studying thermal analysis of fluid flow through biomass cookstoves is a more complex phenomenon; however, it is good to make some assumptions to reduce the complexity of solving with approximate accuracy. The energy analysis and the numerical prediction of the new model have been estimated by taking the following considerable assumptions into account.

- One-dimensional heat transfer
- Cookstove operates under steady-state condition
- The combustion products are considered fluid
- All stove zones are taken as a fixed and non-deformable control volume
- Pressure drop across a combustion chamber is negligible
- Flow within the stove is symmetric

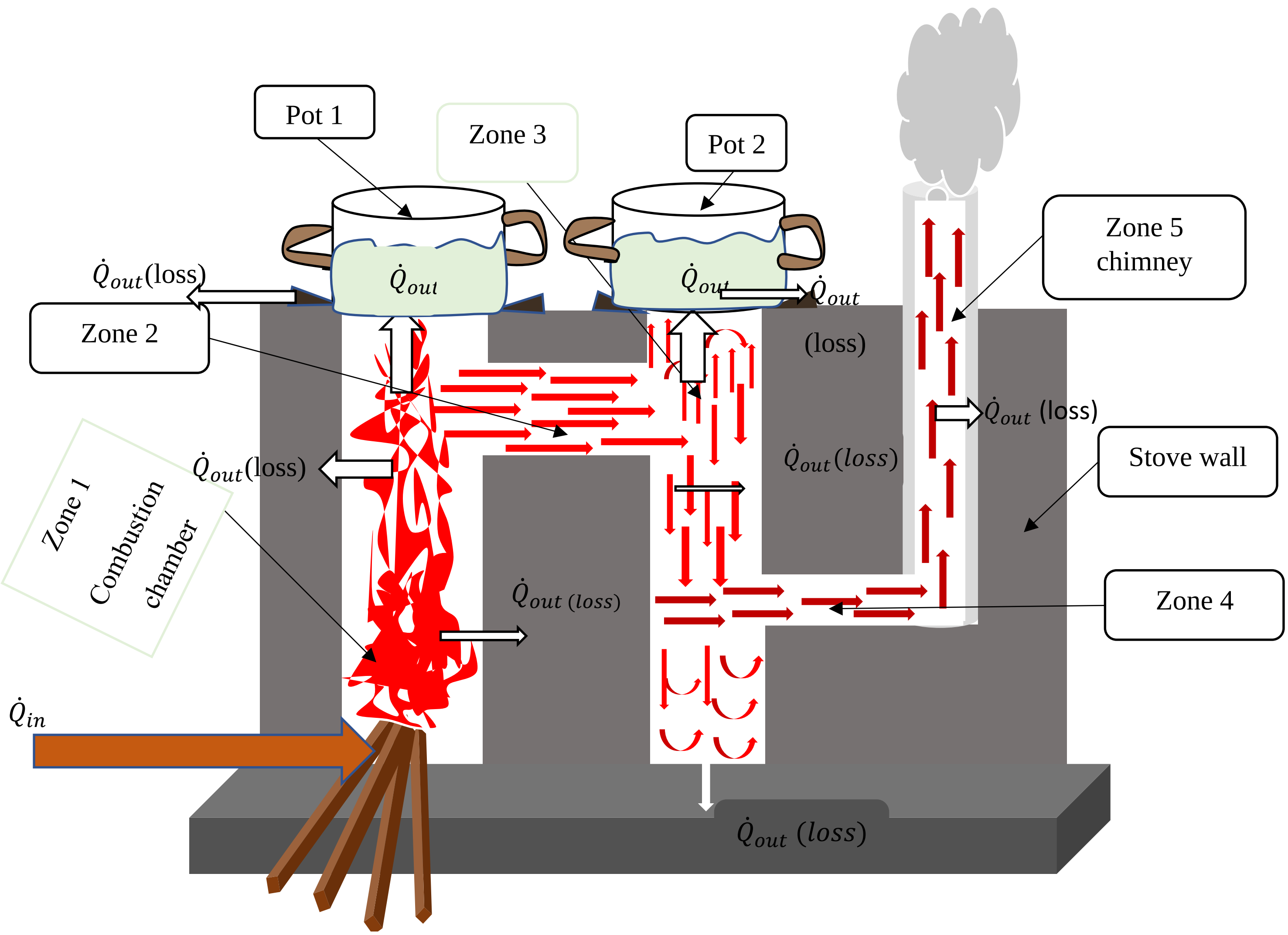

Figure 4.1 Overall energy transfer on the stove

The conduction heat transfer on the stove is occurred in between different walls of the stove. (Yusuf, 2011). Heat transfer by conduction of the cookstove is calculated by the Fourier law of conduction (Crump, 1981).

$$\dot{Q}_{cond} = -kA\frac{\Delta T}{\Delta X} \quad (2)$$

Where, $\dot{Q}_{cond}$ is a rate of heat transfer by conduction (J/s or W), *k* is a thermal conductivity of the materials, A is the area of the cross-sectional surface, ΔT is the temperature difference between the endpoints of the stove, ΔX is the distance between the two ends or length (Parajuli *et al*., 2019). The rate of heat transfer ($\dot{Q}$) depends on the thickness of the medium (insulation part), type of materials that are used as insulation, and temperature difference across the medium.

Convection mode of heat transfer is the type of heat transfer between a solid surface and a moving fluid. For the natural draft biomass cooking stoves, the type of heat transfer is free convection at which the driving force is higher temperature gases and the convection velocity is low compared with forced convection. This mode of heat transfer is done to or from; the wall of the stove to the surrounding, the bottom of a cooking pot to the entire fluid (food or water) in motion, and the sidewalls of the pan to the surrounding and the food. The heat that transfers through convective mode can be estimated as;

$$\dot{Q}_{conv} = \ h\ A\ \Delta T \quad (3)$$

where, $\dot{Q}_{conv}$ is the rate of heat transferred by convection (W), A is heat transfer area (m^2), h convective heat transfer coefficient ($W/(m^2$°C).

The convective heat transfer coefficient 'h' is determined by taking the following assumptions,

- ✓ The flow field of convective heat transfer is taken as horizontal plate
- ✓ The one-dimensional heated surface facing up the horizontal cylinder.

$$N_u = \frac{hL}{K} = 0.53(G_r * P_r)^{0.25} \quad (4)$$

$$h = \frac{k}{L} * N_u \quad (5)$$

$$G_r = \ \frac{L^3\rho^2 g\beta\left(T_{fl} - T_\infty\right)}{\mu^2} \quad (6)$$

and T_∞ is ambient temperature is Grashof's number and Pr is Prandtl number

$$T_f = \frac{T_{fl} + T_a}{2}\,°\mathrm{C} \quad (7)$$

$\beta = \frac{1}{T_f + 273\,K}$ where β is a constant and T_f is average of ambient and desired temperature;

$$P_r = \frac{\mu C_p}{K} \tag{8}$$

Radiation is the third mode of heat transfer occurred due to the fire and char radiation in the combustion chamber to the bottom of the pot, from the char bed to the stove wall, from the stove body to the pot, and the surrounding. By using Stefan-Boltzmann law, the rate of radiation heat transfer is given by;

$$\dot{Q}_{radi} = \varepsilon \sigma A s T^4 \tag{9}$$

where, $\dot{Q}_{radi}$ is heat transfer by radiation, ε is the emissivity which is dependent on the temperature (T) and the characteristic length (L_b) (Howell et al., 2010), σ is Stephen Boltzmann constant (i.e. 5.67×10^{-8} W/m^{2}K^4), A is an area of a combustion chamber and T is the absolute temperature (K).

$$\varepsilon = exp\{(0.848 + 9.02 \times 10^{-4} \times T) + (0.9589 + 4.8 \times 10^{-6} \times T) \times ln(0.2 \times L_b)\} \tag{10}$$

Where L_b is the characteristic length and is estimated by;

$$L_b = 3.6 \times \frac{volume}{Surface\ Area} \tag{11}$$

Where the constant 3.6 accounts for the geometry of the combustion chamber. Heat transfer by radiation depends on surface geometry (A_s), nature of fluid motion i.e., Reynolds number of the fluid flow, properties of the fluid (density, viscosity, specific heat (Cp), and fluid velocity (Núñez et al., 2020).

4.4 Heat Balance Equation

Correlations are established for different properties of air to design and study the analysis of two pot cookstoves at atmospheric pressure and 300 to 1500 K temperature range (Pande, Sharma, *et al.*, 2019).

$$\mu = 0.03501 \times T^{0.69} \times 10^{-6} \tag{12}$$

$$k = 8 \times 10^{-5} \times T^{1.0152} \tag{13}$$

$$\rho_g = \frac{359.7}{T^{1.003}} \tag{14}$$

$$v = 0.0009 \times T^{1.7097} \times 10^{-6} \quad (15)$$

$$h_s = 0.00032273 \times T^2 + 1.64833661388 \times T + 2021.531847 \quad (16)$$

$$C_p = 415.6 \times T^{0.1591} \quad (17)$$

$$R_e = \frac{\rho v L}{\mu} \; and \; P_r = \frac{\mu C_p}{k} \quad (18)$$

Due to the different losses that occur in the stove, the study of different heat transfer processes is very important and necessary to understand the mechanism of heat transfer in a cookstove (Husain *et al.*, 2019). In addition, increasing the flow velocity often leads to more turbulence that improves heat transfer efficiency (HTE) compared to laminar flow behavior however if the turbulence is beyond the extent limit that might reduce the thermal efficiency. The heat energy balance for the combustion chamber can be expressed as;

$$Q_{fl} = Q_{ac} - \left(Q_{cr} + Q_{fr} + Q_{loss} + Q_{H_2 loss} + Q_{moisture\ loss} + Q_d\right) \quad (19)$$

Where, $Q_{fl,}$ Q_{ac}, Q_{cr}, Q_{fr}, Q_{loss}, $Q_{H_2 loss}$, $Q_{moisture\ loss}$ and Q_d are heat gain by a flue in zone 1, supplied heat by the fuel combustion, heat transfer by radiation from char to the pot, heat transfer by radiation from a flame to the pot, loss through combustion wall, heat loss due to hydrogen in the fuel, moisture loss and loss through a door opening in the feeding zone respectively. Heat addition (Q_{ac}) is the amount of heat supplied from the fuel added to a combustion chamber.

i. Combustion Chamber (Zone 1)

The combustion chamber region of the stove is considered as the control volume of the system which is surrounded by the *Aircrete* wall. In a cookstove which is a natural draft type, the buoyancy force drives the airflow against the flow resistance. Where a force when a fluid exerts an upward direction against the weight of a partially or fully immersed item is a buoyant force. Besides, the airflow that enters the chamber determines the combustion and heat transfer efficiency and wood-burning rate of the stove. In this specific zone, mainly combustion of fuel is the main process that is taken place. Even though radiative heat transfers to the pot from char, the flame from the combustion of wood and different zonal heat losses through the wall of the stove and door opening are the conditions in this zone. By using the general stack equation natural draft mass flow rate can be calculated which is a methodology adopted by stoves and solar chimney researchers previously (Andersen, 2003).

In the combustion of solid biomass fuel, the heat might be lost due to several means from the heat source to the surrounding. In this process, the losses are:

- ✓ Char loss
- ✓ Lose due to door opening in the feeding zone
- ✓ Fuel moisture loss
- ✓ Hydrogen related moisture loss
- ✓ Stove wall loss
- ✓ Flame radiation loss

Flue gas is sensible heat that is exchanged by a body or thermodynamic system, which causes the body's or system's temperature to fluctuate as a result of the heat exchange. Using the first law of thermodynamics, for a system that is assumed to be isobaric, no mechanical work, constant kinetic and potential energy, and also assuming that the ideal gas behavior is considered, the heat addition can be investigated from correlation given by Agenbroad *et al.*, (2011);

$$Q_{fl} = m_{act} \times C_{p,fl} \times \left(T_{fl} - T_a\right) \quad (20)$$

In a cookstove which is a natural draft type, the buoyancy force drives the airflow against the flow resistance. By using the general stack equation (Andersen, 2003) natural draft mass flow rate can be expressed by:

$$\dot{m}_{act} = C_d * A * \rho_g * \sqrt{2 * g * H * \left(\frac{T_{fl}}{T_a} - 1\right)} \quad (21)$$

where; C_d is the coefficient of discharge which occurred by different means of losses on the cookstove due to viscous effects and the value is calculated by (Kshirsagar *et al.*, 2015). The calculated values of C_d is less than 1 and usually between 0.35 and 0.42 for different types of chimneys. For this study, the value of the coefficient of discharge is taken as 0.42. T_{fl} is the flame temperature inside the cookstove combustion chamber, and 950 K has taken the average temperature of the test.

$$C_d = \frac{\dot{m}_{act}}{\dot{m}_{th}} \quad (22)$$

$$\dot{m}_{the} = \rho_{fl} * A * \sqrt{2 * g * H * \left(\frac{T_{fl}}{T_a} - 1\right)} \quad (23)$$

and the density of flue gas is also given as;

$$\rho_{fla} = \frac{359.7}{{T_{fl}}^{1.003}} \quad (24)$$

$$\dot{m}_{act} = m_{fl} * \dot{m}_{fl} \quad (25)$$

$$m_{fl} = \left(m_a + 1 + \frac{M}{100 - M}\right) \quad (26)$$

The fuel mass flow rate can be obtained from firepower and net calorific values of fuel as shown in equation (27):

$$\dot{m}_{fl} = \frac{P}{NCV} \quad (27)$$

The firepower P of the process of cooking is equal with heat addition or the heat supplied by fuel in the combustion and implemented as Zube, (2010);

$$P = \dot{m}_{fl} * NCV = Q_{actual} = \dot{m}C_p\left(T_{fl} - T_a\right) \quad (28)$$

$\dot{m}_{fl}$ is fuel burn rate with the value of 0.3 kg/s (Kshirsagar and Kalamkar, 2015).

$$\dot{m}_{act} = C_d * A * \rho_{fl} * v_{th} \quad (29)$$

$$thoretical\ velocity\ (v_{th}) = \sqrt{2 * g * H * \left(\frac{T_{fl}}{T_a} - 1\right)} \quad (30)$$

The radiative mode of heat transfer from char and flame (Q_1&Q_2) to the bottom pot in the combustion zone of the cookstove can be evaluated as;

$$Q_{c-r} = \frac{\sigma \times A_{cross} \times \left({T_{ch}}^4 - {T_{p1}}^4\right)}{\frac{1 - \epsilon_{ch}}{\epsilon_{ch}} + \frac{2}{1 + F_{c-p}}} * \frac{1}{\dot{m}_{fl} * 1000} \quad (31)$$

$$Q_{f-r} = \sigma A_{cross}\left(\epsilon_{fl}{T_{fl}}^4 - \alpha_{fl}{T_{p1}}^4\right) * \frac{1}{\dot{m}_{fl} * 1000} \quad (32)$$

where, Q_{c-r} and, Q_{f-r} are char bed and flame radiation heat transfer, ϵ_{ch} & ϵ_g are the emissivity of char and flue gas, σ is Stephen Boltzmann constant 5.67×10^{-8} W/m^2K^4, A is the cross-sectional area of a combustion chamber and T_{ch}, T_{fl}, T_{p1} are the char, flue gas, and pot surface temperatures respectively. From (Shah and Date, 2011) expressions emissivity and absorptivity of the zonal wall of the stove can be found as;

$$\varepsilon_{fl}(T, L_b) = exp\{(0.848 + 9.02 \times 10^{-4} \times T) + (0.9589 + 4.8 \times 10^{-6} \times T) \times ln(0.2 \times L_b)\} \quad (33)$$

where L_b is the characteristic length and estimated by and the characteristic length.

$$L_b = 3.6 \times \frac{volume\ (v)}{Surface\ Area\ (A)} \quad (34)$$

$$v = L * W * H\ and\ area\ A_{surface} = 2lh + 2lw + 2wh \quad (35)$$

The absorptivity of a flue gas α_g also given as

$$\alpha_{fl} = \varepsilon_{fl}\left(\frac{T_{fl}}{T_s}\right)^{0.5} \quad (36)$$

Based on Dittus–Boelter (Smith *et al.,* 2002) equation of radiative and convective heat transfer coefficients are the combustion chamber inside and outside convective heat transfer coefficients h_{ci1} calculated as;

$$h_{fl} = h_{c-i} = \frac{k_{fl}}{L_b} \times N_u \quad (37)$$

$$N_u = 0.023 \times R_{eLb1}{}^{08} \times P_r{}^{0.4} \quad (38)$$

By assuming that the outer wall of the cookstove is subjected to constant heat flux and the flow is fully developed on the duct;

$$h_2 = h_{c-o} = \frac{k}{H} * 0.59 * (G_{rH} * p_r)^{0.25} \quad (39)$$

Heat loss from the combustion chamber through a wall of the stove body is normally considered as a heat transfer through a plane wall; which is combined heat transfer conduction, convection, and radiation modes. The heat flow from the combustion chamber on the concrete wall of the stove is shown in 4.3.

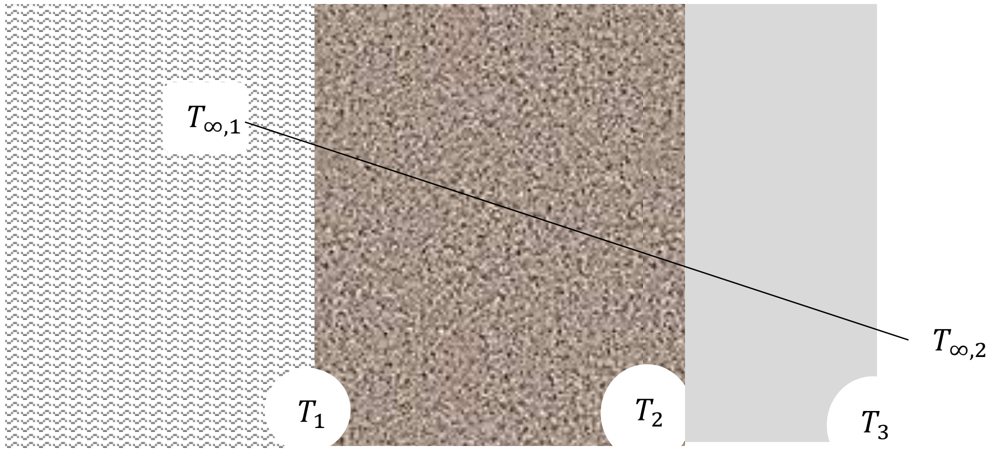

Figure 4.2 Heat transfer walls

For this case, there are three layers namely air, *Aircrete*, and galvanized sheet

$$Q_{loss} = \frac{T_{fl} - t_{\infty 2}}{\frac{1}{(h_{ci1} + h_{fl} + h_{chr})A} + \frac{L}{K_{ins}A} + \frac{1}{h_{co} + h_{ro1}}} \tag{40}$$

$$h_{ro1} = \sigma\epsilon_2({T_{wol}}^2 - {T_{amb}}^2)(T_{wol} + T_{amb}) \tag{41}$$

$$h_{rfl1} = \frac{\sigma(\epsilon_{fl}{T_{fl1}}^4 - \alpha_{fl}{T_{wi1}}^4)}{T_{fl1} - T_{wi1}} \tag{42}$$

Where ϵ_g and α_g are emissivity and absorptivity of the flue gas in the combustion zone and assuming the stove inner and pot outer surface treat as a black body and emissivity are 1.

$$h_{chr} = \frac{\sigma({T_{char}}^2 + {T_{wi1}}^2) \times (T_{char} + T_{wi1})}{\frac{1 - \epsilon_c}{\epsilon_c} + \frac{F_{c-w} + F_{c-p}}{F_{c-w}(F_{c-w} + 2 \times F_{c-p})}} \tag{43}$$

From the value obtained by Howell *et al.*, (2010) the shape, view, or configuration factor between the char bed and the fuel feeding door is taking as ($F_{c-d} = 0.2$) by approximating the region as rectangle to perpendicular circular segment.

The other factor that must be taken into account is the radiation shape factor. Based on *Smith et al.*, (2002) Shape factor can be defined as the fraction of energy that leaves one surface and strikes the other surface. Assuming the first zone to be cylindrical, and the radiation shape factor) between two parallel plates of a cylinder is implemented as;

$$F_{c-p} = \frac{1}{2B^2}\left(Y - \sqrt{Y^2 - 4B^2C^2}\right) \quad (44)$$

$$B = \frac{\sqrt{0.5}\, D_{pot\,1}}{2H_1} = 0.4949 \;\; and\; C = \frac{D_{pot\,1}}{2H_1} \quad (45)$$

$$Y = 1 + B^2 + C^2 \quad (46)$$

and the value of 'H' is 100 mm

$$F_{c-w} = 1 - F_{c-p} - F_{c-d} \quad (47)$$

The heat loss through the feeding opening is given as Q_d

$$Q_d = F_{c-d} \times \sigma \times A_{cross} \times ((T_{char})^4 - (T_{amb})^4) \quad (48)$$

The heat is lost due to sensible heating of hydrogen-related to moisture (KJ/kg of dry fuel and due to evaporation of fuel moisture (kJ/kg of dry fuel). sensible heat is the heat or energy that moves from one system to another which changes the temperature, not its phase. The heat lost through those two mechanisms was examined using equations M and W.

$$Q_{H_2\,moi} = (h_s - 2547) * 0.09 * H_2 \quad (49)$$

$$Q_{fuel_{moi}} = \{(h_s - 4.187) * (T_a - 273)\} * \left(\frac{M}{100 - M}\right) \quad (50)$$

The correlation of specific enthalpy for super-heated steam h_s given by

$$h_s = 0.00032273 * T^2 + 1.64833661388 * T + 2021.531847 \quad (51)$$

From Pande *et al.*, (2019) the heat loss from an inner wall of the combustion chamber (Q_{c-in}) heat loss from the inner wall to the outer wall (Q_{i-o}) = heat loss from the outer wall to the surrounding (Q_{o-s}).

Therefore,

$$Q_{c-in} = Q_{i-o} = Q_{o-s} = \frac{T_{fl1} - T_{wi1}}{\frac{1}{\left(h_{ci1} + h_{fr1} + h_{char}\right) \times A_{i1}}} = \frac{(T_{wi1} - T_{wo1})}{\frac{L}{kA}}$$
$$= \frac{(T_{wo1} - T_{amb})}{\frac{1}{(h_{co1} + h_{ro1})} \times A} \quad (52)$$

ii. Zone 2

Zone 2 is the region that the flue gas released from the combustion chamber pass by to the second pot section. The heat transfer to the bottom of pot 1 can be calculated by taking the assumption that no heat loss has occurred in the region.

$$Q_{pot\ 1} = (h_{conv\ 2} + h_{rad\ 2}) \times A_{pot\ 1} \times \left(\frac{T_{fla} + T_{flu\ 1}}{2} - T_{p1}\right) \tag{53}$$

$$h_{rad2} = \varepsilon_2 \times \sigma \left(\frac{T_{fla\ 1} + T_{flu\ 1}}{2} + T_{wi\ 1}\right)\left(\left(\frac{T_{fla1} + T_{flu\ 1}}{2}\right)^2 + {T_{wi1}}^2\right) \tag{54}$$

From (Kshirsagar & Kalamkar, 2015) correlation the convection heat transfer coefficient for the bottom wall of the pot calculated using equation 55.

$$hp_{conv2} = \left(\frac{k_{bottom}}{D_3} \times 0.726 \times {R_{e\ D2}}^{0.53} \left(\frac{W_i}{D_2}\right)^{-0.191}\right) \tag{55}$$

$$Nu_{pbottom} = 0.726 \times {R_{e\ D2}}^{0.53} \left(\frac{W_i}{D_2}\right)^{-0.191} \tag{56}$$

iii. Zone 3

Zone three is the secondary pot section of the stove. under this combustion of fuel does not take place and the section uses only the energy that propagates from the primary zone and is accumulated for an additional cooking application.

$$Q_{f-i} = \frac{T_{flu\ 2} - T_{wi\ 3}}{\frac{1}{(h_{ci3} + h_{flu\ 2})A}} = Q_{i-o} = \frac{T_{wi\ 3} - T_{wo3}}{\frac{L}{kA}} = Q_{o-a} = \frac{T_{wo\ 3} - T_a}{\frac{1}{(h_{co\ 3} + h_{ro\ 3})A}} \tag{57}$$

$$Q_{pot2} = (h_{conv\ 3} + h_{rad\ 3}) \times A_{pg\ 2} \times \left(\frac{T_{flu\ 2} + T_e}{2} - T_{p2}\right) \tag{58}$$

$$h_{conv\ 3} = \frac{k_{bottom}}{D_{p2}} \times 0.726 \times {R_{e\ D2}}^{0.53} \left(\frac{W_i}{D_{p2}}\right)^{-0.191} \tag{59}$$

$$h_{rad\ 3} = \sigma \times \epsilon_3 \left(\frac{(T_{flu2} + T_e)}{2} + T_{wi\ 3}\right)\left[\left(\frac{T_{flu} + T_e}{2}\right)^2 + {T_{wi\ 3}}^2\right] \tag{60}$$

The change in enthalpy of the flue gas that leaves zone three

$$Q_{entalphy,2} = h_{conv\ 2} \times A \times \left(\frac{T_{flu\ 2} + T_e}{2} - T_{p\ 2}\right) \tag{61}$$

iv. Zone 4

The heat transfer analysis in the gap between pot 2 and the upper surface of the stove can be calculated using equation 62.

$$Q_{pg} = h_{pg2}A_{pg} \times \left(\frac{T_{flu\,2} + T_e}{2} - T_{p\,2}\right) + \sigma \times A_{pg} \times \left(\varepsilon_8 \left(\frac{T_{flu\,2} + T_e}{2}\right)^4 - \alpha_8 (T_p)^4\right) \tag{62}$$

The heat transfer coefficient of the pot gap is also evaluated as

$$h_{pg2} = \frac{k_{pg2}}{D_{p2}} \times 0.726 \times Re_{Dp2}{}^{0.53} \times \left(\frac{W_i}{D}\right)^{-0.191} \tag{63}$$

v. Zone 5

The heat transfer analysis on pot two sides was calculated using equations 64 and 65. The convective and radiative heat transfer flue gas coming out through zone 3 increases the heat that transfers to the content inside the pot or the food that is going to cook.

$$Q_{conv\,side\,2} = h_{side\,2} \times A_{side\,2} \times \left(\frac{T_{flu\,2} + T_o}{2} - T_{p\,2}\right) \tag{64}$$

$$Q_{rad\,side\,2} = \sigma \times A_{side\,2} + \left\{\varepsilon_4 \left(\frac{T_{flu\,2} + T_o}{2}\right)^4 - \alpha_4 \times T_{p\,2}{}^4\right\} \tag{65}$$

$$h_{side\,2} = \frac{k_{side\,2}}{D_2} \times 0.726 \times R_{e\,D2}{}^{0.53} \left(\frac{W_i}{D_2}\right)^{-0.191} \tag{66}$$

On the other hand, the loss of convective and radiative heat from the sides of the pot to the surroundings is also considered in this zone. By assuming the combined convective and radiative heat transfer coefficient is 10 W/m^2K, the heat lost to the surrounding evaluated using equation 67.

$$Q_{conv\,side\,loss} = 10 \times A_{side\,2} \times \left(\frac{T_{flu\,2} + T_o}{2} - T_a\right) \tag{67}$$

$$h_{side\,2} = \frac{k_{side\,2}}{h} \times 0.664 \times (Re_2)^{0.5} \times Pr^{0.333} \tag{68}$$

4.5 Proximate Analysis of the Fuel

It is a process of determination of the characteristics of the biomass feedstock. Under this section moisture content, volatile matter, ash content, and the amount of volatile was discussed and determined.

4.5.1 Moisture Content

A proximate analysis starts from determining the amount of moisture found in a sample of feedstock. Determining the moisture content of the fuel is necessary since the moisture content of the fuel has a direct effect on the process of combustion by lowering the CV (calorific value) of the fuel therefore a high percentage of the moisture is undesirable. By taking a sample of a pre-weighed eucalyptus wood log feedstock, the moisture content of the fuel was determined using the formula given by;

$$[m] = \frac{M_i - M_e}{M_e} * 100\% \quad (69)$$

Where m is the mass of moisture in the sample fuel on a dry basis in percent, M_i is the initial mass of the fuel sample which is placed in an oven where a temperature of 105℃ is maintained and M_e is the final mass of the fuel founds after drying the sample.

4.5.2 Volatile Matter

The determination of volatile matter for biomass fuel can be investigated by using equation 69. It is a component of fuel that can burn in the presence of oxygen are known as volatile substances (Muthu and Anand, 2019). Volatile matters are formed by the thermal degradation of biomass fuel when the fuel is exposed to heat (Caillat and Vakkilainen, 2013). The volatile matter content in almost all types of biomass fuel is the function of carbon to hydrogen ratio is high and commonly about 70%-80% of the weight of the dry biomass (Li *et al*., 2001; Volborth, 1979).

$$[v] = \frac{V_i - V_e}{V_e} \times 100\% \quad (70)$$

The amount of volatile matter is determined by heating a dried ground sample of biomass with an initial mass of V_i in a closed crucible in an oven with a temperature of 600°C for seven minutes followed by heating the sample in an oven with a temperature of 900°C for another seven minutes. The amount of volatile matter [v] in percent, in the biomass, is equal to the loss in the weight and is calculated as (Miller, 2013; Volborth, 1979).

4.5.3 Ash Content

Determination of ash content is the way of calculating the non-combustible and useless matter in the fuel that reduces the calorific value (CV) of the feedstock. If the fuel has a high amount of ash content; it affects the heat flow by lowering the temperature of the flue gas due to the formation of clinker. Ash content in the fuel is determined using equation 71.

$$\% \, ash = \left[\frac{weight\ of\ ash}{weight\ of\ wood\ sample}\right] \times 100 \tag{71}$$

4.5.4 Fixed Carbon

The final step is a determination of fixed carbon content [c] by mass balance equation. Fixed carbon is the amount of carbon in the fuel that is going to burn. It is possible to determine the amount of fixed carbon difference of 100 and the sum of moisture content [m], the amount of ash [a], and the number of volatiles [v] in a sample of biomass.

$$[c] = 100\% - ([m]\% + [a]\% + [v]\%) \tag{72}$$

4.5.5 Calorific Value of the Fuel

The calorific value of the fuel is defined as the amount of heat presented or obtained in a food or a fuel. It can be classified as higher/Gross heating/calorific value (HHV) or lower/net heating/calorific value (LHV). HHV is the maximum amount of heat that can be extracted from the combustion of desired fuel theoretically and LHV is the minimum that can be extracted from the feedstock. The calorific value of any given species of biomass is dependent on the moisture content and its density. The lower calorific value of the fuel can be evaluated from the following relations.

$$LHV = HHV - 10.55(W + 9H) \tag{73}$$

Where: LHV = lower heating value of fuel, HHV = higher heating value of fuel, W = Weight % of moisture in fuel, and H = Weight % of hydrogen in fuel. The net or lower calorific values of the sample biomass fuel were taken from literature which is between 16,613.51 MJ/kg and 1864 MJ/kg (Adem *et al*., 2019; Adem and Ambie, 2017; Bantelay, 2014).

4.5.6 Fuel Consumed

It is the amount of fuel burned or consumed during the experiment to boil a two and half-kilo gram of water. It can normally calculate by taking the difference of the mass of fuel before the test and after the test respectively.

$$F_c = m_{fi} - m_{ff} \tag{74}$$

Where m_{fi} and m_{ff} are the initial and final weight of the feedstock, respectively.

4.5.7 Mass of Water Vaporized

Mass of water vapor lost (released) during the experimental test can be calculated by subtracting the final weight of water from the initial weight of water. By the time of measuring the mass of water, consideration must be taken on the weight of a pot.

$$W_{mv} = P_{wi} - P_{wf} \tag{75}$$

4.5.8 The Effective Mass of Water Boiled

This is the mass of water at the end of the experiment which possibly calculates by simple subtraction of the weight of pot from the final weight of water. So that the effective mass of water can be calculated as follows;

$$W_{we} = W_{wf} - W_p \tag{76}$$

Where W_{we}, $W_{wf,}$ and W_p are effective mass boiled water, the final weight of water, and mass of pot respectively.

4.5.9 Time to Boil

The total time that takes to boil or cook the given sample is calculated by subtracting the starting time of the test from the time that the water is boiled. The time that takes to boil the entire water is calculated by using Equation 77.

$$\Delta t_c = t_{cf} - t_{ci} \tag{77}$$

4.5.10 Specific Fuel Consumption

SFC is the fuel that has been used to boil a two and a half kilogram of water. It is a measured amount of fuel required to cook the entire food. It can be expressed as;

$$SFC = \frac{Fuel\ used\ (Kg)}{Food\ cooked\ (Kg)} \tag{78}$$

The other stove parameter is firepower (FP) which tells the average power output of the stove (in Watts) or the amount of energy output from the combustion process.

$$FP = \frac{SFC \times LHV}{\Delta tc * 60} \tag{79}$$

4.5.11 Thermal Efficiency

The thermal efficiency (η_{th}) of the stove from the experiment was calculated as the ratio of the amount of heat gained by the water inside the pot and evaporated to the energy of the fuel used for heating. The complete mathematical relation is given in Equation 80 (Adem and Ambie, 2017).

$$\eta_{th} = \frac{m_{wi} \times C_{pw} \times (T_f - T_i) + m_e \times L}{m_f \times NCV} \times 100 \tag{80}$$

where, Where m_{wi}, $C_p w$, T_i,T_f, m_e, L, m_f and NCV are the initial mass of water (kg), specific heat capacity (kJ/kg/°C), initial temperature of the water (°C), final (boiling) temperature of the water (°C), the mass of water evaporated (kg), Latent heat of evaporation of water (kJ/kg), a mass of fuel, and heating value of the fuel (kJ/kg).

4.6 Computational Modeling and Analysis of Double-Pot Biomass Cookstove

To predict the performance of double-pot biomass cookstove, three different numerical models with different geometry were analyzed using ANSYS fluent software. The results can be used to show the velocity field and the temperature distribution in the combustion chamber and also it generates the contour of different output parameters. The aim of developing more than one model is to analyze the performance of the cookstove by varying the geometrical parameters. After finding the results from the former two designs, the last model of the cookstove with modified geometry is developed on fluent to find out better performance. Using the temperature distribution on the stove body from the CFD result the performance of the designed cookstove with better performance has been investigated experimentally.

4.6.1 Model Description and Meshing

The simulation of the stove is started by creating a geometry of the desired domain of the fluid flow section on the DM (design modeler) which is considered as a pre-processor. In this section of ANSYS software, the geometry of the fluid flow of each zonal section of the stove has been developed separately and at the end, the separate parts are made as one part for the sake of the flow analysis. The performance prediction of the new cookstove was used as an input for the actual development of the stove. Three 3D models are built on ANSYS fluent software with different flow sections and their results are analyzed to decide on the preparation of the experimental model. The basic geometrical effect studied in the present study was the size of the combustion chamber. Those three developed numerical models that were designed on ANSYS fluent are discussed below.

Based on (Parajuli *et al*., 2019) the dimensions of the stove were been seized and the temperature distribution of three numerical models was evaluated on ANSYS fluent and the model with better heat distribution on the bottom of pot one selected for an experimental model. The first CFD model that was designed for the analysis of the geometrical effect on the double-pot cookstove was a 3D object that consists of all the actual stove geometries. The model geometry was developed on an ANSYS design modeler with 350 mm combustion height, 300 widths, and 320 mm length of the combustion chamber. This unit has a 20 mm distance of grate from the bottom of the stove and 10 mm of pot support height. The second numerical model was made on the same geometrical configuration by keeping all the dimensions the same and made the height of the chamber 450 mm. The analysis is carried out for the same considerable boundary conditions. The last numerical model was developed with a modified geometry size based on the results of the previous two ANSYS results. The modified geometry was having a 400 mm height, 300 mm length, and 320 mm of width. From the temperature distribution of the three numerical models, the last model (model 3) were selected and studied the other numerical parameter for the validation of the experimental model.

4.6.1.1 Geometry

The decision has been made by taking the comparison of the outlet temperature value from the developed three geometries. The model geometry (model 3) has been selected and further analysis was carried on it. Figure 4.3 shows the numerical model description of the selected geometry of the study.

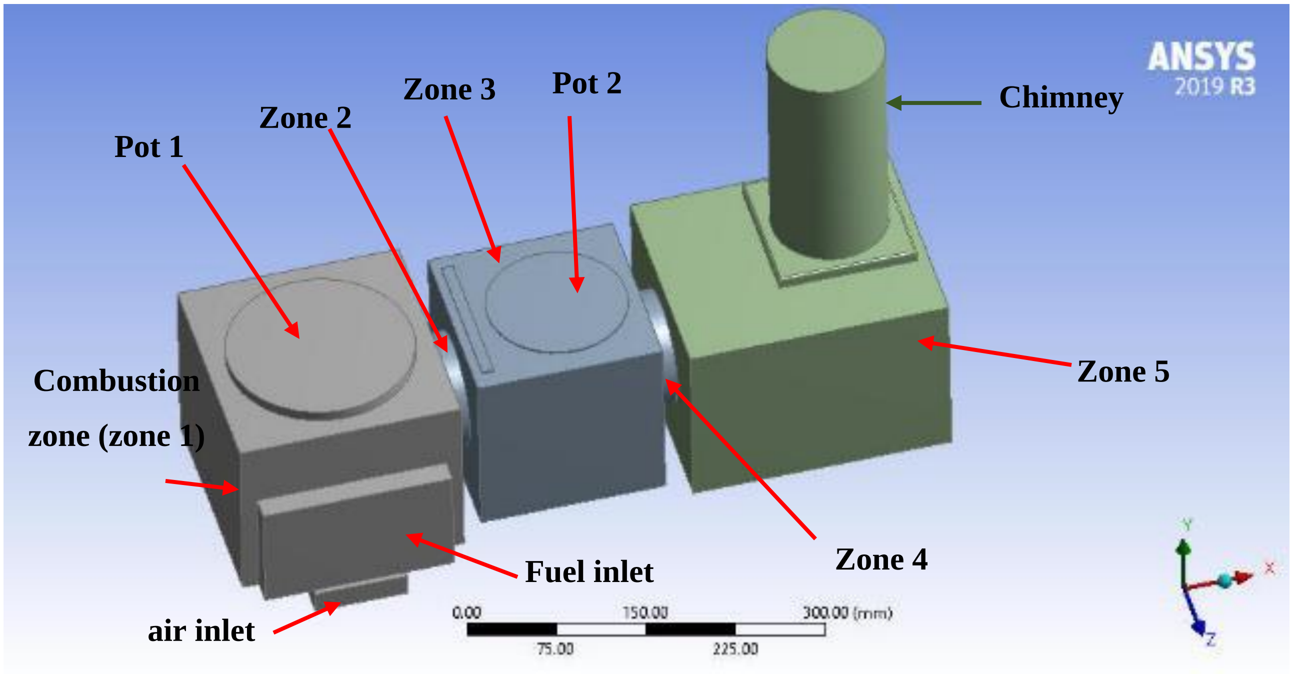

Figure 4.3 Model description of the selected cookstove

4.6.1.2 Meshing

Meshing is the way of discretizing the flow domain into fine grids. Meshing a domain is the language of ANSYS fluent that considers the physical discretization of the geometry into different elemental and nodal points. A good meshing can result from accurate results. Under this part of the simulation, some basic terms must be taken into consideration for the analysis and the result of the stove outputs i.e., sizing, mesh quality, material type (fluid or solid), identifying the geometrical parameter i.e., inlet, outlet.

A note must be taken to check the mesh independent test. This is the method of whether the outputs are dependent on the number of meshes or not. The selected computational numerical model was discretized element size of 2e-3 m using quadrilateral mesh type and it consists of 1,027,299 nodes and 710,302 elements. The discretized view of the model is described in Figures 4.4.

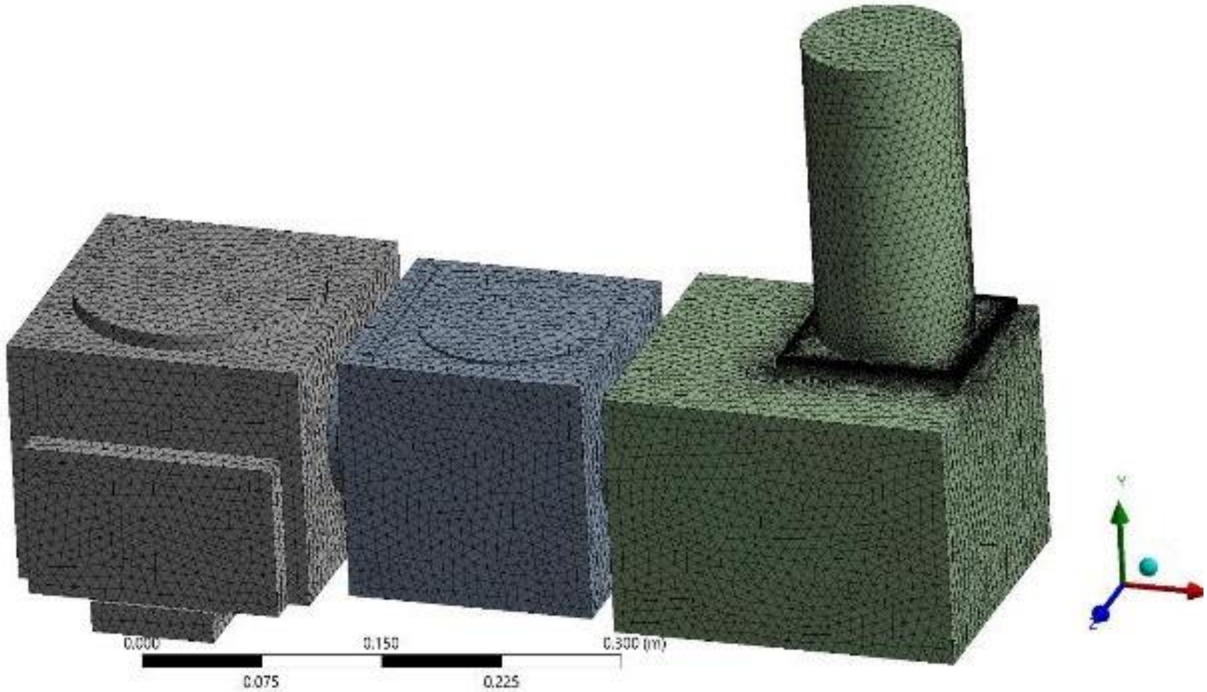

Figure 4.4 Computational grid of the stove

4.6.1.3 Grid Independence Test

The mesh independent test has been done to determine the level of grid enhancement or reduction of the mesh size.

Table 2 Grid independency test

No.	No. of nodes	No. of element	Element size	T_{fl} (K)	T zone 2	T_{p1}	T_{p2}	T_e
1	59,511	57,422	5e-3	598.6	566.48	555.4	518.5	402.9
2	108,004	105,430	3e-3	591.6	558.35	548.3	513	401.5
3	1,027,29	710,302	2e-3	585.5	538.15	541.3	502.8	398.3

Although the GIT test helps to examine the variation of temperature output whether it keeps changing or not. Beyond the 5e-3 size of the mesh, the output temperature did not show a considerable change. Succeeding the grid independence test, decisions had been made for the mesh that has been used for the model, and table 2 shows the meshing property of the model.

4.6.2 Setup

Setup is the section identifying the boundary conditions of the problem which is the backbone of the solution. The governing equations of the problem, the boundary conditions, and flow defining as well. The pressure-based solver under steady-state condition has been chosen and since the combustion process is a turbulent flow, $k - \varepsilon$ model with reliable and enhanced wall treatment is selected for the flow process. This indicates that k is the turbulence kinetic energy and ε is the turbulence eddy dissipation rate. There are various models for turbulent flow analysis but $k - \varepsilon$ model is the most commonly used model which can be able to analyze the turbulent simulation in ANSYS fluent (Husain *et al*., 2019; Zuckerman and Lior, 2006). Moreover, along with the accuracy with the reasonable and less computational cost, this model is preferable to the other higher-order turbulent models (Li *et al*., 2001). From the previous studies, it can be concluded that this model would be the most appropriate for this specific case.

4.6.3 Governing Equations

In the non-premixed combustion model, conservation of mass, conservation of momentum, and conservation of energy equation were solved.

a) The continuity equation is given as

$$\nabla . \rho \bar{v} + \frac{\partial \rho}{\partial t} = 0 \tag{81}$$

b) Energy equation

$$\frac{\partial}{\partial t}(\rho h) + \nabla(\rho \bar{v} h) = -\nabla q + \dot{S}_h \tag{82}$$

where *h* is specific total enthalpy and v is velocity.

c) Conservation of momentum

$$\frac{\partial(\rho \bar{v})}{\partial t} + \nabla . (\rho \bar{v}^2) = -\nabla P - \nabla \tau + \rho g \tag{83}$$

wherein equations 83 and 84 the pressure gradient and molecular transport terms are represented respectively and τ is viscosity stress tensor.

$$\tau = -\mu\left[2S - \frac{2}{3}\nabla\bar{v}\right] \quad (84)$$

$$S = \frac{1}{2}(\nabla\bar{v} + \nabla\bar{v}^T \quad (85)$$

Where $\nabla\bar{v}^T$ is the transpose of the velocity gradient and μ is the dynamic viscosity.

4.6.4 Computational Procedure

Under the boundary condition, the turbulent intensity is 10% which means that the velocity fluctuation is high. In this case, the combustion generates high turbulence intensity. Assumptions that were made while numerical analysis of the stove;

- ✓ The different sectional temperatures (i.e., combustion chamber, an inner and outer wall of each zone, flame, each pot bottom and content of the pot, fuel bed (grate), and ambient temperatures) are steady as well as different (Gogoi and Baruah, 2016).
- ✓ The operation of the cooking stove is considered a steady-state. The reason is the operating parameter that needs to be considered is the average parameter (Pande, *et al*., 2019; Shah and Date, 2011).
- ✓ In the computational domain, the exhaust type is and does not undergo any further chemical changes**.**

i. Boundary conditions

In the CFD simulation, the material and thermal properties of the components of the system that has impacts on the performance of the cookstove based on heat transfer and temperature distributions are involved. Types of material and working fluids, and their thermal properties are the major input parameters in a boundary condition. The velocity of fluid domain, temperature distribution, exhaust emissions, and other related variables are investigated from the post-processing of CFD analysis. To obtain appropriate findings in CFD analysis, it is critical to use proper beginning and boundary conditions that are close to experimental values. Three basic boundary conditions are done on the analysis of cookstove such that inlets, outlets, and walls.

The working parameter's boundary conditions are quantitatively and computationally indicated. The inflow variable for the state of the cookstove flow process is a blend of wood volatiles and air for all circumstances. Because the entrance is exposed to the atmosphere, the model input is air velocity, and the stove output is atmospheric pressure conditions (zero-gauge pressure). At 300 K, the bottom of the pot is treated as a wall. The walls are provided with no-slip boundary constraints.

The air and fuel input temperatures were both set to 300 K. Furthermore, the input's turbulence resistance and turbulent viscosity ratio are both 5 and 10%, respectively (Fluent, 2011). Walls-For flowing fluid, these are solid boundaries that allow heat and other variables to enter and leave the domain. The boundary conditions for the zonal walls are put no-slip conditions.

ii. Components and Material Properties

In the current double-pot cookstove simulation, the materials used include incompressible gas (air), *Aircrete* wall, and galvanized Sheetmetal. The working fluid for the fluid phase is modeled as an incompressible ideal gas in the simulation.

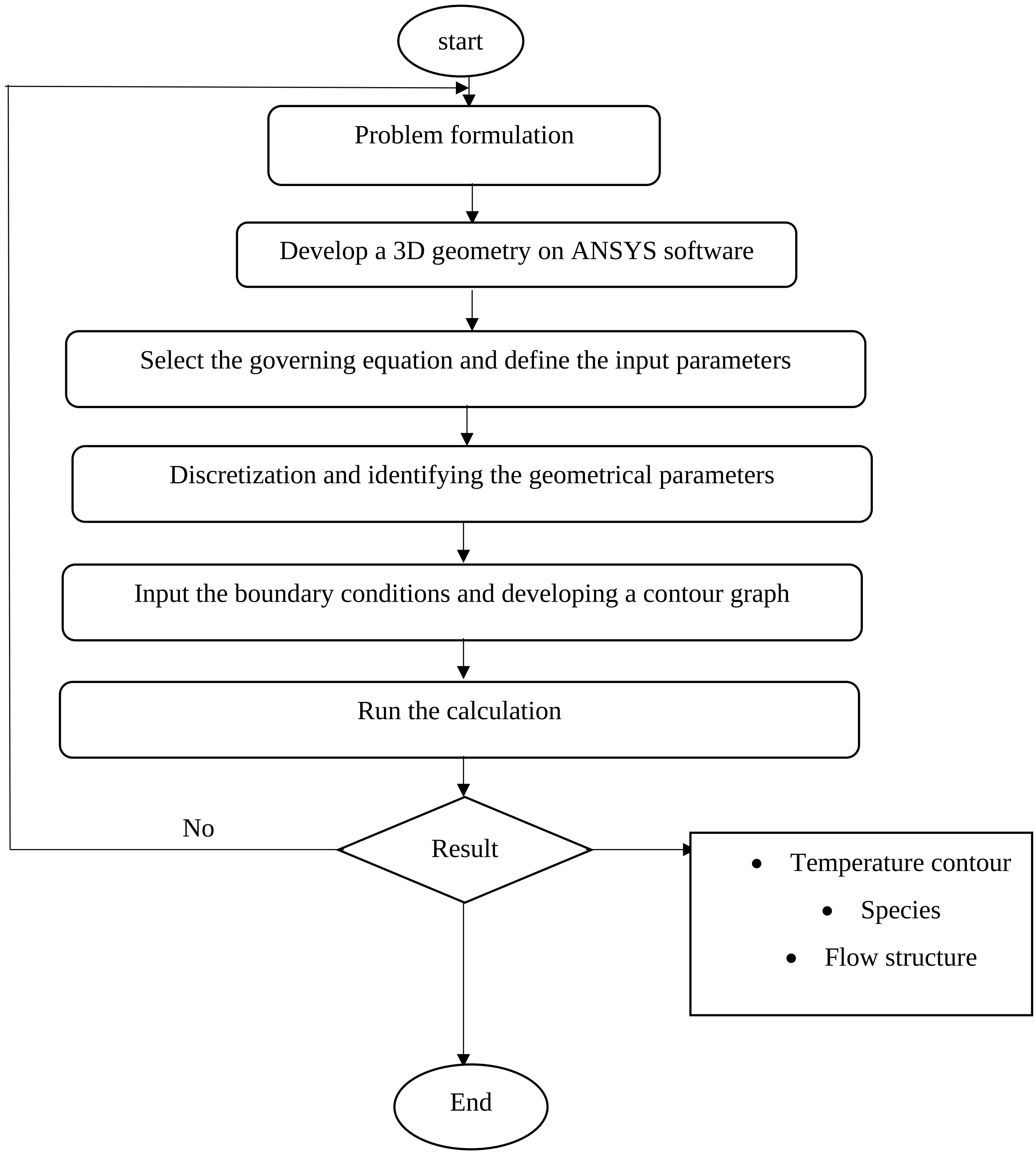

Figure 4.5 Computational algorithm of double-pot biomass cookstove

4.7 Performance Parameters of the Stove

The efficiency of the cookstove is determined (measured) by the performance of the cookstove. Equation 86 is used to predict the total efficiency of the stove based on the CFD findings. The overall efficiency of the stove can be estimated using equation 86 after calculating heat transmission and heat losses owing to various methods.

$$\eta_o = \frac{Q_{pot\ 1} + Q_{pot\ 2} + Q_{conv\ side\ 2} + Q_{rad\ side\ 2} + 0.67\ Q_{c-r}}{FP} \times 100 \qquad (86)$$

CHAPTER FIVE

5. EXPERIMENTAL SETUP AND CONSTRUCTION OF DOUBLE-POT BIOMASS COOKSTOVES

5.1 Introduction

The manufacturing process, the experimental setup, and procedure, as well as the working principle of the double-pot biomass cookstove, are all described in detail. The procedure of creating the experimental model of the new stove begins with the selection of the right material for a specific application. Different factors were taken into account before making the decision. Those concerns are based on a variety of characteristics of end-user life, including technological aspects, economic aspects, mechanical aspects, durability (life span), and material accessibility.

5.2 Deign of Double-Pot Biomass Stove

SOLIDWORKS 19 was used to create a novel design for a double-pot biomass cookstove. Various considerations were addressed when determining the size and design of the current stove, based on CFD data and the most recent studies. The stove was constructed with many components such as the fuel bed, grate, hearth zone, and chimney. The three zones of the new cookstove model are referred to as zone 1, zone 2, and zone 3. The combustion chamber is the initial section of the stove. The combustion of biomass fuel takes place in this portion. The design of this zone has a significant impact on the remainder of the zones. Because the fuel must have ample room to burn completely. According to the study (Parajuili et al., 2019), the combustion chamber was constructed by changing the geometries of the stove's height, length, and width. The experimental prototype's combustion has a height of 400 mm, a length of 300 mm, and a width of 320 mm.

The flue pass passage section follows the combustion chamber and is located between the combustion chamber and the second pot portion. The firepower and amount of energy required to reach the pot two portions must be considered when deciding on this interface. Taking this into account, the distance between them was calculated to be 40 mm. The flue gas that reaches pot two must also be considered in the design of zone three, which is pot two parts. Because boiling is the most prevalent technique of food preparation, the energy or heat that comes from this division is required to boil water. The dimensions of this portion of the stove are 200 mm in length, 300 mm in height, and 320 mm in width. The final chimney component measured 320 mm wide, 120 mm long, and 450 mm tall. The fuel grate was installed above the ash hopper, at a height of 90 mm from the bottom. The gaps between the round bars on the grate allow the ash door's limited air to enter. The fuel inlet door has a width of 280 mm, a height of 180 mm, and a length of 300 mm. *Aircrete* walls were used to create all of the zonal geometries, which were then covered with galvanized sheet metal. The upgraded biomass cookstove with two pots is designed to be as simple to make as possible for any craftsman shop.

5.3 Preparation of the *Aircrete* Mixture

To reduce energy losses, the most relevant technique to design an efficient cookstove is to use insulation material on the heat transmission region. Insulation is full of air holes and light in weight, according to the cookstove method (Bantelay D., 2014). As a result, the current study developed a new insulation material for biomass cookstove construction.

Figure 5.1 Preparation of *Aircrete* mixture

Clay, steel (sheet metal), and a mixture of cement and sand were the most common materials used to make biomass cookstoves, according to local biomass cookstoves and recent literature studies. The alteration on the wall on cookstoves has been studied in light of this. Mud and concrete walls make up the majority of locally accessible double-pot biomass cookstoves. This could harm a country's economy by consuming too many resources. To lower the cost of using a biomass cookstove and to improve the function of the new *Aircrete* wall on the stove. The appropriate combination of foam and other additives is required for the construction of high-quality *Aircrete* walls. The foam material in this circumstance is made from a mixture of water and liquid detergent soap that can be used to build a light and porous wall by creating an air gap between the wall particles. The detergent soap was well mixed between 873 and 1050 m/s torque to generate foam, and the mixer utilized during the foam production was a drill machine with swirl-bladed long steel on the drill tip. The current stove was made from a combination of readily accessible detergent soap, cement, and lightweight gravel. The goal of making an *Aircrete* mix is to create a porous wall with low thermal conductivity.

Figure 5.2 All *Aircrete* wall samples

To test the thermal conductivity and porosity of each sample, four samples were made using varied ratios of the main element and other inputs. Each *Aircrete* sample had a thickness of 30 mm, a width of 78 mm, and a length of 120 mm.

The first sample (Figure 5.3) consisted just of water, cement, and foam. The sample was made in a quantity ratio of 25.9, 664, and 200 grams, or 1:25.63:7.722 for Water, Cement, and Foam, respectively.

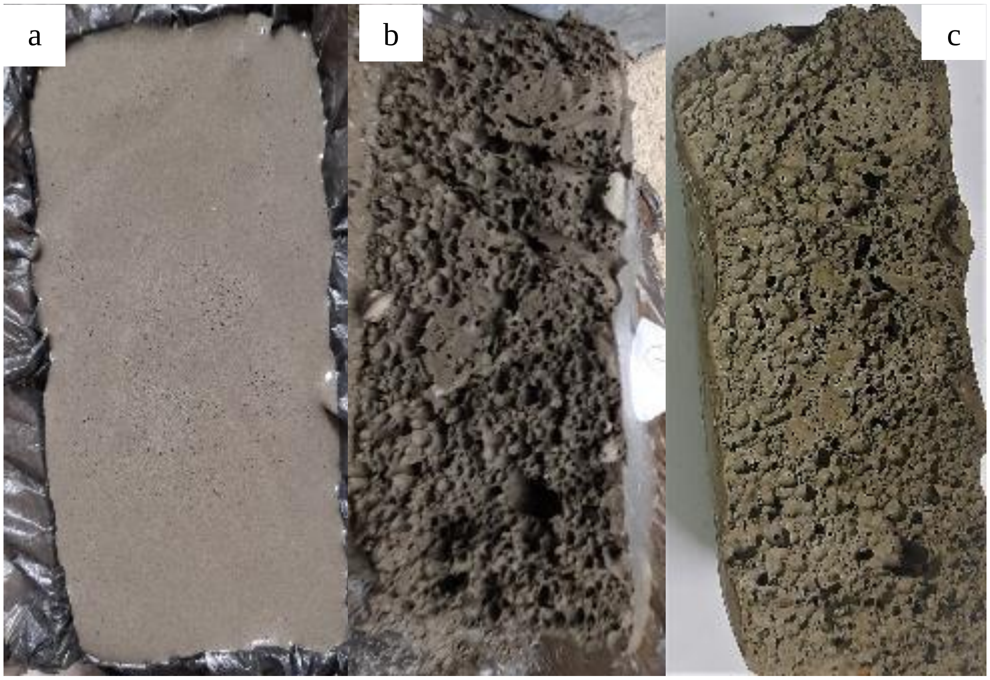

Figure 5.3 Sample 1: a) preparation, b) drying stage and c) final (dried) sample

The other sample was made with a 1:25.63:7.722:9.652 ratio, which is 25.9 g water, 664 g cement, 200 g foam, and 250 g light (porous) gravel. Figure 5.4 depicts the outcome of this composition.

Figure 5.4 Sample 2

As shown in figure 5.5 sample three were prepared from 1:27.237:7.722:9.652 which is 25.9 g:700 g:200g:250 g of Water, Cement, Foam, and sand respectively.

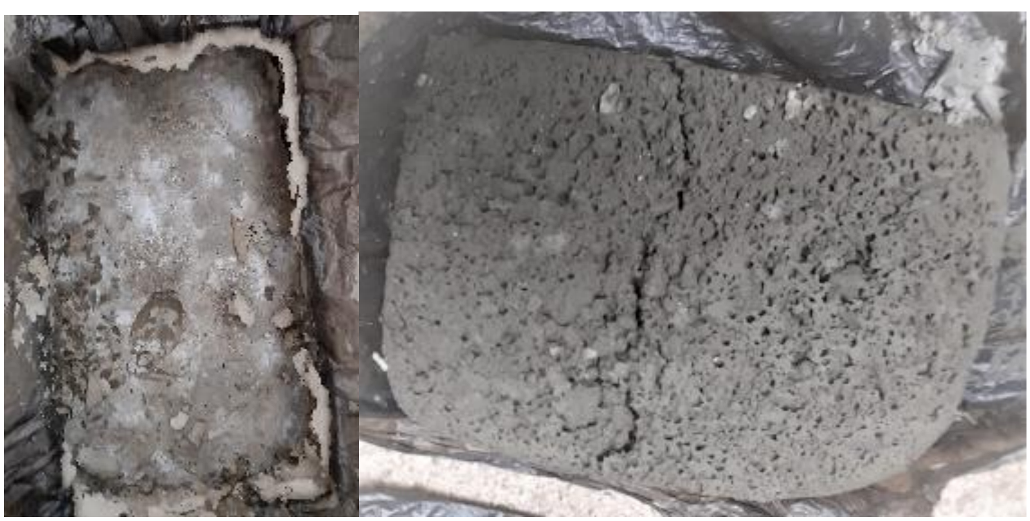

Figure 5.5 Sample 3

The other sample was made by combining water, cement, and light gravel in the ratio of 1:28.312:1.9 (water: cement: light gravel), as shown in figure 5.6. For 1 hour and 15 minutes, all of the sample combinations were mixed at a constant speed of 1040 m/s.

Figure 5.6 sample 4

5.4 Thermal Conductivity Test

The prepared samples' thermal conductivity is tested using fast thermal conductivity meter equipment. The heat flow is measured using a heat flow meter in conjunction with a heat flow sensor. The material to be tested is placed between the two plates with varying temperatures to create a heat flow from the hot plate to the cold plate, which the transducer measures. As a reference, the instrument is calibrated for materials with a specified thermal conductivity.

The thermal conductivity of each dried *Aircrete* slab was evaluated using a rapid thermal conductivity meter QTM-500, which is a hot wire (probe) method after the spaceman was prepared in rectangular form with a thickness of 30 mm.

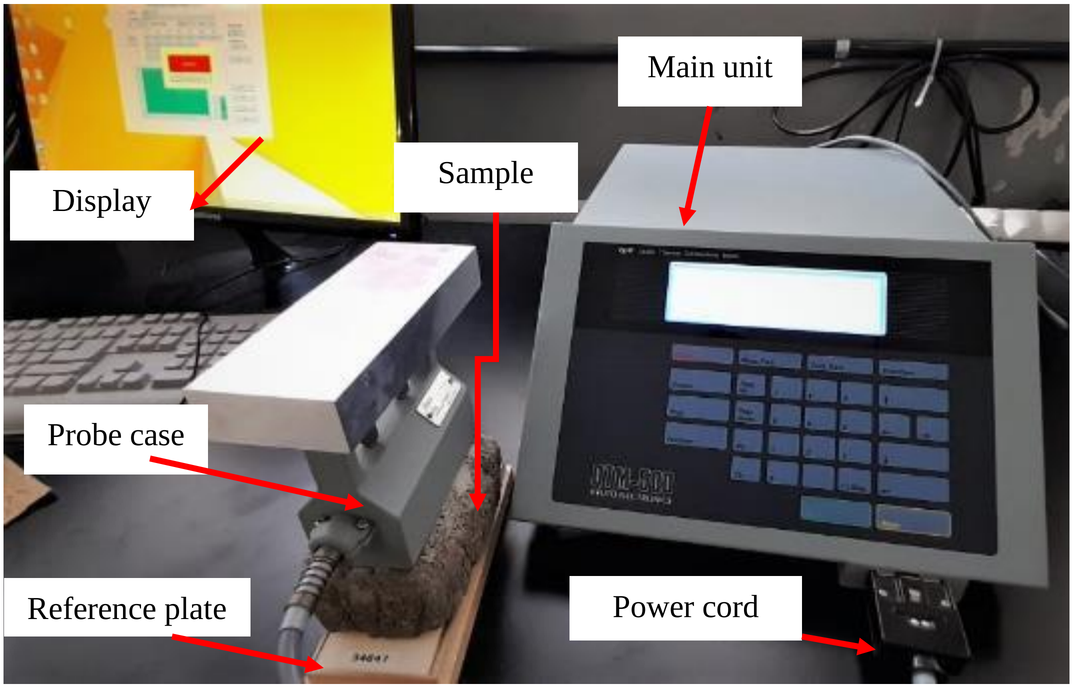

Figure 5.7 Thermal conductivity test

The ASTM C 518 foam concrete test was used to determine the results (Baldinelli et al., 2019). The dried specimen was dried until the mass stayed unchanged, and then the *Aircrete* slab with dimensions of 120 mm x 75 mm x 30 mm was tested using three known thermal conductivity references: rubber, polymer, and glass. The choice to build the current stove was taken based on the thermal conductivity test findings shown in Table 3. The 1:27.237:7.722:9.652 sample containing water, cement, foam, and lightweight gravel was chosen for the development of the experimental stove model.

5.5 Porosity (P) Distribution

Two samples with lower thermal conductivity values and one sample with the highest thermal conductivity value were chosen based on the results of the thermal conductivity test, and the density of those two samples was tested to calculate the porosity of the selected sample plate using Archimedes' principle. The porosity of each sample's specimens was estimated using equation 87, which was based on ASTM C 373.

$$P = \frac{([M - D])}{([M - S])} \times 100 \quad (87)$$

where, M, D, S, and P are saturated mass, dry mass, mass suspended in water, and Porosity of the prepared samples.

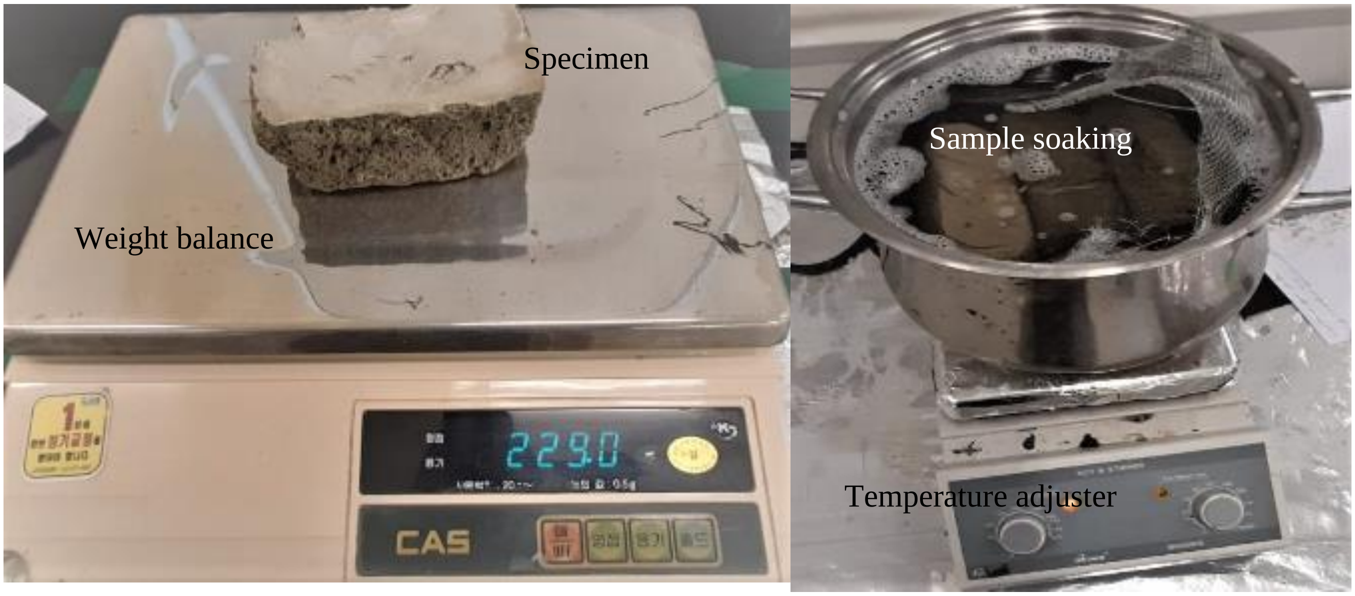

Figure 5.8 Density testing procedures

Table 3 Thermal conductivities and porosity of the samples

Sample no.	Water	Cement	Foam	Poros (light)gravel	Sand	Ratio	Thermal conductivity (K) (W/mK)	P (%) (porosity)
1	✓	✓	✓	X	X	1:25.63:7.722	0.1839	37.0353
2	✓	✓	✓	✓	X	1:25.63:7.722:9.652	0.1962	31.84768
3	✓	✓	✓	X	✓	1:27.237:7.722:9.652	0.329	-
4	✓	✓	X	✓	X	1:28.312:1.9	0.5469	20.1859

The slabs were soaked in distilled water for 24 hours at 37 ℃. After impregnation, the saturation mass and the mas suspended in water were measured.

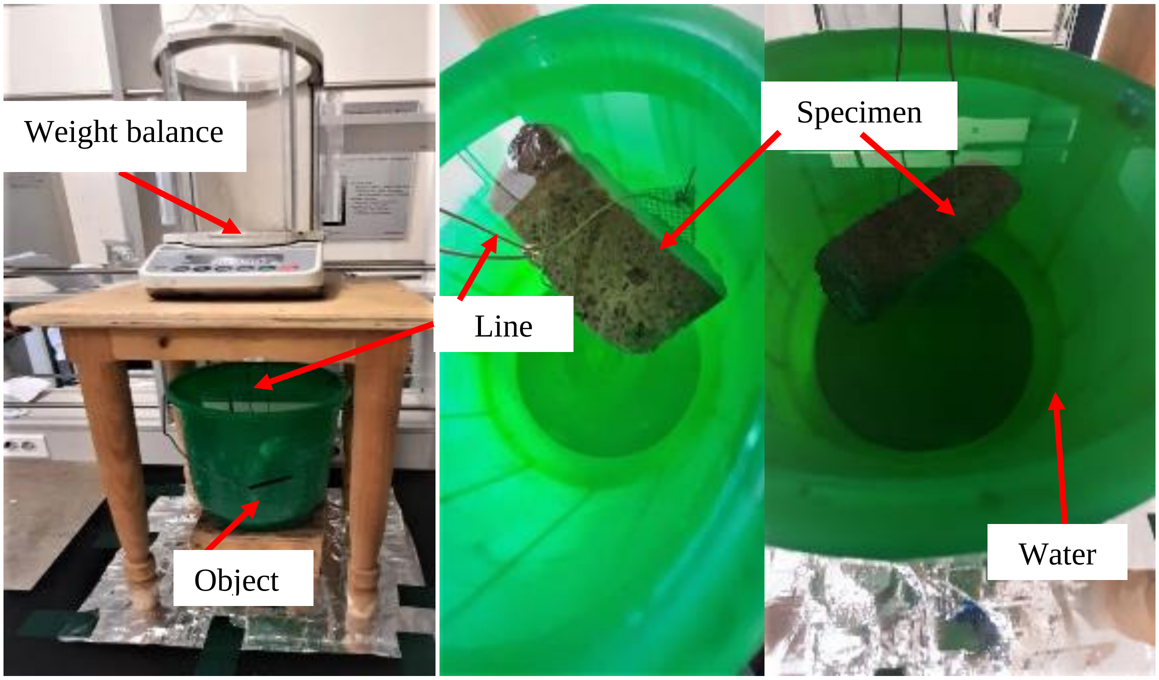

Figure 5.9 Density setup for measurement of suspended weight of samples

5.6 Manufacturing Process of Double-Pot Biomass Cookstove

Galvanized aluminum sheet metal has been employed in the design and construction of the stove. The cookstove's mold was created in the ASTU mechanical workshop. The sample of *Aircrete* walls with the best thermal conductivity and density was chosen and utilized to make the stove. Following the creation of the foamed cement combination, the produced cement and foam mixture is poured into the prepared stove mould to obtain the desired shape. The thermal conductivity of the produced wall was investigated in order to assess heat transmission through the system's wall (stove).

Figure 5.10 Manufacturing process of 2-pot BCS pattern a) preparing the edge supports and b) preparation of the internal pattern

To determine the mold of the designed cookstove, the stove's frame was prepared and welded with a specific dimension. Galvanized aluminum sheet metal with a thickness of 0.7 mm was utilized for the external body of the stove, and flat bar steel with a 20 mm by 2 mm was used as support during the formation of the mold manufacture. Following that, a mixture of sawdust and wood glue was used to close the openings around the mold. The *Aircrete* mixture is then made and poured into molds that have been built.

Figure 5.11 Assemblies and mold of the stove

5.7 Experimental Setup

A water boiling test is used to evaluate the new design's performance. To validate the numerical result and come to a conclusion, the thermal efficiency was calculated, the exhaust gases were recorded, and the temperature of various portions was measured. The setup was established in the chemical engineering department of ASTU, Adama Ethiopia, to investigate the current cooking stove experimentally. A combustion chamber, flue gas zones, two pots, chimney, fuel feeding door, air intake, ash hopper, and grate make up the stove's entire experimental setup. Figure 5.12 depicts a photograph of the entire arrangement.

Figure 5.12 Experimental setups of double-pot biomass stove

The experiment was carried out in a controlled lab with no wind, and tests were carried out at a rate of one per day to minimize the background concentration and allow the cookstove to cool before the cold-start test began. The amount of fuel used, each zone, wall and flame temperatures, an exterior body temperature of the stove, exhaust emissions emitted from the stove, and the time to boil 2.5 kg of water are all measured and recorded during the test. Table 4 lists the instruments that were used throughout the experiment.

Table 4 Instrumentation used in experimentation

No.	Instrument	Range
1	Thermometer	300-1300 (K)
2	Weight balance	0.5 -50 kg
3	Flue gas analyzer	CO_2 0.01 % volume
		CO 0.002 % volume
		O_2 20.03% volume

5.8 Working Principles of **Double-Pot Biomass Cookstove**

The basic concept behind biomass stoves is to transform the carbon present in solid biomass fuels into useful energy (heat). The fuel is added to the newly adopted stove through the door on the combustion chamber side. The model is divided into five portions (zones), which are zone 1, zone 2, zone 3, zone 4, and zone 5. The first zone is the part of the stove where the combustion process happens. The primary pot is positioned on top of the stove in this portion, with no gap between the upper part of the stove and the bottom of the pan. Only flue gasses move through the remaining three parts, which are not in direct contact with the combustion process. The flue gas from the combustion zone escapes through the pot section in the next portion, zone two. The flue gases from zone one will flow through this segment and reach the next pot in two portions. That is, the extra energy lost in section one flows via this medium, allowing the energy to be used for other purposes without the expenditure of additional fuel. So that the energy that escapes the combustion chamber can be stored and applied to another cooking task.

The secondary pan part continues, and this time it's a pot side with no direct combustion. Only the flue gas from the combustion zone is delivered to this area. The stove's fourth segment is the other flue gas flow zone, which leads to the last section, which is the chimney zone. The emissions in this zone are not expected to be hazardous or dangerous. The section in question is the chimney section, and combustion will not reach below it. This section's goal is to eliminate indoor air pollution. It is placed in the corner of the stove to allow emissions to escape into the environment, hence reducing indoor air pollution.

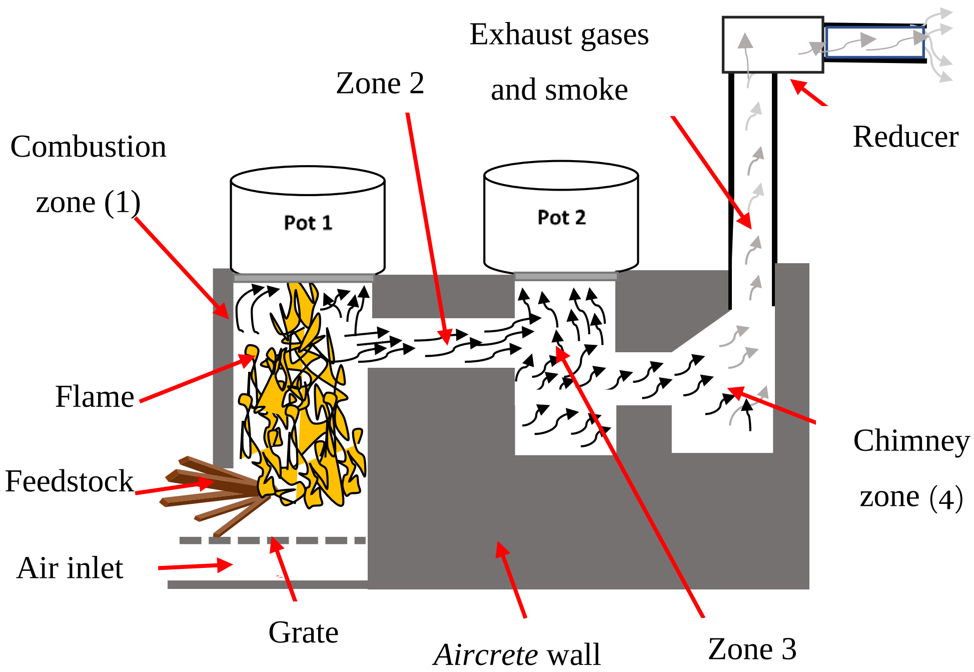

Figure 5.13 Schematic diagram of working principles of double-pot biomass cookstove

5.9 Experimental Procedure

Different measuring devices were utilized to measure various readings before, during, and after the experimental test of the double-pot cookstove. The transport of heat energy from the combustion of fuel to the two pots placed on top of the cookstove was investigated in this experiment. The WBT was done in two stainless pots, each with a capacity of 3.5 liters. During the boiling of water, the experimental protocols were followed.;

- Prepare weight balance and make ready the thermocouple that is used t measure the weight and temperatures.
- Preparing the eucalyptus tree login to the approximately same size (15 mm x 30 mm) (Adem and Ambie, 2017)
- 20 ml to 30 ml sanitizer to initiate (ignite) the fire
- Measure the initial mass of fuel and water
- Measure the initial temperature of the water in both pots and ambient temperature
- Measure and record each zonal temperatures and each pot temperatures within 5minutes until the interval
- Remove, measure, and record the fuelwood and char left as soon as the temperature of the first pots reached the local boiling point (94.506 ℃ for Adama)
- Measure and record the weight of water in both pot 1 and pot 2

The temperature of each zone, including the flame temperature, was measured using a K-type thermocouple with a range of 300°C to 1300°C. The weight measurements were taken before and after the test using a digital weight balance that could weigh up to 50 kg with a resolution of 2 grams. The experiment took place at ASTU, which is located at 8.558°N 39.28°E at an elevation of 1712 meters (Chandraprabu et al., 2019), with a local boiling point of 94.506 ℃.

CHAPTER SIX

6. RESULTS AND DISCUSSIONS

6.1 Introduction

This chapter presents and discusses the numerical and experimental data on the performance of double-pot biomass cookstoves. The computational and experimental output temperatures were used to calculate mass flow rates, thermal efficiency, and different zonal heat transfers. The outcomes of all numerical models produced for the study are described, and the results of the numerical models chosen for validation are compared to the experimental findings. The effect of air velocity and combustion chamber height on the output parameters is explored based on the computational fluid dynamics analysis of the current stove's model.

6.2 Numerical Results of Double-Pot Biomass Cookstove

Temperature distribution across the present ICS was examined using heat transfer simulations. The highest temperature was found near the stove's combustion point, while the lowest temperature was found on the stove's outermost surface, according to a general tendency. To better comprehend the results, examinations were done on the temperature-based and velocity-based results in graphical mode and compare their numerical values.

6.2.1 Effect of Height of Combustion Chamber

On ANSYS fluent, the variation in the height of the combustion chamber is investigated. The outlet temperatures that reach the bottom of the pot are investigated, and a choice is taken on how to proceed with the real model development. The output temperatures of three 3D numerical models were investigated while other parameters remained constant. The temperature fluctuations of the three numerical models with varied combustion chamber heights are shown in Figure 6.1.

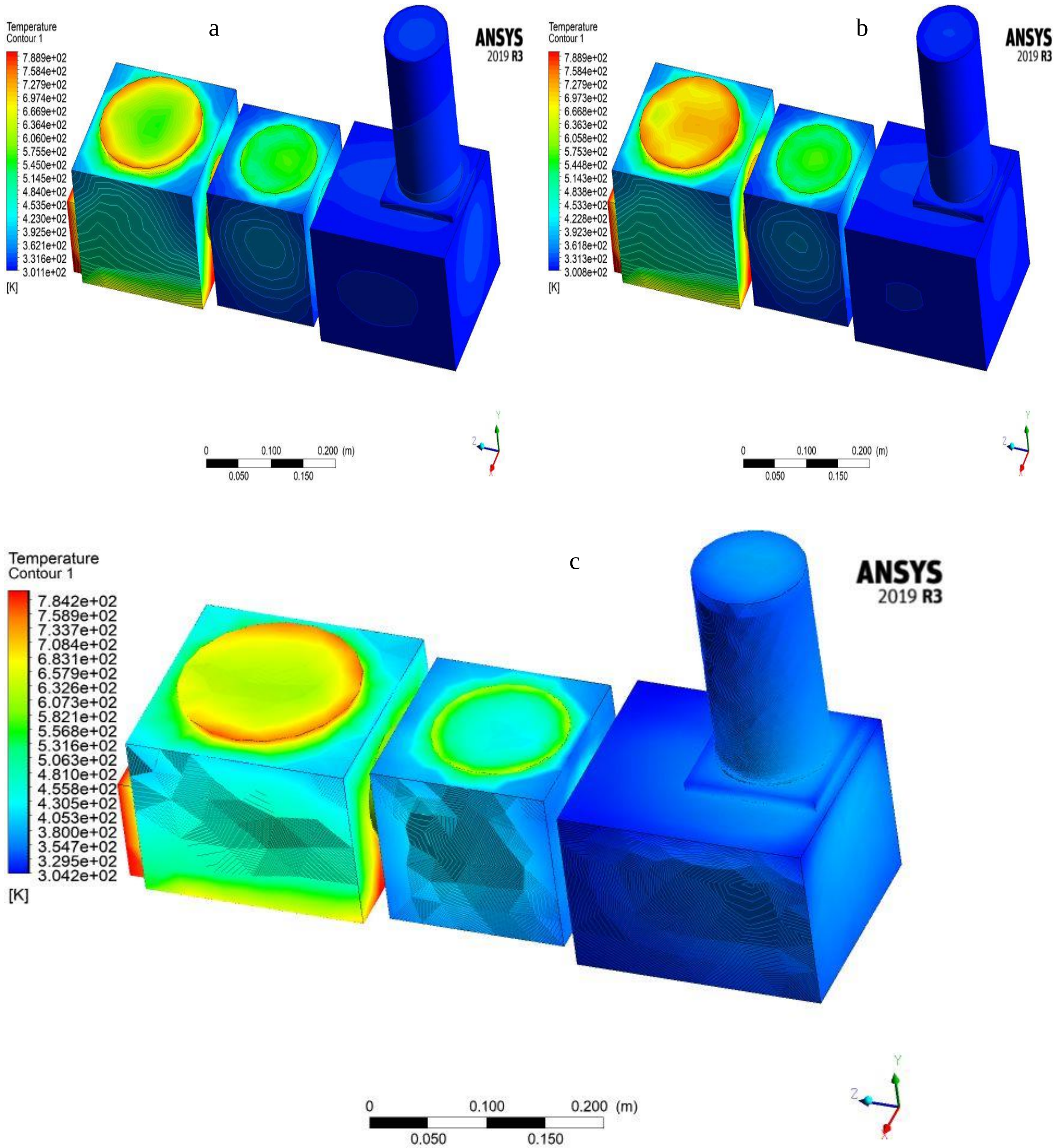

Figure 6.1 Temperature contour for different height of combustion chamber a) H@350 mm b) H@400mm and c) @ 450 mm

As the temperature contour shows, as the height of the combustion chamber rises, the temperature of the flame striking the bottom of the pot decreases. It has an effect on lowering the quantity of energy received by the pot in addition to lowering the flame temperature. As a result, raising the combustion chamber's height reduces its thermal efficiency. As a result, decreasing or raising the height of the combustion chamber beyond its maximum extent has an impact on temperature distribution as well as the combustion process. As a result, for the current investigation, a combustion chamber height of 40 cm was chosen, and lowering this figure will have a significant impact on flame temperature.

6.2.2 Effect of Air Velocity

Increased turbulence usually leads to an increased flow rate, which can improve heat transfer efficiency. The combustion chamber's flow velocity was maximum near the air inlet, as expected, and increased rapidly as height climbed. Figure 6.2 shows that the entrance air velocity is around (0.01 m/s) at a 50 mm chamber height and that it increases as the chamber height grows to 250 mm when the flow velocity is around 0.075 m/s. This increase in velocity causes greater turbulence, which can improve the stove's heat transmission efficiency. Nnez et al., (2019) estimated an air velocity of 0.075m/s, which increases as it approaches the combustion chamber, making the flow more turbulent.

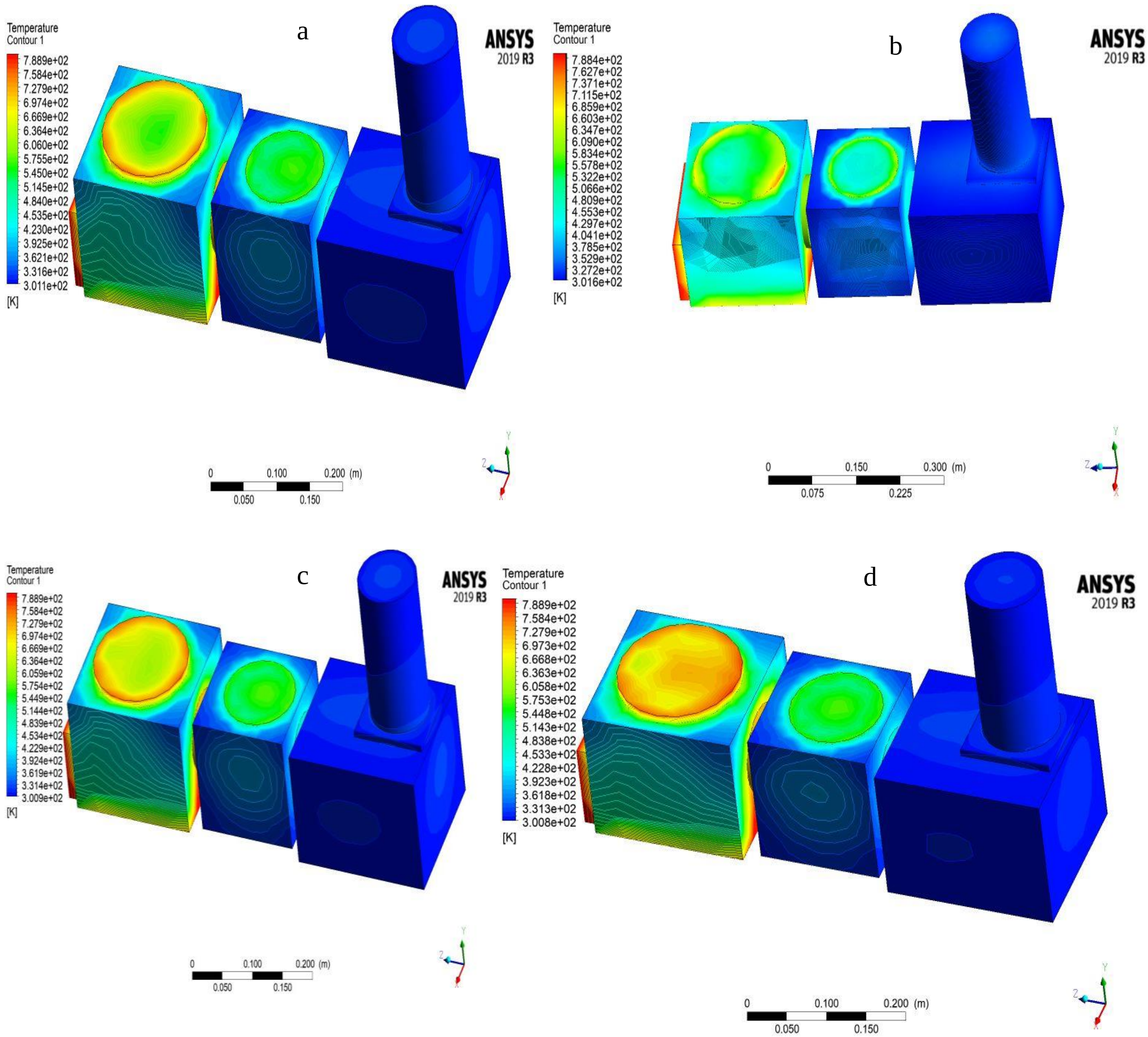

Figure 6.2 Output temperatures at different air velocity a) Temperature @0.0207 m/s, b) Temperature output @ 0.207 m/s, c) temperature @0.08 m/s and d) Temperature output 0.0107m/s

The fluctuation in air entry velocity affects the temperature in the stove, as shown in figure 6.2. Figure (a) shows that the outlet temperature that reaches the pot center is rather low, despite the fact that it should be quite high at this point. The next (b and c) contours continue the same pattern, and it improves in Figure (d).

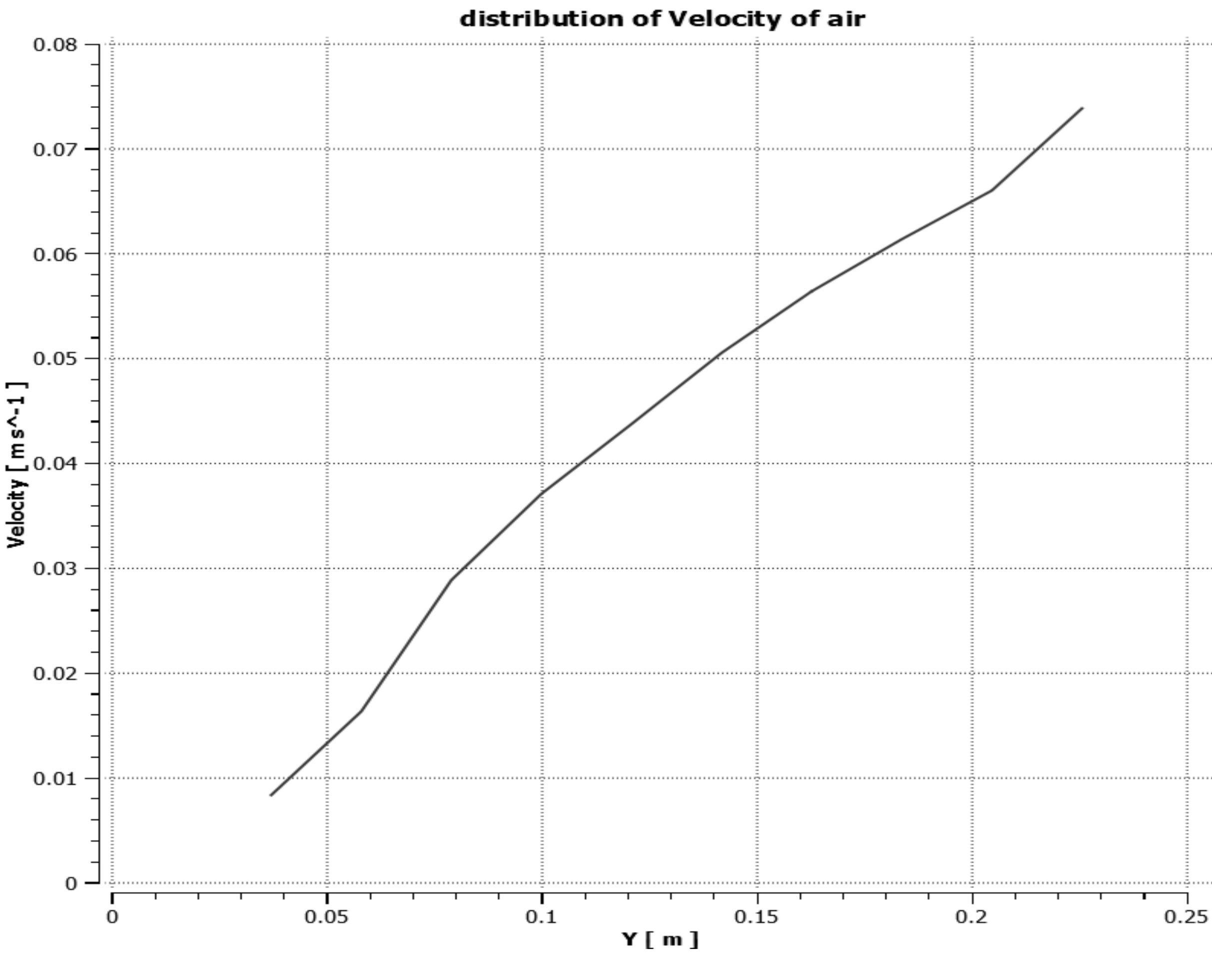

Figure 6.3 Inlet air velocity distribution on the combustion chamber

The temperature distribution is greatest at the middle of the bottom of the pot and diminishes as the diameter of the pot increases. This demonstrates that the highest flame energy reaches the pot's bottom center. The flow velocity was found to be lowest near the fire inlet, which had the highest combustion temperature. As the temperature rises, the velocity inside the combustion chamber increases. This means that the temperature of the combustion chamber is directly proportional to the flow of hot gases within the chamber.

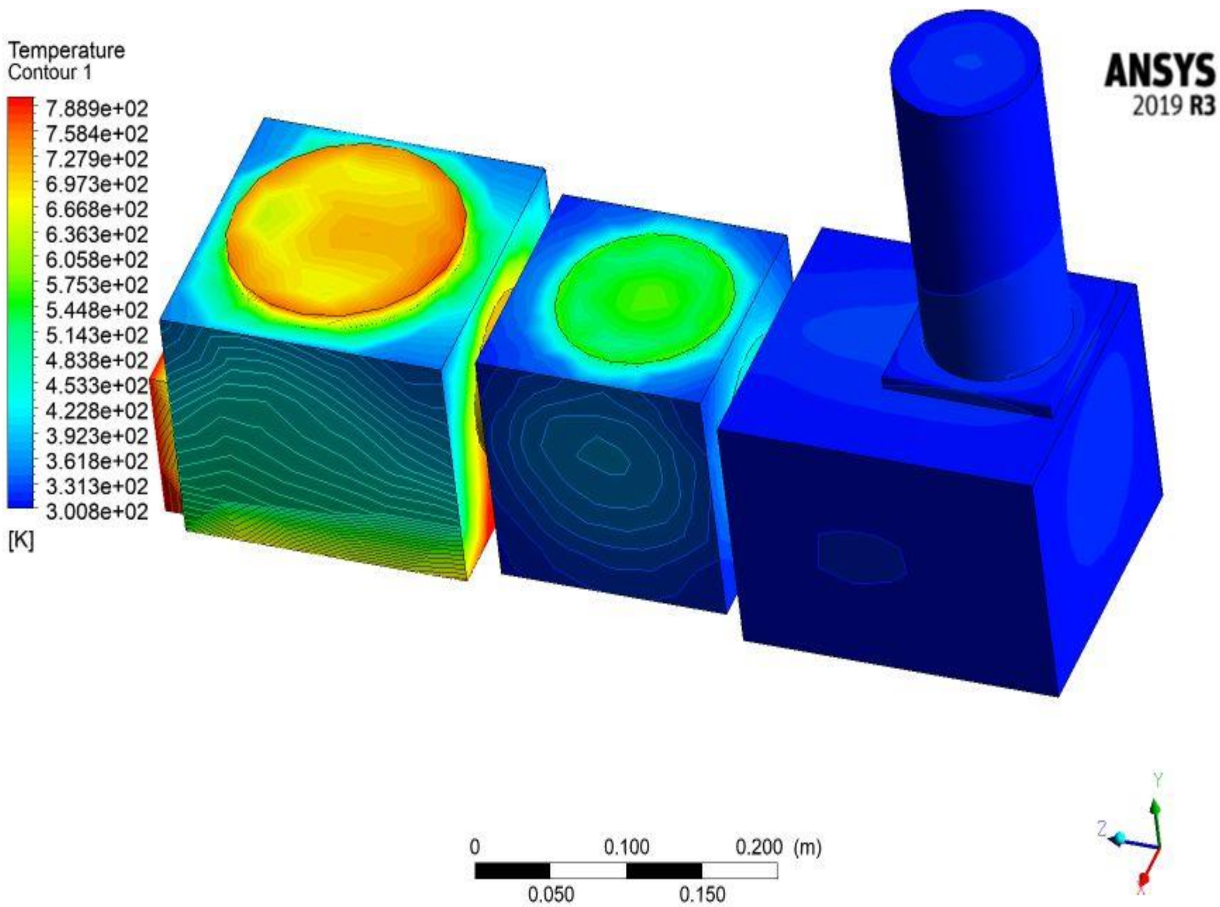

Figure 6.4 Temperature contour @ 0.0107 m/s

6.3 Water Boiling Test Results

The cookstove's performance was assessed using three sets of water boiling tests. The boiling point of water for Adama city at an altitude (height) of 1648 m was taken as 94.506°C while calculating thermal efficiency. Some output characteristics were measured and recorded from the three sets of water boiling tests on the double-pot cookstove, and the average results were used to determine the stove's performance. The experimental test output parameters (specific fuel consumption, firepower, time to boil, thermal efficiency, output temperatures, and exhaust emissions) are listed in Table 5. A eucalyptus wood log with a moisture level of 10.03 percent was used as feedstock for the stove in the experiment.

Table 5 Results of water boiling test

Phase	Parameter	Value	Unit
Cold start (high power) test	Time to boil	15.667	Min
	Burn rate	32	g/min
	Thermal efficiency	35.25	%
	Specific fuel consumption	165	g/l
	Firepower	8.684	kW
	CO	0.10175	%Volume
	CO_2	5.19	%Volume
Hot start (high power) test	Time to boil	14.67	Min
	Burn rate	35	g/min
	Thermal efficiency	36.66	%
	Specific fuel consumption	115	g/l
	Firepower	9.502	kW
	CO	0.321	%Volume
	CO_2	7.7075	%Volume
Average	Time to boil	15.166	Min
	Burn rate	33.1667	g/min
	Thermal efficiency	35.8 %	%
	Specific fuel consumption	140	g/l
	Firepower	6.686	kW
	CO	0.211	%Volume
	CO_2	6.448	%Volume

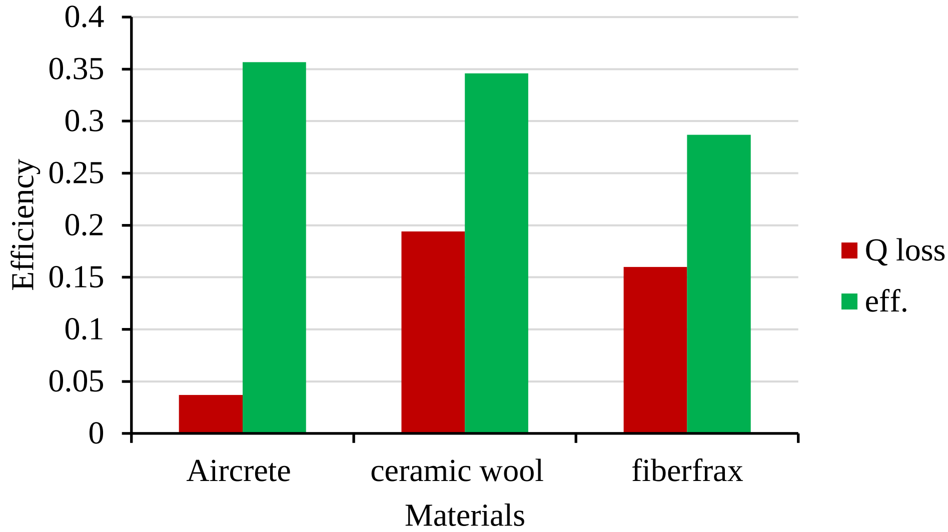

Figure 6.5 Thermal efficiency and specific fuel consumption of stoves with different materials

6.3.1 Temperature Variations

During the experiment, the zonal temperatures of the stove were measured by inserting a K-type thermocouple into an important component of the stove. During the experiment, thermocouples were inserted in each zone of the stove at various positions to measure the flame temperature, flue temperature, and interior and exterior wall temperatures of the stove. Figure 6.6 shows how increasing firepower raises the flame temperature and flue gas temperature in zone two.

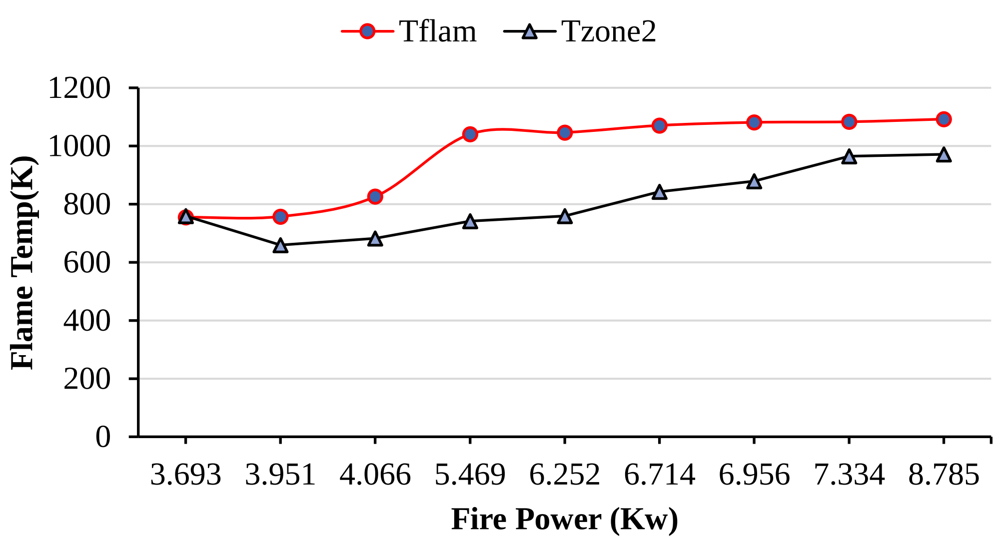

Figure 6.6 Variation of flame temperatures with firepower

Figure 6.7 shows the experimental results of temperature at various zones of the stove, including inner and outer-wall temperatures, plotted against time. The average firepower (6.686 kW) was used to determine the experimental findings.

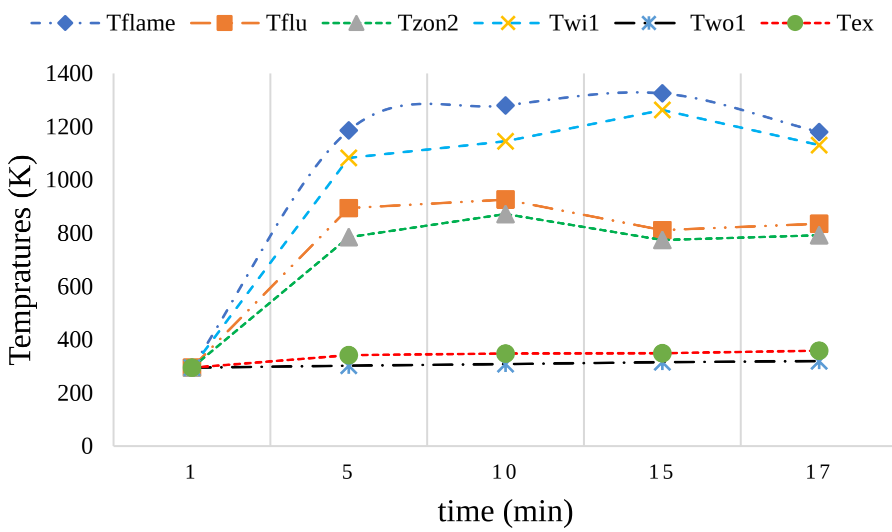

Figure 6.7 Output temperatures with time

The outlet temperatures in a different region of the stove are growing higher as the boiling duration increases, according to the WBT results in cold and hot start runs, as shown in Figure 6.8.

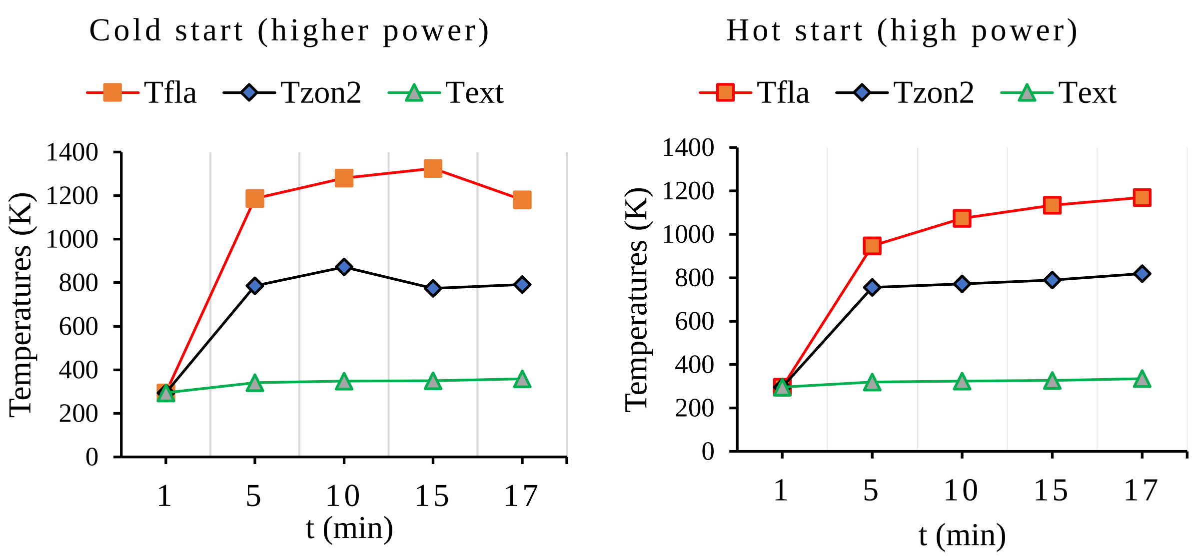

Figure 6.8 Different zonal temperatures during WBT a) Cold start b) Hot start

6.3.2 Mass Flow Rate

The mass flow rate of the flow impacted by various parameters such as Cd, firepower, and inlet area ratio is likewise in reasonable agreement with the mass flow rate of the predicted model and the experimental test. Maintaining a steady-state flow in a natural draught biomass cookstove is challenging and impractical. As a result, the fundamental unpredictability of firepower allows for such fluctuations.

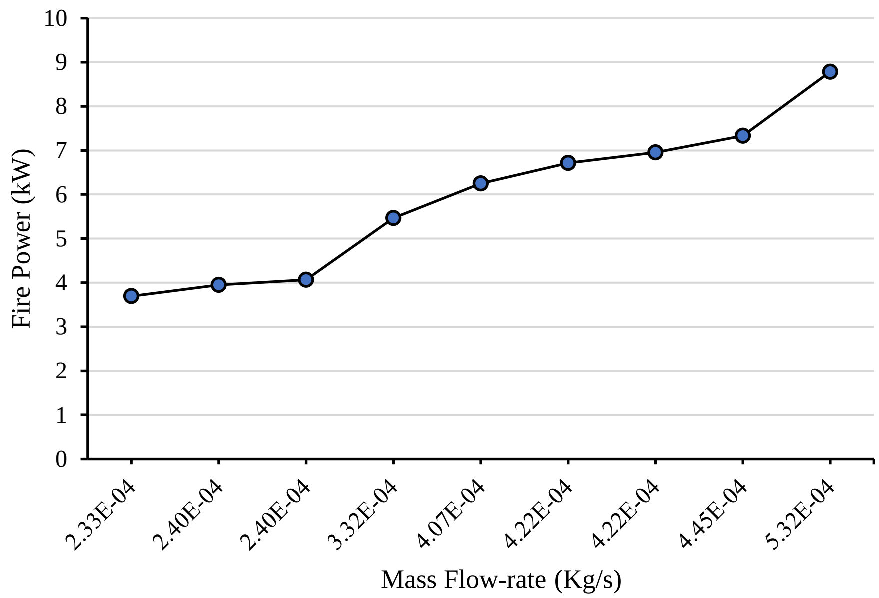

Figure 6.9 Variation of firepower with a mass flow rate

Increasing the height of the combustion chamber zone and the pot support revealed a change in mass flow rate, according to the numerical data. The mass flow rate is increased by varying the height of the combustion chamber and the distance between pot and support. Figures 6.9 show how mass flow rate varies with firepower.

6.3.3 Exhaust Gases

Knowing the specific exhaust emissions from a then-developed cooking stove is critical for the future; controlling emissions by exploring alternative fuels that result in lower emissions or optimizing the stove's operating characteristics. An infralyt gas analyzer was used to measure the exhaust gases exiting from the stove during the experiment. The average quantity of CO emission from the experimental test was 0.21 percent volume as a result of incomplete combustion. The average output concentrations of CO and CO2 emissions are inversely related, as seen in figure 6.10.

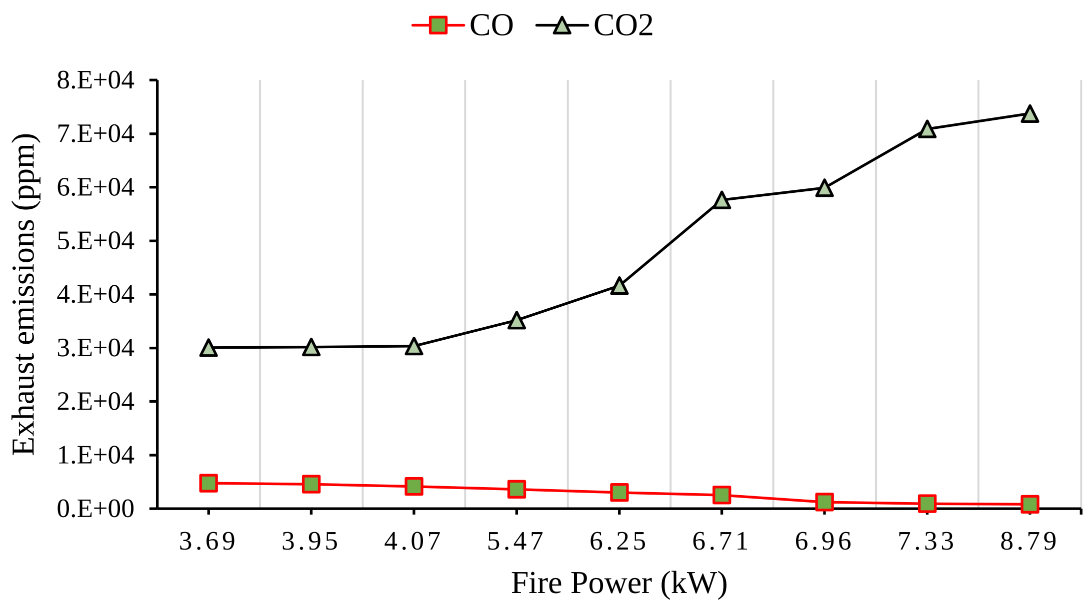

Figure 6.10 Variations of exhaust emissions Versus firepower

The variation in carbon dioxide content has a direct link with output temperatures, as seen in figure 6.10. As the temperature in the combustion chamber rises, the concentration of CO2 rises as a result of the increased conversion of feedstock to CO2. It's reasonable since the conversion of carbon in the fuel increases and the flame produced from the feedstock increases as the burning process improves, i.e., the fuel-to-oxidizer (air) ratio in the system (combustion chamber) improves. The average CO2 gas from the stove was reported as 6.448 percent volume based on the experimental test results.

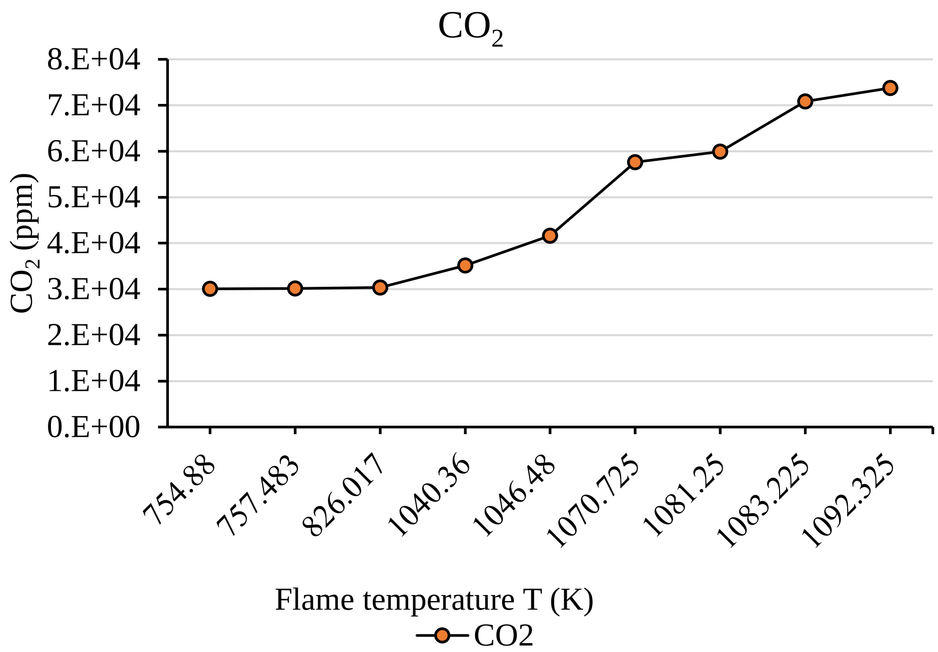

Figure 6.11 Variations of CO_2 versus flame temperature

The CO emitted by the stove, on the other hand, ranged from 0.0818 to 0.476 percent volume. As a result, in terms of CO emissions, the WHO requirements were met. The measured temperature trend is similar to the almost linear dependence of CO level on firepower.

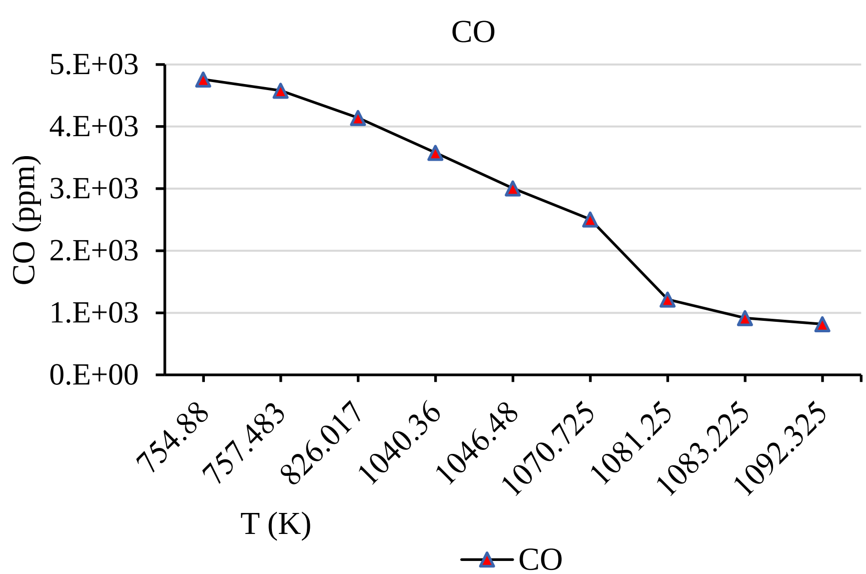

Figure 6.12 CO emission with temperature

6.3.4 Percent of O_2

As for firepower increases, the change in percent O2 in the system (cooking stove) was shown to decrease, as predicted by previous literates such as Dasappa and Paul (2001); Kshirsagar and Kalamkar, (2015); Pande et al (2019). Figure 6.13 depicted the relationship between percent O2 and firepower.

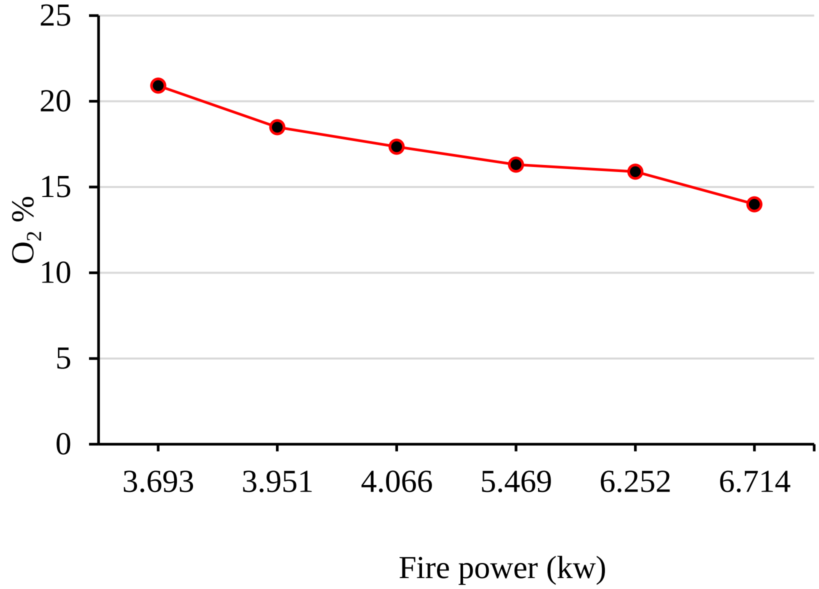

Figure 6.13 Variation of oxygen during experimental test

6.3.5 Specific Fuel Consumption

The stove's efficiency was assessed in specific fuel consumption (SFC), which was the quantity of fuel necessary to cook the entire meal. To boil two and a half kilograms of water, 140 g/l of fuel was used on average. The raw material for cookstove input fuel was a log of Eucalyptus woody biomass, and the addition of alternative feedstocks may bring a different value in terms of thermal efficiency and indoor air pollution.

6.3.6 Fire Power

Figures 6.14 show the fluctuation in firepower with flame temperatures in the established experimental model. As the feeding rate of the fuel in the stove increases and the temperature rises, the value of firepower grows. When the combustion process becomes incomplete owing to a lack of air supply or an inappropriate combination of air and fuel in the combustion chamber, the output firepower decreases.

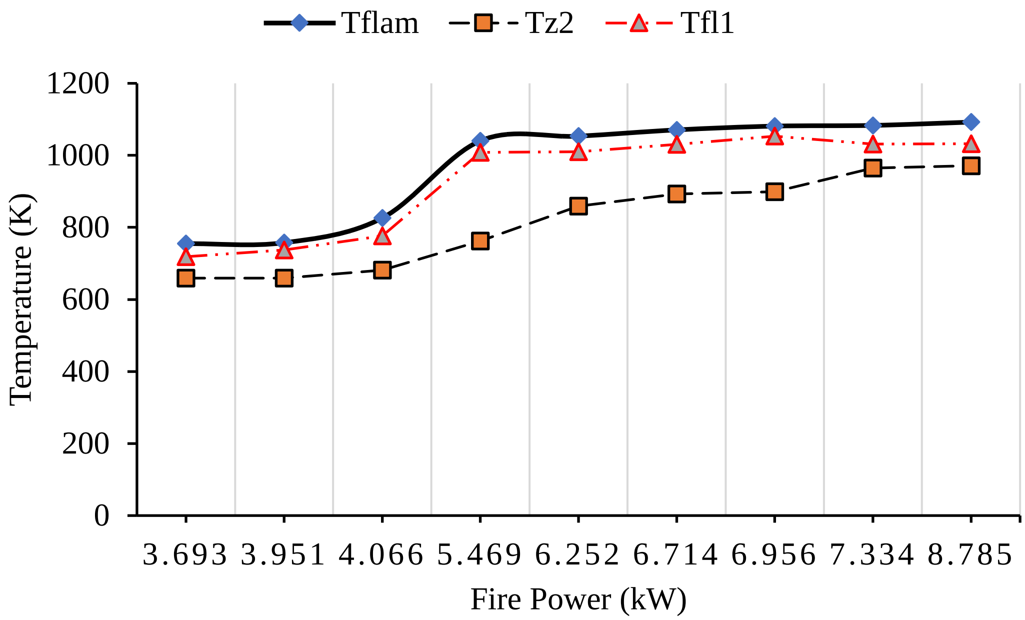

Figure 6.14 Variation of firepower with temperature

For a non-premixed flame, where the maximum local flame temperature around the first pot is substantially higher than in other locations with firepower, this outcome is expected. According to the research (Honkalaskar et al., 2013), the average firepower employed in single-pot biomass cookstoves is 8.46 kW. According to the results of this study, the WBT's maximum firepower was 8.785 kW. This can be used to demonstrate that the energy wasted in the first pot was saved and employed in the second. The heat loss through the combustion chamber wall is found to be 182.037 Watt, which is 3% of the overall loss, according to the figures provided in Table 6. According to recent studies by Kshirsagar & Kalamkar, (2015) and Pande, et al., (2019), the value of heat energy lost from the stove chamber to the surrounding was 469 W (16%) and 604.60 W (19.39%) of the total loss, respectively.

Table 6 Energy balance of entire stove

Parameter	**Symbol**	**Value (Watt)**	**Percent (%)**
Heat gain by a flue in zone 1	Q_{fl}	4421.704381	89.31653499
Heat transfer by radiation from char to the pot	Q_{cr}	27.93055579	0.564185266
Heat transfer by radiation from a flame to the pot	Q_{fr}	22.0606018	0.445614709
Loss through combustion wall	Q_{loss}	182.0372118	3.677073724
Heat loss due to hydrogen in the fuel	$Q_{H_2 loss}$	123.8798593	2.502320109
Moisture loss	$Q_{moisture\ loss}$	83.85721292	1.693879791
Loss through a door opening in the feeding zone	Q_d	89.13017755	1.800391418
Total		4950.6	100

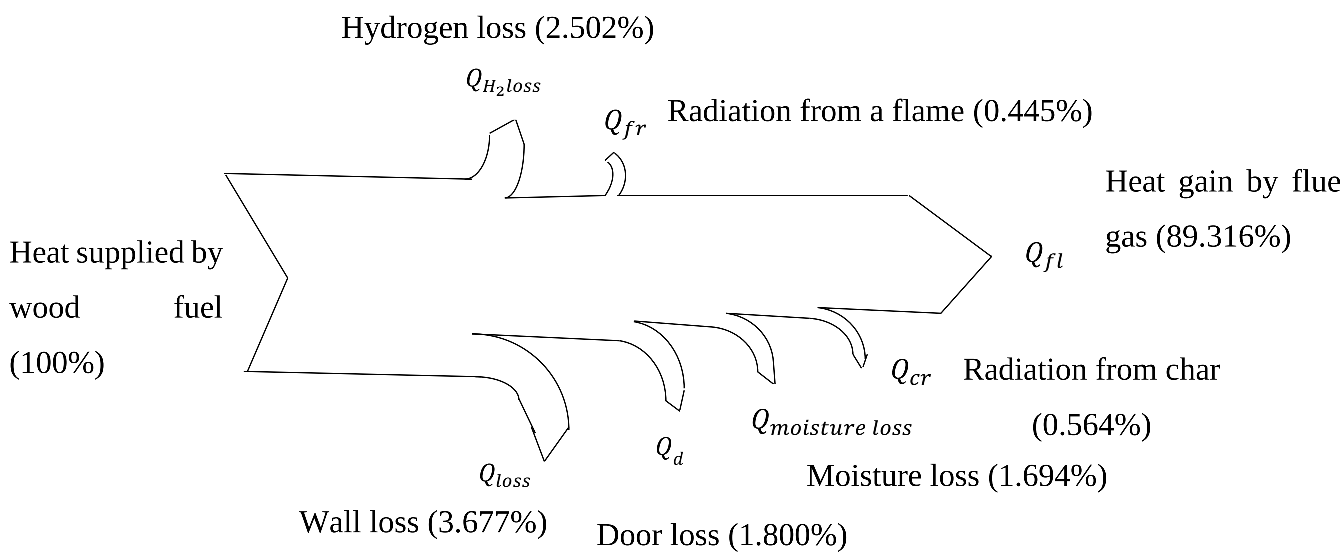

Figure 6.15 Sankey diagram for heat balance of the stove

This finding indicates that the newly released *Aircrete* insulation material for cookstoves has a lower thermal conductivity than traditionally used cooking stove materials, allowing for greater energy savings from the cookstove.

6.4 Thermal Efficiency

The water boiling test in the laboratory is used to explore the parameter thermal efficiency (th), which is used to measure the performance of cookstoves. The numerical analysis and experimental test findings were compared and validated. The thermal efficiency of the water boiling test was calculated to be 35.68 percent. Other feedstocks could bring a different value in terms of thermal efficiency and indoor air pollution if the feedstock was not limited to woody biomass.

6.5 Evaluation of Experimental against Numerical Results

The current improved model achieves a thermal efficiency of 35.8% in the water boiling experiment, which is higher than the previous models, which achieved a thermal efficiency of 18.13 percent (Parajuli et al., 2019), 32.23 2.36 pande et al (2019). Furthermore, for the current investigation, the average discrepancy in numerical and experimental temperature data is 2.446 percent. Figure 6.16 demonstrates that the average deviation of CFD and experimental data is modest and acceptable. As a result, the numerical model's accuracy is appropriate for the current investigation. The temperature of the exterior wall of the combustion chamber was 324.28 °C during the experiment, which was close to the model's expected value of 342 °C.

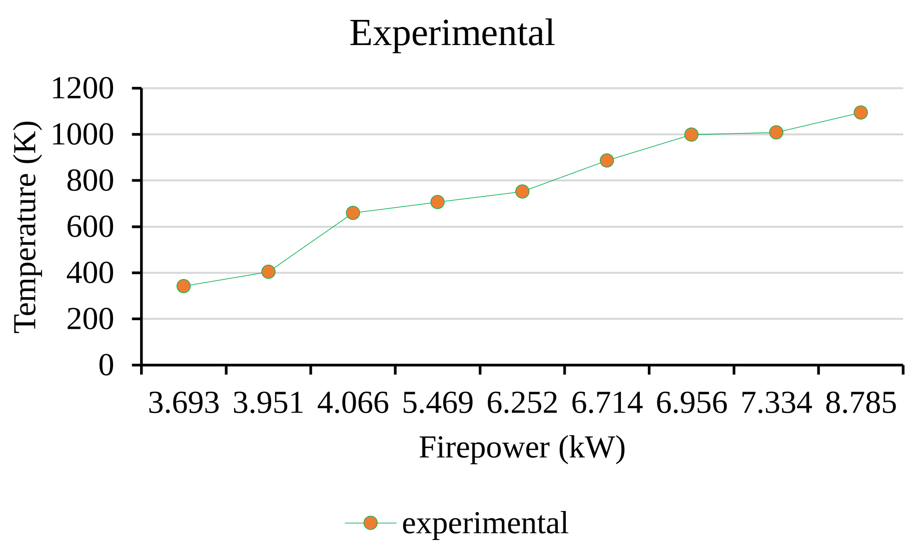

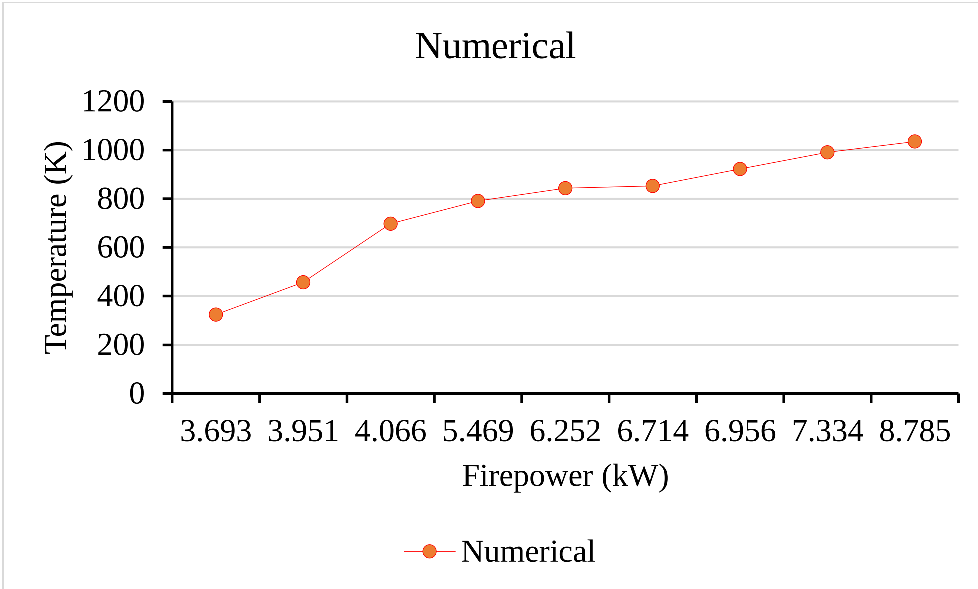

Figure 6.16 Variation of temperature with firepower (experimental and numerical)

The average recorded flame temperature from the WBT was 1035.1325 K, which is close to the flame temperature anticipated by the computational model of 1099.28 K. The average flame temperature was also 693 K and 723 K, according to Parajuli et al., (2019) and Pandit et al., (2010). Average temperatures in zones 1, 2, 3, 4, and 5 differ by 0.418 %, 0.539 %, 0.241 %, 0.65 percent, and 0.067 %, respectively, from computational model and experimental results.

In comparison to the theoretical results, the temperature achieved from the experiment is lower, as shown in Table 7. This is due to the fact that numerical outcomes are always based on a reliable assumption and are unaffected by natural impediments.

Table 7 Average values of numerical and experimental results

	Parameter	Experimental Value (K)	The numerical value (K)	Sd
Zone 1	T_{fla}	1035.1325 k	1099.28	41.82536611
	T_{wi1}	990.73	1008.53	12.58650071
	T_{wo1}	324.28	342	12.52993216
	T_{flu1}	922	998.22	53.89567886
Zone 2	T_{zon2}	852.55	886.57	24.0557727
Zone 3	T_{flu2}	843.75	751.809	65.01210457
	$Tz_{one\ 3}$	698.2	658.521	28.05728997
	T_{wi2}	790.859	705.968	60.02700176
	T_{wo2}	309.2	338.582	20.77621144
Zone 4	T_{zone4}	376.7	394.713	36.76036023
Zone 5	T_{zone5}	341	337.56	9.503515139
	T_{wo3}	309	323.345	10.14344678
	Te	324.28	333.795	6.728121023

Table 7 shows that the differences are reasonable and acceptable because the actual experiment was influenced by uncontrollable natural phenomena such as inlet air, flame temperature nonuniformity, and unaccounted losses.

CHAPTER SEVEN

7. CONCLUSIONS AND RECOMMENDATIONS

7.1 Conclusions

The experimental and numerical performance of a double-pot natural draft biomass cookstove with an *Aircrete* wall as insulation material was investigated in this work. The actual stove's model geometry was created in SOLIDWORKS, and the numerical model was created with ANSYS fluent software. The influence of combustion chamber height and then inlet air velocity on output parameters were investigated and forecasted. The experimental model was built based on the numerical results from ANSYS fluent, and WBT was used to investigate the performance of the actual dual-pot performance. In terms of temperatures at various sections and locations, efficiency, and emissions, the experimental and numerical data were in good accord. As a result, it may be considered that the numerical model accurately represents the physical phenomena of the double-pot biomass cookstove. The following conclusions were drawn from an experimental and numerical performance assessment of a double-pot natural draft biomass cookstove using an *Aircrete* wall as an insulation material:

- The use of *Aircrete* insulation resulted in a 3.68 percent reduction in heat loss through the combustion chamber wall. This demonstrates that *Aircrete* reduces loss by 12.33 percent and 15.33 percent more than ceramic wool and fiberfrax, respectively.
- It was discovered that 40 cm is the ideal combustion height for achieving the needed optimal temperature output. The porosity (air gap) of the concrete wall has a significant impact on the stove's thermal conductivity.
- • The results of the CFD technique, such as temperature distribution, geometrical effect, and inlet air velocity, show good agreement. The average variation of the temperature distribution in the stove was found to be 2.446 % based on the experimental and numerical data.
- • The thermal efficiency, fuel consumption, cooking time, heat loss through the environment, and CO gas emitted from the stove have all been improved by 35.8%, 140 g/l, 15.166 min, 3%, and 0.21 %, respectively. In general, the study answers certain questions about the performance of cookstoves, environmental protection, health, and energy conservation when utilizing the system.

7.2 Recommendations

The model is only applicable to combustion chamber stoves that operate under natural draft conditions and use wood as a fuel source. It does not apply to charcoal stoves, forced draft stoves with a fan, or gasifier-type stoves. Additionally, both mathematical and computational models can be used to obtain results that are much closer to the experimental values. The model generates a wide range of solutions for varied geometrical and operational inputs. The following areas for further research can be addressed in future studies.

- Optimization of the geometrical design parameters of biomass cookstoves.
- Improvement of the thermal property of *Aircrete* materials for biomass cookstoves.
- Analyzing the combustion flow field of the biomass cookstove using CFD.

“This research project is funded by Adama science and technology university under the grant number ASTU/SM-R/366/21, Adama, Ethiopia”.

REFERENCES

A. Mohammed, "Addis Ababa university institute of technology school of energy center " Design, and Development and Performance Evaluation of Thermoelectric Stove using CFD" a thesis rese, 2020.

Adem, K. D., and Ambie, D. A. (2017). Performance and emission reduction potential of micro-gasifier improved through better design. AIMS Energy, 5(1), 63-76.

Adkins, E., Tyler, E., Wang, J., Siriri, D., and Modi, V. (2010). Field testing and survey evaluation of household biomass cookstoves in rural sub-Saharan Africa. Energy for sustainable development, 14(3), 172-185.

Agenbroad, J., DeFoort, M., Kirkpatrick, A., and Kreutzer, C. (2011). A simplified model for understanding natural convection-driven biomass cooking stoves—Part 1: Setup and baseline validation. Energy for Sustainable Development, 15(2), 160-168.

Ali, H., and Wei, T. T. J. (2017). CFD study of an improved biomass cookstove with reduced emission and improved heat transfer characteristics. Journal of Clean Energy Technologies, 5(6), 427-432.

Alliance, C. C. (2013). The water boiling test, version 4.2. 3: Cookstove emissions and efficiency in a controlled laboratory setting. Glob. Alliances Clear. Cookstoves., 2, 52.

Amare, D., Endeblhatu, A., and Muhabaw, A. (2015). Enhancing biomass energy efficiency in rural households of Ethiopia. Journal of energy and Natural Resources, 4(2), 27-33.

Andersen, K. T. (2003). Theory for natural ventilation by thermal buoyancy in one zone with uniform temperature. Building and Environment, 38(11), 1281-1289.

Ballard-Tremeer, G., and Jawurek, H. H. (1996). Comparison of five rural, wood-burning cooking devices: efficiencies and emissions. Biomass and Bioenergy, 11(5), 419-430.

Balmes, J. R. (2019). Household air pollution from domestic combustion of solid fuels and health. Jphournal of Allergy and Clinical Immunology, 143(6), 1979-1987.

Bantelay, D. T., and Nigus, G. (2014). Design, manufacturing and performance evaluation of household gasifier stove: A case study of Ethiopia. American Journal of Energy

Engineering, 2(4), 96-102.

Bantu, A. A., Nuwagaba, G., Kizza, S., and Turinayo, Y. K. (2018). Design of an improved cooking stove using high-density heated rocks and heat-retaining techniques. Journal of Renewable Energy, 2018.

Beyene, A. D., and Koch, S. F. (2013). Clean fuel-saving technology adoption in urban Ethiopia. Energy Economics, 36, 605-613.

Beyene, G. E., Kumie, A., Edwards, R., and Troncoso, K. (2018). Opportunities for transition to clean household energy in Ethiopia: application of the household energy assessment rapid tool (HEART) .

Boafo-Mensah, G., Darkwa, K. M., and Laryea, G. (2020). Effect of combustion chamber material on the performance of an improved biomass cookstove. Case Studies in Thermal Engineering, 21, 100688.

Bryden, K. M., and Ragland, K. W. (1996). Numerical modeling of a deep, fixed bed combustor. Energy and Fuels, 10(2), 269-275.

Bryden, Mark, Still, Dean, Scott, Peter, Hoffa, Geoff, Ogle, Damon, Balis, Rob, and Goyer, Ken. (2005). Design Principles for Wood Burning Cook Stoves Aprovecho Research Center Shell Foundation Partnership for Clean Indoor Air:

Caillat, S., and Vakkilainen, E. (2013). Large-scale biomass combustion plants: an overview. Biomass Combustion Science, Technology and Engineering, 189-224.

Chica, E., and Pérez, J. F. (2019). Development and performance evaluation of an improved biomass cookstove for isolated communities from developing countries. Case Studies in Thermal Engineering, 14, 100435.

Clarke, R. E., Pianella, A., Shabani, B., and Rosengarten, G. (2017). Steady-state thermal measurement of moist granular earthen materials. Journal of Building Physics, 41(2), 101-119.

Cookstoves, H. (2011). Environment, Health, and Climate Change: A New Look at an Old Problem. Washington: The World Bank.

Dasappa, S., and Paul, P. J. (2001). Gasification of char particles in packed beds: analysis and results. International journal of energy research, 25(12), 1053-1072.

Deng, S., Wang, X., Tan, H., Li, Y., Hu, Z., and Niu, B. (2015). Optimization of operating conditions of a household up-draft biomass gasification stove. BioResources, 10(3), 4178-4190.

Downward, G. S., van der Zwaag, H. P., Simons, L., Meliefste, K., Tefera, Y., Carreon, J. R., ... and Smit, L. A. (2018). Occupational exposure to indoor air pollution among bakery workers in Ethiopia; a comparison of electric and biomass cookstoves. Environmental Pollution, 233, 690-697.

Gogoi, B., and Baruah, D. C. (2016). Steady-state heat transfer modeling of solid fuel biomass stove: Part 1. Energy, 97, 283-295.

Grabow, K., Still, D., and Bentson, S. (2013). Test kitchen studies of indoor air pollution from biomass cookstoves. Energy for Sustainable Development, 17(5), 458-462.

Hall, D. O., Rosillo-Calle, F., Williams, R. H., and Woods, J. (1993). Biomass for energy: supply prospects. Biomass for energy: supply prospects., 593-651.

Husain, Z., Tiwari, S. S., Kataria, A., Mathpati, C. S., Pandit, A. B., and Joshi, J. B. (2020). Computational Fluid Dynamic Study of Biomass Cook Stove—Part 2: Devolatilization and Heterogeneous Combustion. Industrial & Engineering Chemistry Research, 59(32), 14507-14521.

Husain, Z., Tiwari, S. S., Pandit, A. B., and Joshi, J. B. (2019). Computational Fluid Dynamics Study of Biomass Cook Stove—Part 1: Hydrodynamics and Homogeneous Combustion. Industrial & Engineering Chemistry Research, 59(9), 4161-4176.

Jain, T., and Sheth, P. N. (2019). Design of energy utilization test for a biomass cookstove: Formulation of an optimum airflow recipe. Energy, 166, 1097-1105.

Jana C, Bhattacharya SC (2017) Sustainable cooking energy options for rural poor people in India: an empirical study. Environ Dev Sustain 19(3):921–937

Jetter, J., Zhao, Y., Smith, K. R., Khan, B., Yelverton, T., DeCarlo, P., and Hays, M. D. (2012).

Pollutant emissions and energy efficiency under controlled conditions for household biomass cookstoves and implications for metrics useful in setting international test standards. Environmental science and technology, 46(19), 10827-10834.

Johnson, M., Lam, N., Brant, S., Gray, C., and Pennise, D. (2011). Modeling indoor air pollution from cookstove emissions in developing countries using a Monte Carlo single-box model. Atmospheric Environment, 45(19), 3237-3243.

Kausley SB, Pandit AB. Modeling of solid fuel stoves. Fuel 2010; 89:782–91.

Kedir, M. F., Bekele, T., and Feleke, S. (2019). Problems of Mirt, and potentials of improved Gonzie and traditional open cookstoves in biomass consumption and end-use emission in rural wooden houses of Southern Ethiopia. Scientific African, 3, e00064.

Kshirsagar, M. P., and Kalamkar, V. R. (2014). A comprehensive review on biomass cookstoves and a systematic approach for modern cookstove design. Renewable and Sustainable Energy Reviews, 30, 580-603.

Kshirsagar, M. P., and Kalamkar, V. R. (2015). A mathematical tool for predicting thermal performance of natural draft biomass cookstoves and identification of a new operational parameter. Energy, 93, 188-201.

Kumar, M., Kumar, S., and Tyagi, S. K. (2013). Design, development and technological advancement in the biomass cookstoves: A review. Renewable and Sustainable Energy Reviews, 26, 265-285.

Kumar, R. M. D., and Anand, R. (2019). Production of biofuel from biomass downdraft gasification and its applications. In Advanced Biofuels (pp. 129-151). Woodhead Publishing.

LaFave, D., Beyene, A. D., Bluffstone, R., Dissanayake, S. T., Gebreegziabher, Z., Mekonnen, A., and Toman, M. (2021). Impacts of improved biomass cookstoves on child and adult health: Experimental evidence from rural Ethiopia. World Development, 140, 105332.

MacCarty, N. A. (2013). Azonal model to aid in the design of household biomass cookstoves.

MacCarty, N. A., and Bryden, K. M. (2015). Modeling of household biomass cookstoves: A review. Energy for sustainable development, 26, 1-13.

Manaye, A., Amaha, S., Gufi, Y., Tesfamariam, B., Worku, A., and Abrha, H. (2020). Fuelwood Use and Carbon Emission Reduction of Improved Biomass Cook Stoves; Evidence from Kitchen Performance Test in Tigray, Ethiopia.

Mapelli, F., Mereu, R., Barbieri, J., & Colombo, E. (2013). CFD feasibility analysis of an Improved Cook Stove (ICS) for electricity production. In *Proc. 31st UIT National Heat Transfer Conference* (pp. 375-384).

McKendry, P. (2002). Energy production from biomass (part 1): an overview of biomass. Bioresource Technology, 83(1), 37-46.

Mehetre, S. A., Panwar, N. L., Sharma, D., and Kumar, H. (2017). Improved biomass cookstoves for sustainable development: A review. Renewable and Sustainable Energy Reviews, 73, 672 687.

Memon, S. A., Jaiswal, M. S., Jain, Y., Acharya, V., & Upadhyay, D. S. (2020). A comprehensive review and a systematic approach to enhancing the performance of improved cookstove (ICS). Journal of Thermal Analysis and Calorimetry, 141(6), 2253-2263.

Miller, B. (2013). Fuel considerations and burner design for ultra-supercritical power plants. In Ultra-Supercritical Coal Power Plants (pp. 57-80). Woodhead Publishing.

Mukhopadhyay, R., Sambandam, S., Pillarisetti, A., Jack, D., Mukhopadhyay, K., Balakrishnan, K., ... and Smith, K. (2012). Cooking practices, air quality, and the acceptability of advanced cookstoves in Haryana, India: an exploratory study to inform large-scale interventions. Global health action, 5(1), 19016.

Núñez, J., Moctezuma-Sánchez, M. F., Fisher, E. M., Berrueta, V. M., Masera, O. R., and Beltrán, A. (2020). Natural-draft flow and heat transfer in a plancha-type biomass cookstove. Renewable Energy, 146, 727-736.

Pal, K., Jha, M. K., Gera, P., and Tyagi, S. K. (2016). Experimental study on the performance evaluation and emission reduction potential of different cookstove models using standard design parameters and testing protocols. Biofuels, 7(4), 313-335.

Pande, R. R., Kalamkar, V. R., and Kshirsagar, M. P. (2019). The Effect of Inlet Area Ratio on the Performance of Multi-pot Natural Draft Biomass Cookstove. Proceedings of the National

Academy of Sciences, India Section A: Physical Sciences, 1-11.

Pande, R. R., Sharma, S. K., and Kalamkar, V. R. (2019). Experimental and numerical analyses for designing double-pot biomass cookstoves. Journal of the Brazilian Society of Mechanical Sciences and Engineering, 41(8), 350.

Pande, R., Kalamkar, V., Tiwari, A., Sharma, S., and Shrivastava, N. (2019, August). A mathematical modeling of two-pot biomass cookstove. In Journal of Physics: Conference Series (Vol. 1276, No. 1, p. 012046). IOP Publishing.

Parajuli, A., Agrawal, S., Tharu, J. K., Kamat, A. K., Jha, A. K., and Darlami, H. B. (2019). A simplified model for understanding the performance of two-pot enclosed mud cookstoves. Clean Energy, 3(4), 288-306.

Pradhan, P., Arora, A., and Mahajani, S. M. (2019). A semi-empirical approach towards predicting producer gas composition in biomass gasification. Bioresource technology, 272, 535-544.

Prapas, J. (2007). Toward the understanding and optimization of chimneys for buoyantly driven biomass stoves (Doctoral dissertation, Colorado State University).

Pundle, A., Sullivan, B., Means, P., Posner, J. D., and Kramlich, J. C. (2019). Predicting and analyzing the performance of biomass-burning natural draft rocket cookstoves using computational fluid dynamics. Biomass and Bioenergy, 131, 105402.

Quist, C. M., Jones, R. B., Jones, M. R., and Lewis, R. S. (2016). Uncertainty analysis and design guidelines of biomass cookstove thermal efficiency studies. Energy for Sustainable Development, 34, 54-61.

Ram, N. P., Kaushik, S. C., and Jain, S. K. (1984). Transient heat transfer for liquid boiling with a cookstove: a start of the art. Chang Village, 6(6), 411-421.

Sagouong, J. M., and Tchuen, G. (2018). Mathematical modeling of traditional stoves using the Thermal Network Approach. International Journal of Engineering Trends and Technology (IJETT), 58(1), 1-9.

Schirnding, Y. V. (2001). Gender differences in the impact of biomass fuel on health. Energia News, 4(4).

Sedighi, M., & Salarian, H. (2017). A comprehensive review of technical aspects of biomass cookstoves. *Renewable and Sustainable Energy Reviews*, *70*, 656-665.

Sedighi, M., and Salarian, H. (2017). A comprehensive review of technical aspects of biomass cookstoves. Renewable and Sustainable Energy Reviews, 70, 656-665.

Setiawan, A. (2018, February). Effective height of chimney for biomass cookstove simulated by computational fluid dynamics. In IOP Conference Series: Materials Science and Engineering (Vol. 308, No. 1, p. 012043). IOP Publishing.

Shah, R., and Date, A. W. (2011). Steady-state thermochemical model of a wood-burning cook-stove. Combustion Science and Technology, 183(4), 321-346.

Sharma, S. K., Sethi, B. P. S., and Chopra, S. (1990). Thermal performance of the "Rohini"—an improved wood cookstove. Energy conversion and management, 30(4), 409-419.

Siegel, R. (2001). Thermal radiation heat transfer. CRC press.

Singh, S. Comparative study of indoor air pollution using traditional and improved cooking stoves in rural households of Northern India, Energy Sustain. Dev. 19 (2014) 1–6.

Tabet, F., Fichet, V., and Plion, P. (2016). A comprehensive CFD-based model for domestic biomass heating systems. Journal of the Energy Institute, 89(2), 199-214.

Tadesse, A. S., Gabisa, E., and Mekonnen, B. A. (2020). Prototyping and Performance Evaluation of Household Cow Dung Gasifier Stove: Cooking and Environmental Performance in the Case of Ethiopia.

Usman, O. Y. (2011). Experimental Performance Evaluation Of Charcoal-Stove (Doctoral dissertation, Ph.D. Thesis, University of Nigeria, Mechanical Engineering, Nsukka. Retrieved June 20, 2019,

Venkatachalam, C., and Solomon, G. (2019). Dataset of solar energy potential assessment for Adama city (Ethiopia). Data in brief, 24, 103879.

Venkataraman, C., Sagar, A. D., Habib, G., Lam, N., and Smith, K. R. (2010). The Indian national initiative for advanced biomass cookstoves: the benefits of clean combustion. Energy for sustainable development, 14(2), 63-72.

Volborth, A. (1979). Problems of oxygen stoichiometry in analyses of coal and related materials. In Analytical methods for coal and coal products (pp. 543-583). Academic Press.

Wassie, Y. T., and Adaramola, M. S. (2021). Analysis of potential fuel savings, economic and environmental effects of improved biomass cookstoves in rural Ethiopia. Journal of Cleaner Production, 280, 124700.

World Health Organization (WHO). (2018). Household air pollution and health. Available via: https://www.who.int/news-room/fact-sheets/detail/household-air-pollution-and-health. Accessed 20 July 2020.

World Health Organization. (2014). WHO guidelines for indoor air quality: household fuel combustion. World Health Organization.

Zube, D. J. (2010). Heat transfer efficiency of biomass cookstoves (Doctoral dissertation, Colorado State University).

APPENDIX A

The porosity of the samples from the experimental test result

Sample no.	Mixture	M (g)	D (g)	S (g)	P
1	Cement, foam and water	362.5	229	2.0335	0.370353417
2	Cement, foam, light gravel and water	418	291	19.2269	0.318476848
3	Cement, light gravel and water	583	501.5	179.2538	0.201859485

APPENDIX B

Thermal conductivity test results of the samples

File name	sample3
Reference Sample	sample3
T / C	0.3290
Unit	[W / mK]

	1 st	2 nd	3 rd	4 th	5 th	Mean	S.D.
T / C	0.3280	0.3353	0.3236			0.3290	0.0059
HEATER(A^2)	0.6250	0.6250	0.6250				
Tm (C)	26.80	27.20	27.30			27.10	
T0 (C)	24.30	24.70	24.80			24.60	

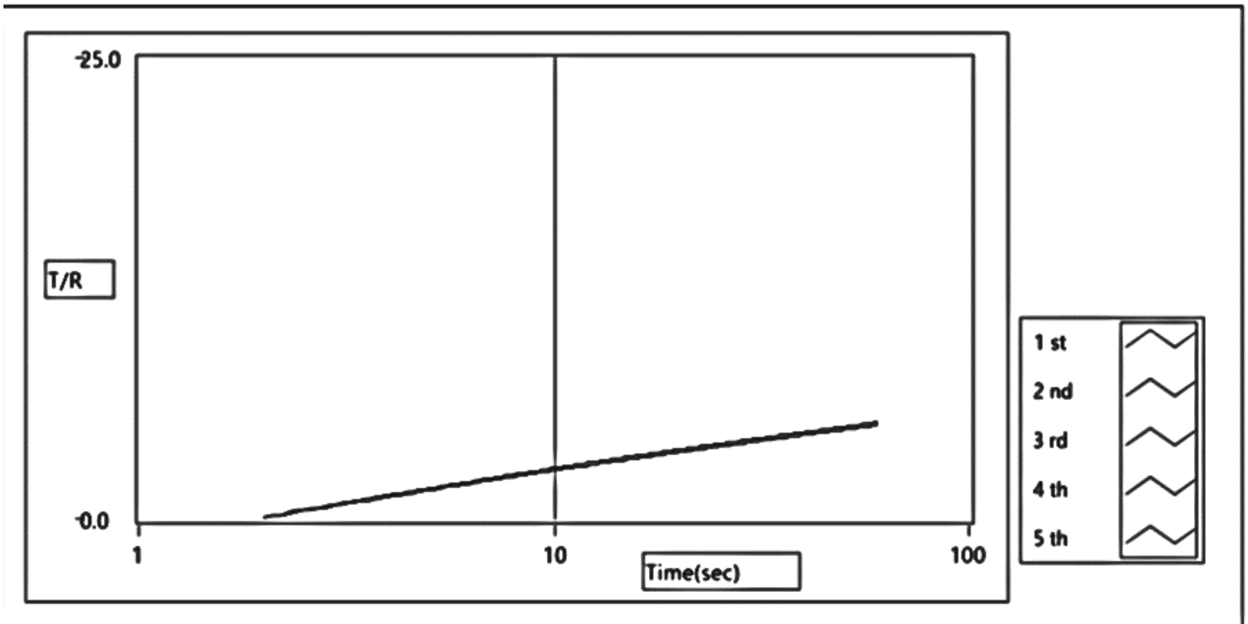

File name	sample2
Reference Sample	sample2
T / C	0.1962
Unit	[W / mK]

	1 st	2 nd	3 rd	4 th	5 th	Mean	S.D.
T / C	0.1923	0.1978	0.1986			0.1962	0.0034
HEATER(A^2)	0.6250	0.6250	0.6250				
Tm (C)	27.50	28.00	28.30			27.93	
T0 (C)	24.00	24.50	24.80			24.43	

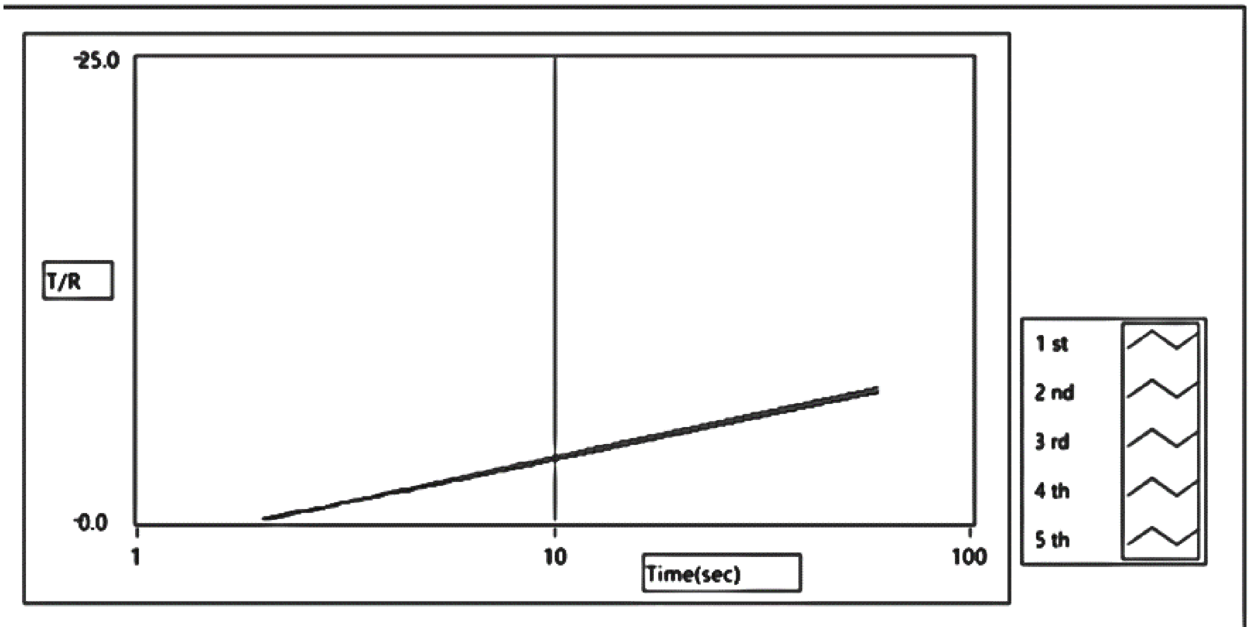

File name	sample1
Reference Sample	sample1
T / C	0.1839
Unit	[W / mK]

	1 st	2 nd	3 rd	4 th	5 th	Mean	S.D.
T / C	0.1615	0.1731	0.2172			0.1839	0.0294
HEATER(A^2)	0.6250	0.6250	0.6250				
Tm (C)	30.90	31.60	31.40			31.30	
T0 (C)	24.60	25.00	25.10			24.90	

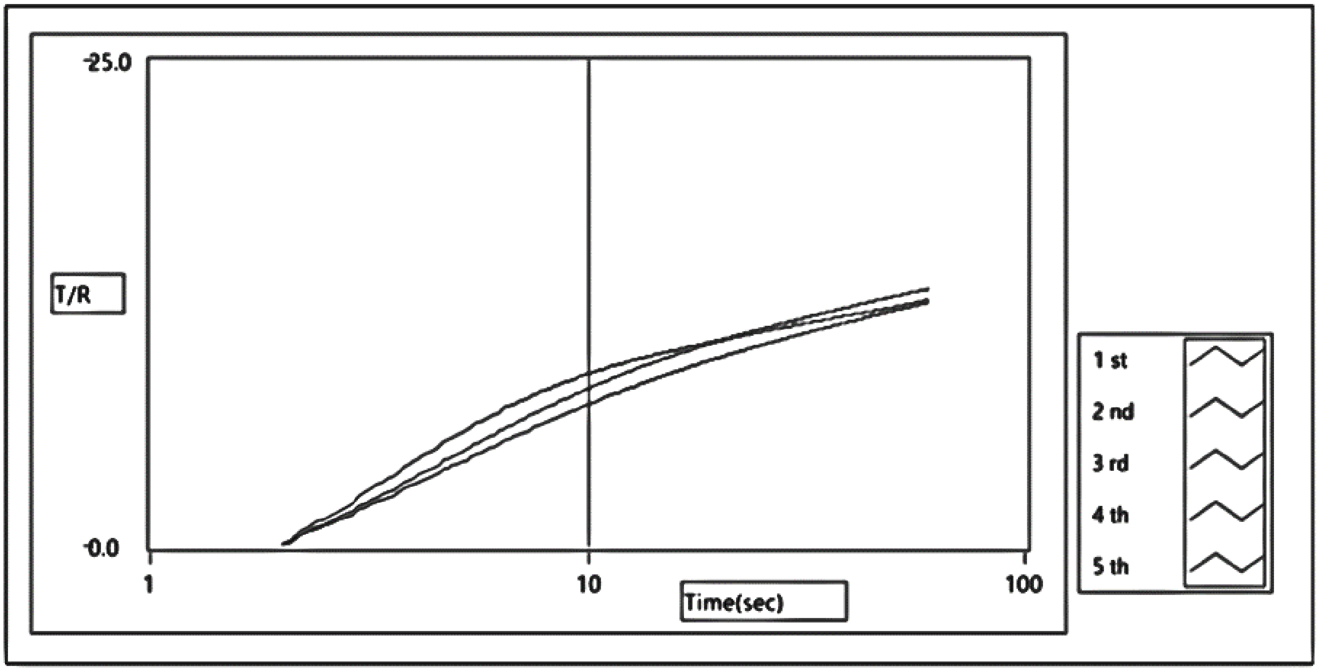

File name	sample4
Reference Sample	sample4
T / C	0.5469
Unit	[W / mK]

	1 st	2 nd	3 rd	4 th	5 th	Mean	S.D.
T / C	0.5346	0.5476	0.5586			0.5469	0.0120
HEATER(A^2)	0.6250	0.6250	0.6250				
Tm (C)	25.60	26.10	26.30			26.00	
T0 (C)	24.10	24.60	24.80			24.50	

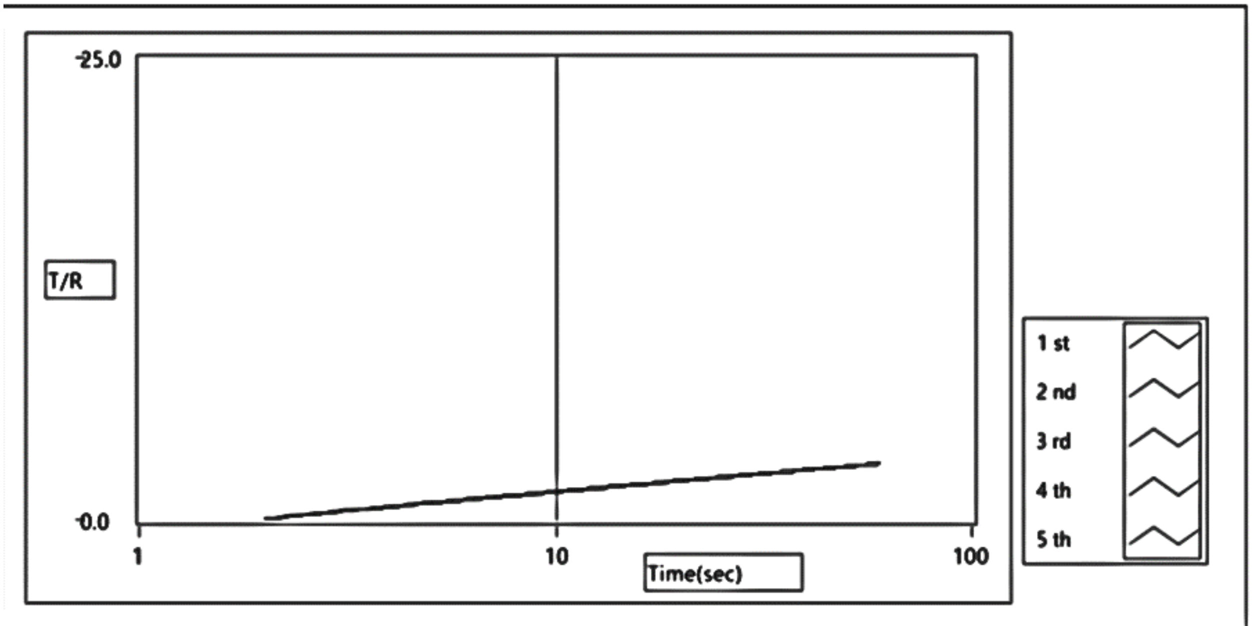

APPENDIX C

Reference materials for thermal conductivity test

APPENDIX D

Specification QTM-500 Quick Thermal Conductivity Meter

Type and model name QTM-500 Quick	Thermal Conductivity Meter
Temperature	-10 to 200℃ (Thermal bath is necessary for measurement at different room temperature)
Heater current precision	±0.1% of setup value
Display	30 digits × 7 lines LCD with back light Display: Thermal conductivity: 0. ××××~×××.×W/m.K Measuring temperature: −100 to 1000 °C Guiding message for measurement
Precision	±5% reading value per reference plate
Reproducibility	±3% reading value per reference plate
Sensor	PD-11 Box Probe Constantan heater wire and chromel-alumel thermocouple
Heater current precision	±0.1% of setup value
Measuring method	Hot Wire method
Measuring range	0.023 to 12W/m.K
Power source	100 to 240VAC, 50/60Hz
Power consumption	Approx. 60W

APPENDIX E

Process of measuring porosity of the slabs

APPENDIX F

Part and Assembly drawings of the stove

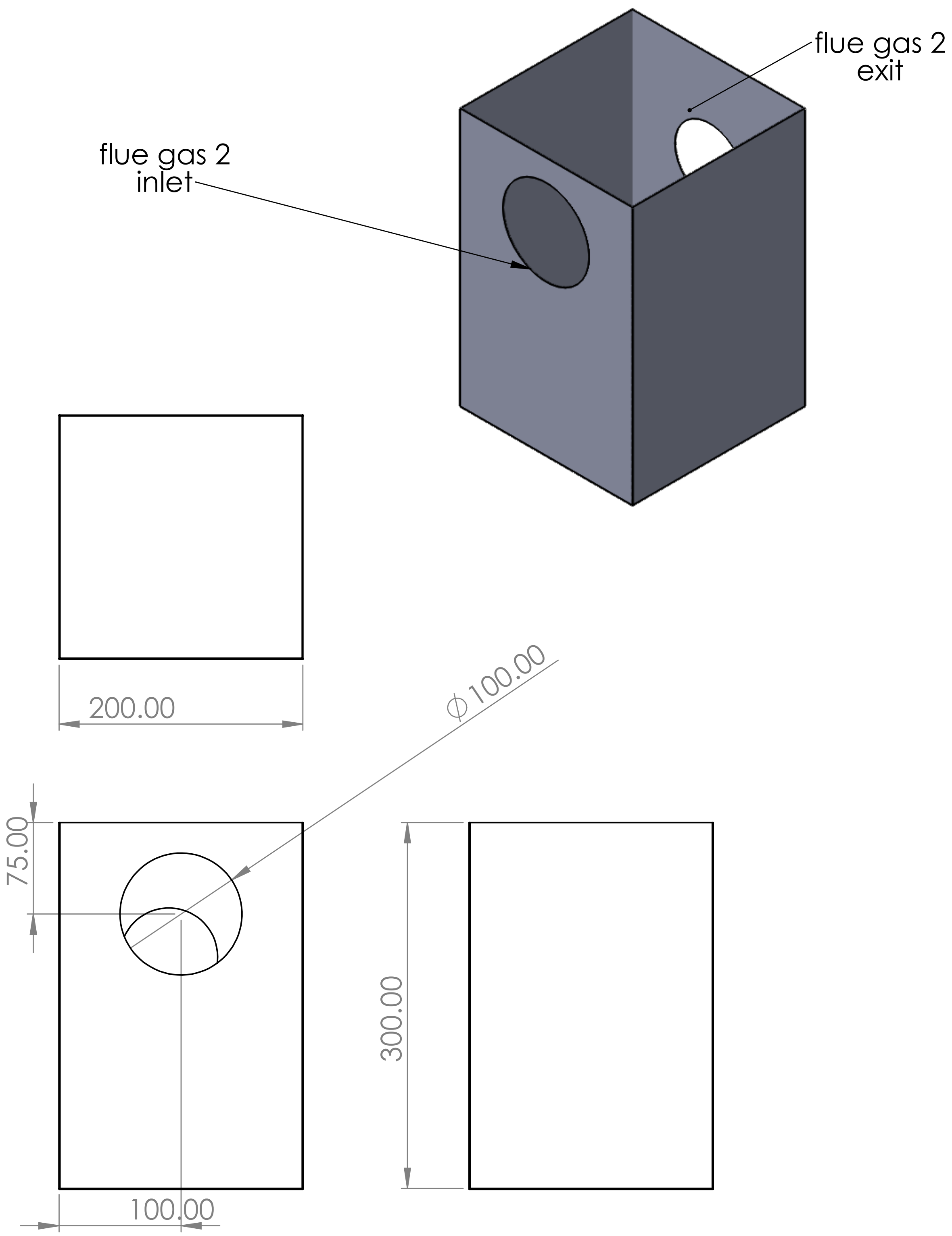

UNLESS OTHERWISE SPECIFIED: DIMENSIONS ARE IN MILLIMETERS SURFACE FINISH: TOLERANCES: LINEAR: ANGULAR:	FINISH:	DEBURR AND BREAK SHARP EDGES	DO NOT SCALE DRAWING	REVISION

	NAME	SIGNATURE	DATE	
DRAWN				
CHK'D				
APPV'D				
MFG				
Q.A				MATERIAL:
				WEIGHT:

TITLE:

zone 2

DWG NO.

A4

SCALE:1:5

SHEET 1 OF 1

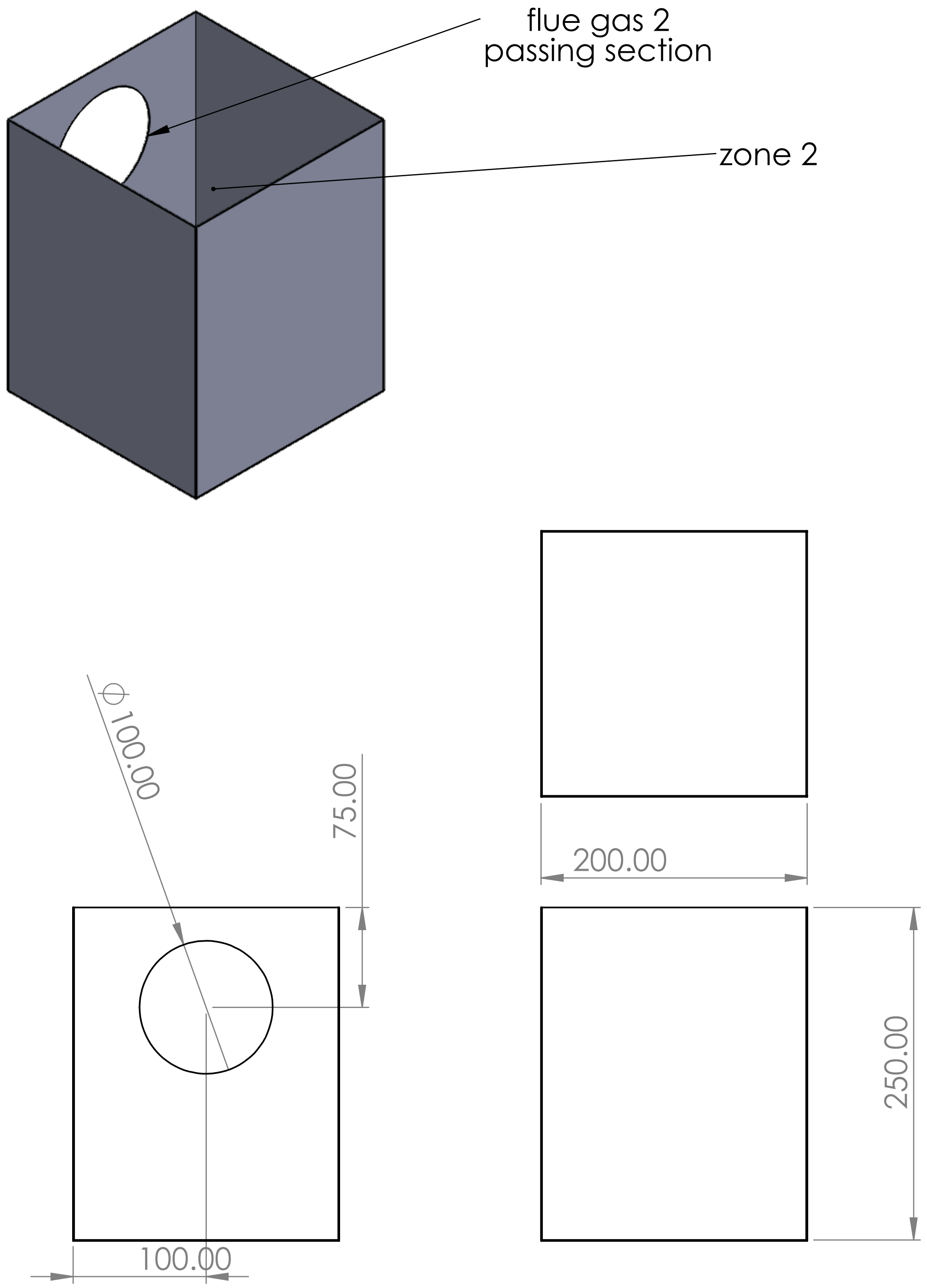

UNLESS OTHERWISE SPECIFIED:
DIMENSIONS ARE IN MILLIMETERS
SURFACE FINISH:
TOLERANCES:
LINEAR:
ANGULAR:

FINISH:

DEBURR AND BREAK SHARP EDGES

DO NOT SCALE DRAWING

REVISION

	NAME	SIGNATURE	DATE
DRAWN			
CHK'D			
APPV'D			
MFG			
Q.A			

TITLE:

zone 3

MATERIAL:

DWG NO.

A4

WEIGHT:

SCALE:1:5

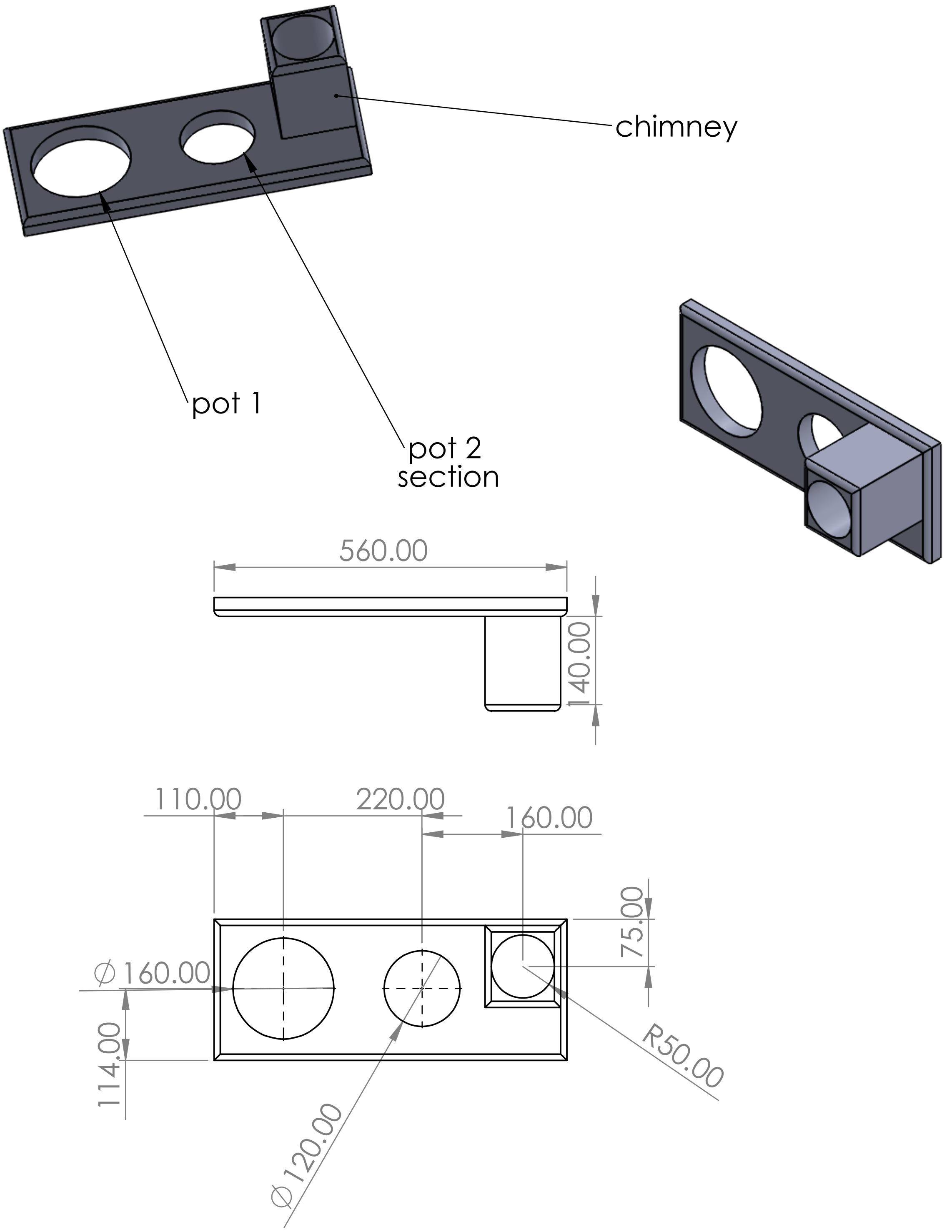

UNLESS OTHERWISE SPECIFIED: DIMENSIONS ARE IN MILLIMETERS SURFACE FINISH: TOLERANCES: LINEAR: ANGULAR:	FINISH:	DEBURR AND BREAK SHARP EDGES

DO NOT SCALE DRAWING

REVISION

	NAME	SIGNATURE	DATE
DRAWN			
CHK'D			
APPV'D			
MFG			
Q.A			

TITLE:

upper part of the stove

MATERIAL:

WEIGHT:

A4

SCALE:1:10

SHEET 1 OF 1

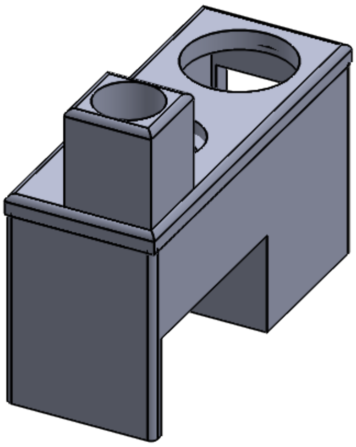

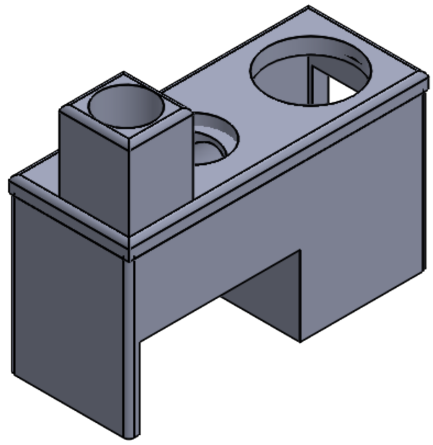

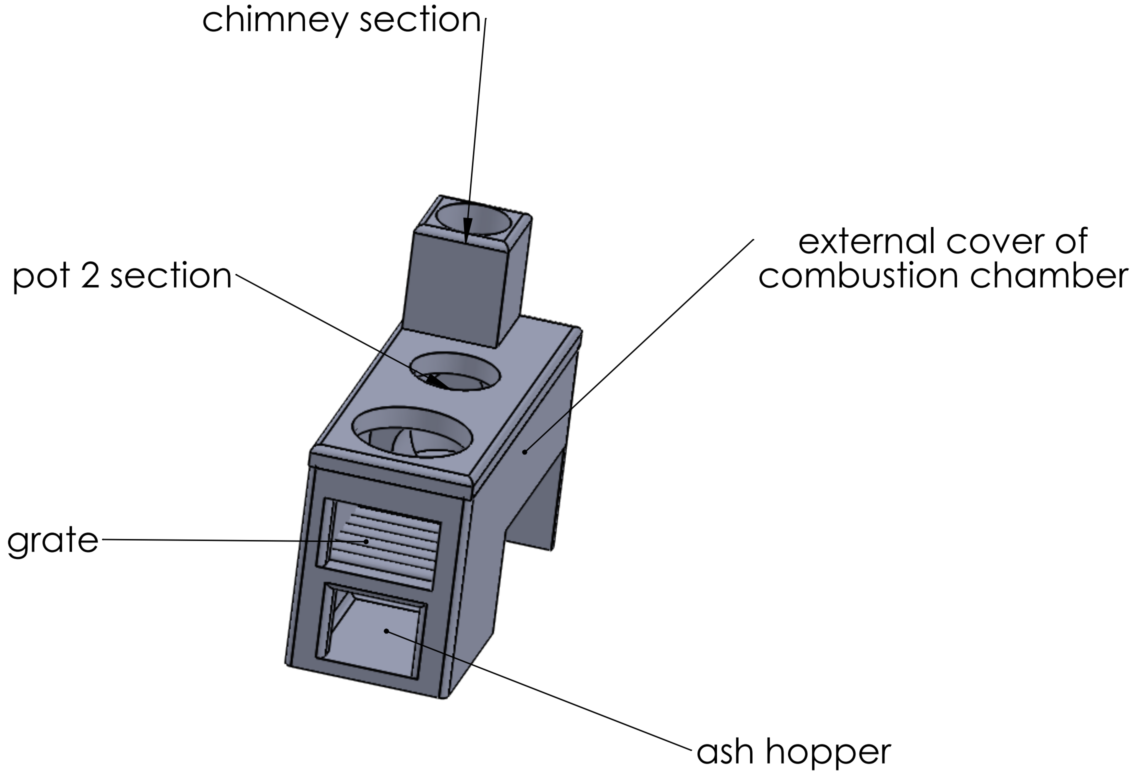

UNLESS OTHERWISE SPECIFIED: DIMENSIONS ARE IN MILLIMETERS SURFACE FINISH: TOLERANCES: LINEAR: ANGULAR:	FINISH:	DEBURR AND BREAK SHARP EDGES	DO NOT SCALE DRAWING

REVISION

	NAME	SIGNATURE	DATE
DRAWN			
CHK'D			
APPV'D			
MFG			
Q.A			

MATERIAL:

WEIGHT:

TITLE:

COMPLETE ASSEMB.

DWG NO.

A4

SCALE:1:10

SHEET 1 OF 1

4 3 2 1

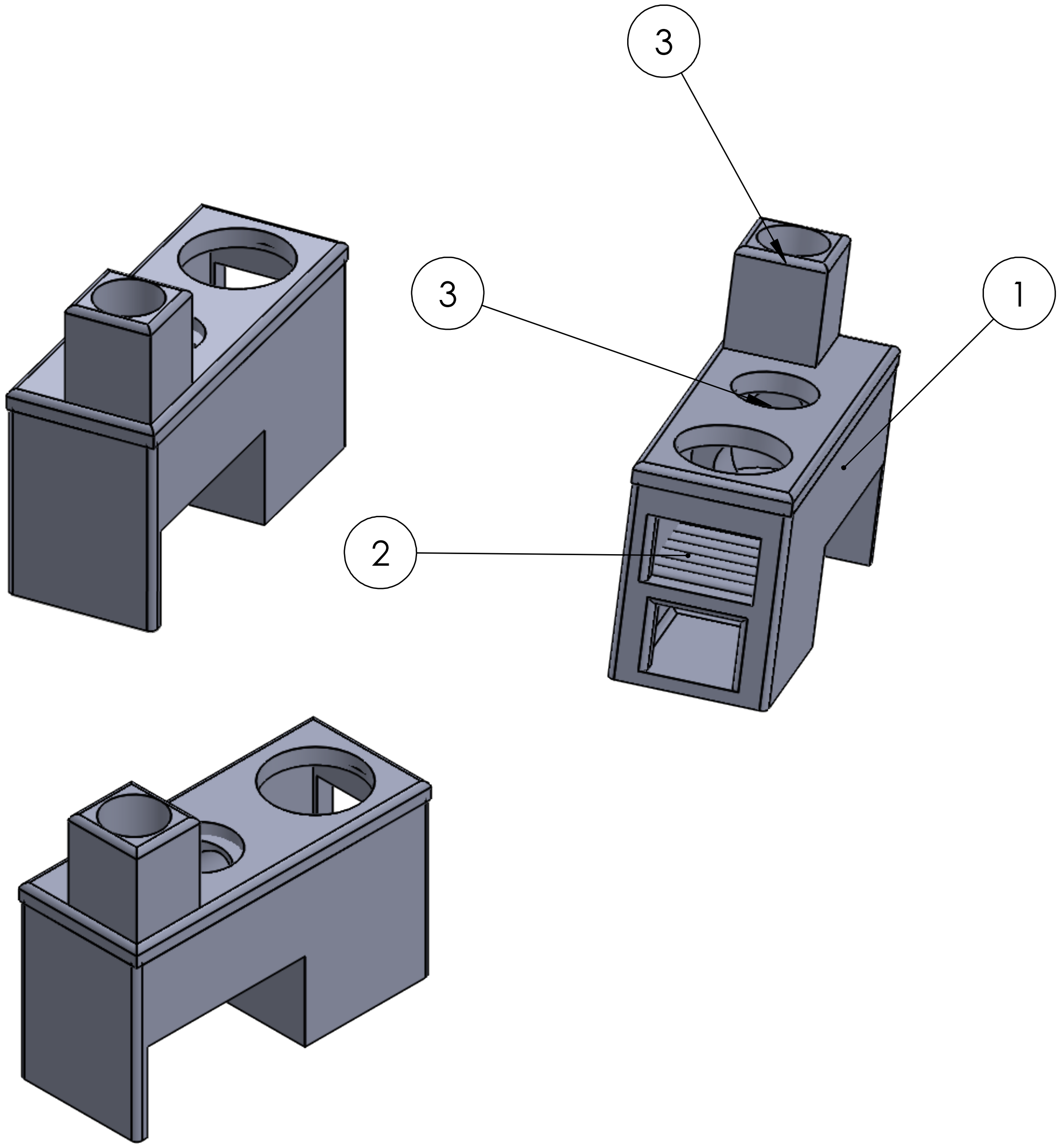

ITEM NO.	PART NUMBER	DESCRIPTION	QTY.
1	combustion chamber with fllet		1
2	grate		6
3	upper part of the stove with fillet		1

UNLESS OTHERWISE SPECIFIED:
DIMENSIONS ARE IN MILLIMETERS
SURFACE FINISH:
TOLERANCES:
LINEAR:
ANGULAR:

FINISH:

DEBURR AND BREAK SHARP EDGES

DO NOT SCALE DRAWING

REVISION

	NAME	SIGNATURE	DATE
DRAWN			
CHK'D			
APPV'D			
MFG			
Q.A			

TITLE:

COMPLETE ASSEMB.

MATERIAL:

DWG NO.

A4

WEIGHT:

SCALE:1:10

SHEET 1 OF 1

4 3 2 1